Acknowledgements

First and foremost I would like to thank my parents. They have been tremendously supportive in almost all my endeavours so far and have given valuable advice when needed. A huge thank-you also to my brother and my sister-in-law for emotional and practical support especially in times of extreme stress.

I thank my supervisor, Rüdiger Klein, who has given me the opportunity to carry out my PhD in a great scientific environment. I am grateful for critical discussions and support. I sincerely appreciate the freedom he has given me to develop my own ideas and interests.

I wish to acknowledge my collaborators at the MPI for Psychiatry in Munich, especially Mathias Eder for performing the LTP experiments.

My deep respect for all the people of all the service units at the MPI who make our work so much easier and more efficient. I am in particular grateful for the excellent service provided by the caretakers in the animal facility in our institute, especially Bettina Hoisl for outstanding work and nice chats that saved me from insanity while genotyping mice.

I acknowledge past and present members of the Klein lab for providing a nice working atmosphere, technical help, discussions and criticism. The international make-up of our lab has truly enriched my life, broadened my horizon and expanded my culinary knowledge. My special thanks go out to Françoise Helmbacher, Archana Mishra, Guido Pantè, Ilona Kadow and Joaquim Egea for conversations, brainstorming and their support. Extra thanks to Joaquim for never tiring to listen to my problems, always trying to find solutions and having his mother offer parsley to the gods of science.

I am grateful for having survived years of doubtful nourishment as provided by the numerous caterers that have run the MPI canteen over the years and sincerely grateful for the temporary lunch-cooking extravaganza with Karl Farrow and John Bailey to which I've had the pleasure of being recruited to.

My sincerest regards for my diploma thesis supervisor, Francesco "Checco" Ramirez, who taught me to be a scientist and without whom I probably would have given up a long time ago. Thanks also for giving me "the elements of style" (Strunk W and White EB, 3rd ed., MacMillan Publishing Co., Inc., New York, 1979), a book that provides excellent advice on the art of writing, probably most which I have shamefully disregarded in this thesis.

I wish to thank colleagues from other departments at the MPI for Neurobiology for interesting and often fruitful discussions. A big hurra to all the fly nerds, especially Karl Farrow, Yong Choe, Virginia Flanagin, Dierk Reiff and Thomas Hendel.

My deepest gratitude to all my friends inside and outside the lab for listening, advice, encouragement, hour-long (phone) conversations, entertainment or other contributions, in particular Françoise Helmbacher, Archana Mishra, Guido Pantè, Ilona Kadow, Karl Farrow, Sonia Paixao, Falko Hampel, Mark Boenke, Simone Helmreich, Francesca Cole, Andrew Bergemann, Ben Short and Uli Löhr.

I thank Yong Choe for critically reading this thesis.

Für Karin, Günter, Andreas und Sylvia

Molecular and functional interaction of Ras/Rab interactor 1 and EphA4 receptor

Dissertation

Der Fakultät für Biologie der
Ludwig-Maximilians-Universität München

Eingereicht am 28. September 2006 von Katrin Deininger

Erstgutachter: Prof. Dr. Rüdiger Klein
Zweitgutachter: Prof. Dr. Heinrich Leonhardt
Tag der mündlichen Prüfung: 16.01.2007

The work presented in this thesis was performed in the laboratory of Prof. Dr. Rüdiger Klein, Department of Molecular Neurobiology, Max Planck Institute of Neurobiology, Martinsried, Germany.

Ehrenwörtliche Versicherung

Ich versichere hiermit ehrenwörtlich, dass die vorgelegte Dissertation von mir selbständig und ohne unerlaubte Beihilfe angefertigt ist.

München, den..... .....

(Unterschrift)

Erklärung

Hiermit erkläre ich, dass ich mich anderweitig einer Doktorprüfung ohne Erfolg nicht unterzogen habe.

München, den..... .....

(Unterschrift)

Abbreviations

aa	amino acid
Abl	Abelson
ACSF	artificial cerebrospinal fluid
ADAM	A-Disintegrin-And-Metalloprotease
AF-6	Afadin-6
AMP	adenosine 5'-monophosphate
amp	ampicillin
AMPA	α-amino-3-hydroxy-5-methyl-4-isoxazole proprionic acid
APS	ammonium persulfate
Arg	Abl-related gene
as	antisense
ATP	adenosine 5'-triphosphate
BBS	BES buffered saline
BCIP	5-bromo-4-chloro-3-indolyphosphate
BDNF	brain derived neurotrophic factor
BES	N,N-bis[2-hydroxyethyl]-2-aminoethanesulfonic acid
Borax	sodium tetraborate
bp	base pairs
BSA	bovine serum albumin
CA	cornu ammonis
CAMKII	Ca^{2+}/Calmodulin-dependent protein kinase II
cAMP	cyclic AMP
Cbl	Casitas B-lineage lymphoma
cdc42	cell division cycle 42
Chaps	3-[(3-Cholaminopropyl)dimethylammonio]-1-propanesulfonate
CNS	central nervous system
CRE	cAMP responsive element
CREB	CRE binding protein
Crk	Chicken Retroviral Kinase
CS	calf serum
C-term	carboxy terminus
Da	Dalton (g/mol)

DG	dentate gyrus
DIG	digoxygenin
DIV	days in vitro
DMEM	Dulbecco's Modified Eagle medium
DNA	deoxyribonucleic acid
dNTP	deoxyribonucleoside triphosphate
DTT	1,4-Dithio-DL-threitol
E	embryonic day
ECL	enhanced chemoluminescence
EDTA	ethylenediaminetetraacetic acid
EGFR	epidermal growth factor receptor
Eph	erythropoietin-producing hepatocellular
Ephexin	Eph-interacting exchange protein
ephrin	Eph receptor interacting
EPSP	excitatory postsynaptic potential
ER	endoplasmic reticulum
Erk1/2	extracellular signal related/regulated kinase 1/2
EtOH	ethanol
FAP-1	Fas-associated protein-tyrosine phosphatase 1
Fas	TNF receptor superfamily member
FBS	fetal bovine serum
FN	fibronectin
GAP	GTPase-activating protein
GEF	guanine nucleotide exchange factor
GluR	glutamate receptor subunit
GPI	glycosylphosphatidylinositol
Grb	growth factor receptor-bound
Grip	glutamate receptor interacting protein
GTP	guanosine triphosphate
h	hour(s)
HBSS	Hank's balanced salt solution
HC	heavy chain
HeLa	Henrietta Lacks
HEPES	N-2-hydroxyethylpiperanzine-N'-2-ethanesulfonic acid
HGF	hepatocyte growth factor

Hras	Harvey rat sarcoma virus oncogene
HRP	horseradish peroxidase
HS	horse serum
IF	immunofluorescence
Ig	immunoglobulin
IHC	immunohistochemistry
IP	immunoprecipitation
JM	juxtamembrane (region)
kan	kanamycin
kb	kilo bases
KD	kinase dead
KO	knock-out
Kras	Kirsten rat sarcoma viral oncogene homolog
LC	light chain
LMW-PTP	low-molecular-weight protein tyrosine phosphatase
LTD	long term depression
LTP	long term potentiation
MAPK	mitogen activated protein kinase
MetOH	methanol
min	minute(s)
ml	milli liter
MS	mass spectrometry
mut	mutant
Nck	non-catalytic region of tyrosine kinase adaptor protein 1
NGF	nerve growth factor
NR	NMDA receptor subunit
Nras	neuroblastoma ras oncogene
N-term	amino terminus
o/n	overnight
°C	degree Celcius
P	postnatal day
PAGE	polyacrylamide-gel-electrophoresis
PCR	polymerase chain reaction
PDZ	postsynaptic density-95/discs-large/zona occludens 1
PFA	paraformaldehyde solution in PBS

pH	potentium hydrogenii
PHIP	pleckstrin homology domain interacting protein
PI3K	Phosphatidylinositol3-kinase
PICK	protein interacting with C kinase
PKC	protein kinase C
PSD	postsynaptic density
PSD-95	postsynaptic density protein 95
PTP-BL	Protein tyrosine phosphatase Burkitts lymphoma
pY/pTyr	phospho-tyrosine
RA	Ras association
Rac1	Ras-related C3 botulinum toxin substrate 1
Ras	rat sarcoma
RBD	Ras-binding domain
RGS	Regulator of G protein Signaling
RhoA	Ras homologue A
rpm	revolutions per minute
RT	room temperature
RTK	receptor tyrosine kinase
s	sense
SAM	sterile-α-motif
SFK	src-family kinase
SH	src homology
SHEP1	SH2-domain-containing Eph receptor-binding protein 1
SLAP	src-like adaptor protein
sol	solution
src	sarcoma virus transforming gene product
SU	subunit
TBS	thetaburst stimulation
TE	Tris-EDTA
tet	tetracycline
TEV	tobacco etch virus
TGN	trans-Golgi network
TK	tyrosine kinase
TM	transmembrane (region)
Tris	Tris[hydroxymethyl]aminomethane

TX·100	TritonX·100
U	units
Ub	ubiquitin
UV	ultra violet
Vav	Vav oncogene
WB	Western blot
wt	wild type

List of Figures

1. Introduction

Undoubtedly one of the most intriguing features in multicellular organisms is how the myriads of cells in the body "talk" to each other. The clear advantage of multicellular over single-cell life forms is that by collaboration and division of labour it became possible to exploit resources that no single cell could utilise so well (Alberts B, et al., 1994). One well known example of a simple multicellular organism is the green algae volvox, comprised of about 50.000 cells forming a hollow sphere. Within the volvox colony there is division of labour among cells, with a small number being specialised for reproduction and serving as the precursors for the next generation. The other cells are dependent on one another and the organism dies if the colony is disrupted. Even in this relatively simple and small life form there arose the need for cells to communicate with each other, setting up signals to govern the character of each cell according to its place in the structure as a whole. How much greater is the necessity in highly complex multicellular organisms, such as vertebrates where more than 200 distinct cell types can be distinguished and many more subtler varieties (Alberts B, et al., 1994).

An animal cell contains an elaborate system of proteins that enables it to respond to signals from other cells. Signals can be transmitted over vast distances in the body in the form of hormones through the blood stream. Another way to cover distances is by extreme morphological adaptation of cells such as neurons, whose processes can contact target cells far away. Signalling molecules can be very diverse and include proteins, small peptides, steroids, retinoids, fatty acid derivates or dissolved gases, such as nitric oxide (Alberts B, et al., 1994). Signals can furthermore be soluble, bound to the extracellular matrix or presented on the surface of neighbouring cells and act in millions of combinations. The way a cell responds to these depends on the combination of signal receptors it possesses and its intracellular machinery through which it integrates and interprets the signals it receives. How it comes about developmentally that subsets of cells express different combinations of receptors and intracellular signalling molecules is itself regulated through intercellular communication. The general principle is that cells respond through receptors on their surface to extracellular signals and pass this information on to the inside of the cell where in turn it is propagated by a cascade of intracellular proteins that eventually determine the cell's response. Cells can respond to signals quickly for example by rearranging their cytoskeleton thus affecting morphology or migratory behaviour, or more slowly by influencing gene expression and thereby changing the molecular composition and

consequently the responsive properties of the cell. With the exception of intracellular receptors that bind to hydrophobic molecules diffusing into the cell, receptors are most often cell surface proteins with high affinity for their specific signal or ligand (Alberts B, et al., 1994). There are three known classes of cell-surface receptors each activating intracellular events through different mechanisms (Alberts B, et al., 1994). Ion-channel-linked receptors or transmitter-gated ion channels, e.g. glutamate-gated cation channels such as the NMDA-receptor are regulated in their open-or-closed state through binding to their ligand and thereby influence the ion permeability of the plasma membrane and thus the excitability of the neuron. G-protein-coupled receptors (GPCRs) are seven-transmembrane domain proteins that act indirectly through a trimeric G-protein to influence a separate protein such as an ion channel or an enzyme. Finally the third class are the enzyme-linked receptors, mostly single-pass transmembrane proteins, the majority of which are protein kinases that phosphorylate intracellular signal transducers. The best known class are the Receptor-Tyrosine-Kinases (RTKs), with such prominent members as Epidermal-Growth-Factor Receptor (EGFR) or the Eph receptors. The Eph receptors and their ligands, the ephrins, shall be of particular interest to this study and will be further introduced in the next chapter.

1.1 Eph receptors and ephrin ligands

Eph receptors and their ligands, the ephrins, are found throughout the animal kingdom but are most numerous in vertebrates. There, they have been reported to be involved in a vast array of biological functions ranging from vascular development, tissue-border formation and cell migration to axon guidance and synaptic plasticity (reviewed in (Klein, 2004; Palmer and Klein, 2003; Poliakov et al., 2004; Wilkinson, 2001). In contrast to vertebrates, only one Eph receptor and 4 ephrins are found in Caenorhabditis elegans (George et al., 1998; Wang et al., 1999) and Drosophila has only a single Eph and a single ephrin, which are expressed within the embryonic CNS at a time when neurons are extending axons towards their targets (Bossing and Brand, 2002; Scully et al., 1999). It has recently been shown that they too act as a functional receptor-ligand pair in vivo since Eph receptor null mutant flies show an axon guidance phenotype in a subpopulation of mushroom body neurons (Boyle et al., 2006).

The Ephs and ephrins differ from most described receptor-ligand pairs in that both the receptor as well as the ligand are membrane residents. Thus signalling is only elicited upon cell-cell contact unlike in systems with diffusible ligands. Another unique feature of this particular system is that also the ligand can induce intracellular signalling, termed “reverse” signalling (Bruckner et al., 1997; Holland et al., 1996) in contrast to “forward” signalling taking place in the receptor cell. This bi-directional signalling can mediate attraction between the cells in contact as has been described for the establishment of the vomeronasal projection in the mouse. Here vomeronasal axons expressing high levels of ephrinA5 project onto regions of the accessory olfactory bulb with high EphA6 receptor concentration (Knoll et al., 2001). Repulsion on the other hand is the more prominent outcome of Eph-ephrin signalling as is well exemplified by the guidance of EphA4-positive corticospinal tract (CST) axons repelled by ephrinB3-positive spinal cord midline cells (Kullander et al., 2001a; Kullander et al., 2001b).

To complicate the picture of Eph and ephrin signalling even further, it has become clear that there are many cell types in which receptor and ligand are co-expressed contrasting the classical complementarity of Eph and ephrin expression domains (Hornberger et al., 1999; Iwamasa et al., 1999). Marquardt and colleagues recently showed that co-expressed EphA and ephrinA in spinal motor neurons segregate to distinct membrane domains and can be activated by their respective binding partner presented by opposing cells (in trans). Within the same growth cone ephrinA and EphA mediate opposite functions, either growth or collapse, respectively. This differential localisation is essential since a forced co-localisation

of receptor and ligand leads to a disruption of correct signalling outcome (Marquardt et al., 2005).
Recent studies have shown that in addition to bi-directional signalling, there is also bi-directional endocytosis of Ephs and ephrins, sometimes termed "trans-endocytosis" (Marston et al., 2003; Zimmer et al., 2003), a phenomenon that will be discussed in detail in chapter 1.3.3).

The Eph receptors

Amongst the family of Receptor Tyrosine Kinases (RTKs), the Eph receptors constitute the most numerous subfamily. Based on sequence similarity and ligand binding preferences they are grouped into ten EphA class receptors that bind to ephrinA ligands and six EphB class receptors that bind to ephrinB ligands. Within the A- and B- classes there is a certain degree of promiscuity, e.g. one EphA receptor is usually able to bind to several ephrinA ligands although with different affinities. A-class receptors generally have no affinity for B-class ligands with the exception of EphA4 that can in addition to A-class ligands also bind to ephrinB2 and ephrinB3 (Pasquale, 2004). The interaction is initiated by one receptor molecule and one ligand molecule coming into contact via the receptor's globular domain and a conserved Eph-binding domain in the ephrin (Lackmann et al., 1997). Crystallography has provided structural details of the receptor ligand interaction showing a high affinity ephrin-binding site within the extracellular part of the Eph receptor that mediates hetero-dimerisation accompanied by a lower affinity site mediating tetramerisation (Himanen and Nikolov, 2003a; Himanen and Nikolov, 2003b). Eph receptors have an evolutionary highly conserved domain structure (Drescher, 2002), with the aforementioned globular domain in the extracellular part which is necessary and sufficient for ligand binding (Labrador et al., 1997; Lackmann et al., 1998), followed by a cysteine-rich linker, an EGF-like motif, and two type III fibronectin domains (Figure 1). A single transmembrane region connects to the cytoplasmic part comprising of a juxtamembrane segment with 2 conserved tyrosine residues, a protein tyrosine kinase domain, a sterile-α-motif (SAM) and a PDZ (PSD-95, Disc large, ZO [Zona Occludens]-1/2) -binding motif (Kullander and Klein, 2002).

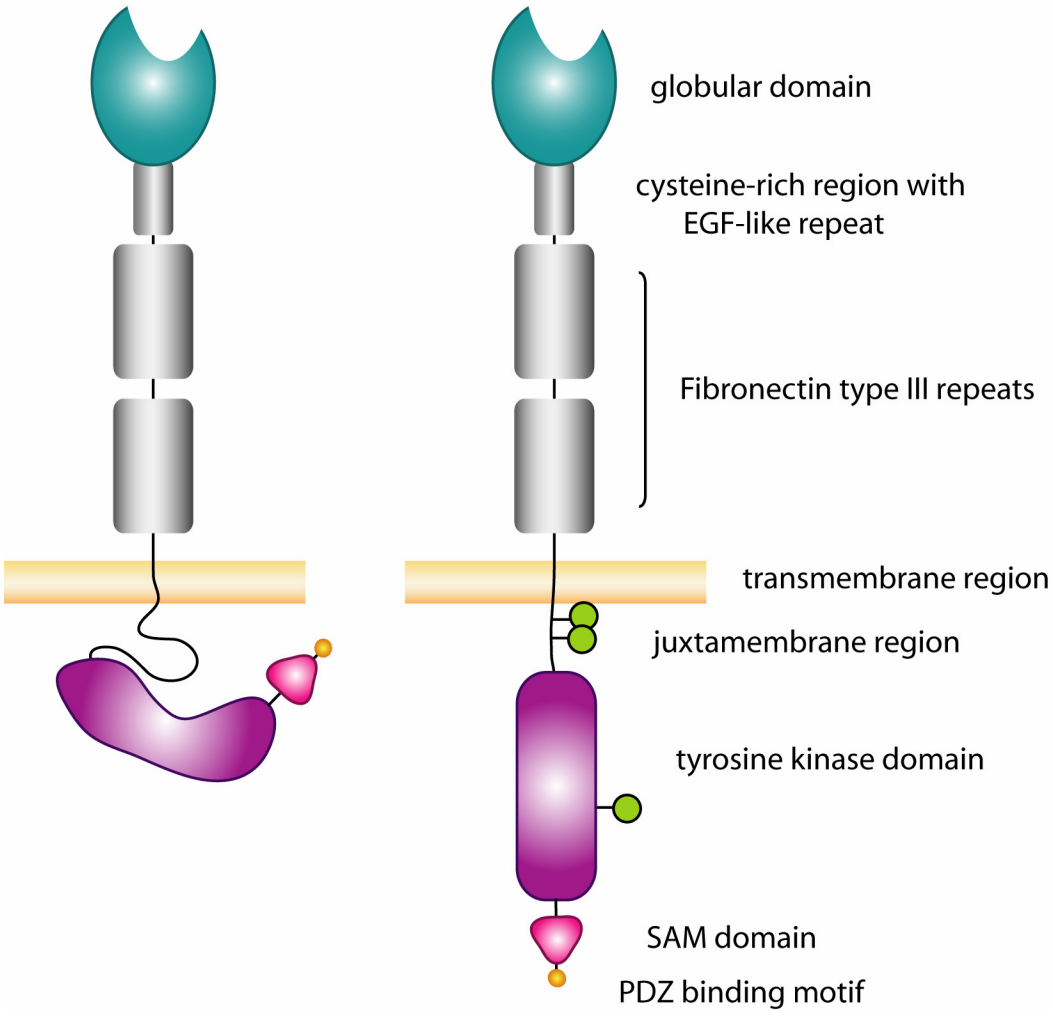

Figure 1 Schematic representation of the Eph receptor structure

The Eph receptor structure shown in its inactive conformation on the left side where the kinase activity is auto-inhibited by interaction with the juxtamembrane (JM) region. On the right side the Eph receptor structure in its active conformation. 2:2 hetero-tetramerisation with ephrin ligands (not depicted) leads to phosphorylation of the two JM tyrosines and thus relieves the auto-inhibition. Phosphate groups in light green. SAM (sterile-α-motif), a protein-protein interaction domain, PDZ (PSD-95, Disc large, ZO [Zona Occludens]-1/2) binding motif, a short stretch of amino acid recognized by PDZ domain containing proteins in a sequence specific manner. Scheme adapted from (Himanen and Nikolov, 2003b)

The ephrins

In vertebrates there are five ephrinA and 3 ephrinB ligands. A-class ephrins are tethered to the membrane by a glycosylphosphatidylinositol (GPI) anchor, while B-class ephrins are transmembrane proteins that contain a cytoplasmic tail with five highly conserved tyrosine residues and a conserved C-terminal PDZ-binding motif (Figure 2) with a consensus sequence of –YKV (Bergemann et al., 1998). As already described for the Eph receptors, intra-class binding is promiscuous but inter-class binding is the exception with ephrinB2 and –B3 being ligands for EphA4 and ephrinA5 which has recently been reported to bind to EphB2 (Himanen et al., 2004). The ephrins do not have any intrinsic catalytic activity but ephrinB ligands can be phosphorylated upon stimulation with EphB receptor (Bruckner et al., 1997; Holland et al., 1996). This can be mediated by src-family kinases (SFK) which are recruited to ephrinB clusters (Palmer et al., 2002).

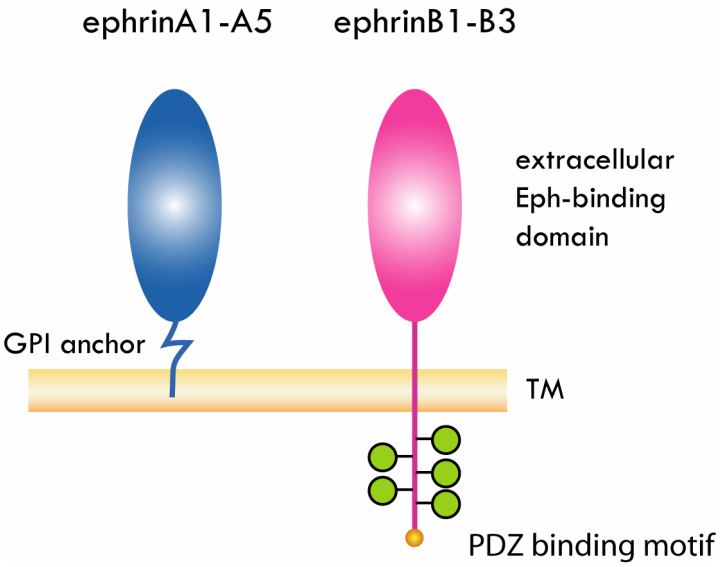

Figure 2 Schematic representation of Ephrin ligand structure

Ephrins are either tethered to the membrane by a GPI anchor (ephrinA1-A5) or have a single membrane-spanning domain (ephrinB1-B3). Both classes bind to Eph receptors via their conserved Eph-binding extra-cellular domains. B class ephrins have a cytoplasmic tail containing five conserved tyrosines that can be phosphorylated (shown as green circles) and a C-terminal PDZ binding motif which provides a docking site for PDZ domain containing adapters. TM (transmembrane domain).

1.1.1 Eph and ephrin signalling

In other receptor-ligand systems, it has been shown that RTK monomers usually dimerise upon binding to their diffusible ligands which leads to trans-autophosphorylation of the receptor monomers and initiation of an intracellular signalling cascade (Schlessinger, 2000). In the case of Eph-ephrin mediated events though, dimerization is not sufficient to elicit physiological signalling. After the initial hetero-di- and hetero-tetramerization, Eph and ephrins form higher-order oligomers and can eventually aggregate into large clusters the size of which might depend on the expression levels of receptor and ligand (Smith et al., 2004). It has been reported by Yancopoulos and colleagues that either membrane attachment or artificial clustering of ephrin ligands is needed to activate Eph receptors (Davis et al., 1994) and vice versa that also receptors need to be pre-clustered in order to achieve ephrinB phosphorylation (Bruckner et al., 1997; Holland et al., 1996). There are low-affinity interactions amongst the ephrins, namely between their extracellular domains and possibly their juxtamembrane cytoplasmic segments, as well as among the Ephs which display homophilic binding with their ephrin-binding domains, cysteine-rich regions and cytoplasmic SAM domains (Himanen and Nikolov, 2003b). In addition to these interactions, PDZ domain containing adapters bound to the cytoplasmic tail of the Eph receptor and/or the ephrinB ligand might help to stabilize the clusters. On the receptor side it has recently been reported that Eph clusters exceed the size of the interacting ephrin surface several fold and that cluster expansion on the membrane of the Eph-expressing cell is independent of ephrin but instead mediated by direct Eph-Eph interactions (Wimmer-Kleikamp et al., 2004).

Forward signalling by Eph receptors

Since signalling by Eph receptors is involved in many different developmental and postnatal processes as well as many different tissues and cell types, this short introduction is by no means trying to give a comprehensive overview. Instead it focuses on general features in the molecular events downstream Eph receptors and some prominent examples of forward signalling in the nervous system. There is a plethora of intracellular signal transducers that have been associated with Eph receptors, some of them identified only through in vitro studies and few of them shown to have biological relevance (Kullander and

Klein, 2002; Pasquale, 2005). For an overview of the Eph receptor interacting molecules see Figure 3.

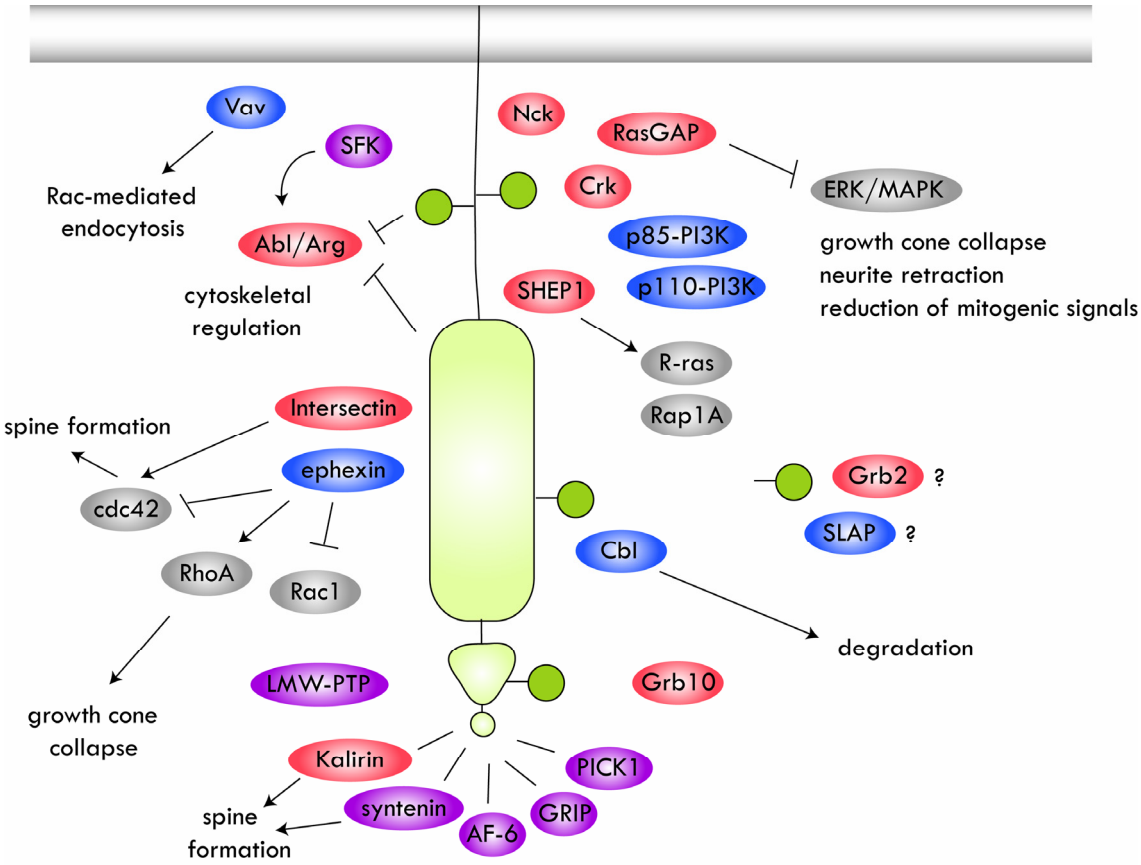

Figure 3 Eph receptor interacting molecules

Proteins so far identified to interact with EphA receptors are depicted in blue, those up to now specific to EphB receptors in red, common interactors for both are shown in purple. Phospho-tyrosines are represented by light green circles, activation of a pathway as arrows, repression by a bar. For simplicity, the interaction (of EphB2) with Syndecan-2 (a cell-surface heparan sulfate proteoglycan) in cultured hippocampal neurons which seems to be involved in positive regulation of spine formation via Intersection/Rac1 and Syntenin/Kalirin (Ethell et al., 2001; Irie and Yamaguchi, 2002; Penzes et al., 2003) is not depicted here.

Abl/Arg (Abelson, Abl-related gene, cytoplasmic tyrosine kinases), AF-6 (afadin-6, tight junction protein and Ras effector), Cbl (Casitas B-lineage lymphoma, an E3 ubiquitin ligase), cdc42 (cell division cycle 42, a Rho-GTPase), Crk (Chicken retroviral kinase, a SH2/SH3 adaptor), Ephexin (Eph-interacting exchange protein, a Rho GEF), ERK (extracellular-signal regulated kinase, a cytoplasmic and nuclear Serine/ Threonine kinase), GAP (GTPase activating protein), GEF (guanine nucleotide exchange factor), Grb (growth-factor receptor-

bound, an SH2/SH3 adaptor), GRIP (glutamate-receptor-interacting protein, a seven PDZ domain scaffolding molecule), LMW-PTP (low-molecular-weight protein tyrosine phosphatase), MAPK (mitogen-activated protein kinase), Nck (non-catalytic region of tyrosine kinase adaptor protein 1, an SH2/SH3 adaptor), PI3K (Phosphatidylinositol3-kinase), PICK (protein interacting with C kinase, PDZ domain containing adaptor), Rac1 (Ras-related C3 botulinum toxin substrate 1, a Rho GTPase), RhoA (Ras homologue A, a cytoplasmic GTPase, a Rho GTPase), SFK (src-family kinases, cytoplasmic tyrosine kinases), SH2 (src-homology2), SHEP1 (SH2-domain-containing Eph receptor-binding protein 1, a Ras GEF), SLAP (src-like adaptor protein), Vav (Vav oncogene, exchange factor for Rho-family GTPases), scheme adapted from (Kullander and Klein, 2002; Pasquale, 2005)

Ligand stimulation by ephrins leads to autophosphorylation of the two juxtamembrane (JM) tyrosines in the Eph receptor which is critical for activation of the protein tyrosine kinase domain (Binns et al., 2000; Kullander et al., 2001a; Zisch et al., 2000). As depicted in Figure 1, phosphorylation of the JM tyrosines relieves the auto inhibitory interaction between the JM and the kinase domain. Furthermore, Eph receptors can be phosphorylated on tyrosine by src-family kinases (SFKs) which can also directly bind to the JM tyrosines via their SH2 domains (Ellis et al., 1996; Zisch et al., 1998). Several studies have been performed mutating the two conserved JM tyrosines to address their biological relevance in vitro and in vivo. Kullander and colleagues replaced the JM tyrosines in EphA4 with phenylalanines (EphA4$^{2F/2F}$) (Kullander et al., 2001b), resulting in a kinase-deficient receptor, whereas Egea and co-workers changed them to glutamic acids (EphA4$^{2E/2E}$) resulting in an open-conformation, hyper-active kinase mutant whose basal kinase activity is comparable or even higher than in ligand-activated wt receptor (Egea et al., 2005). In primary cortical cultures derived from EphA4$^{2F/2F}$ homozygous mutant mice, no receptor autophosphorylation can be detected in response to ephrinB3 stimulation and although trans-phosphorylation mediated by EphA4$^{2F/2F}$ can still occur, it is reduced. The signalling capabilities are further compromised in EphA4$^{2F/2F}$ mutants due to the disruption of the SH2 adaptor binding site, since EphA4$^{2F/2F}$ failed to co-precipitate with SH2 domains of known interactors like Src tyrosine kinase or Grb10.

Since both EphA4 kinase dead (EphA4$^{KD/KD}$) mutants as well as EphA4$^{2F/2F}$ but not EphA4$^{2E/2E}$ mice display aberrant recrossing of CST fibres at lumbar levels it could be concluded that CST axon guidance depends on a functional but not necessarily a ligand-regulated kinase domain (Egea et al., 2005). Interestingly though, EphA4$^{2E/2E}$ mutants displayed the same defects in thalamocortical projections (of dorsal thalamic axons to the

somatosensory cortex) that had previously been described for EphA4 null mutants (EphA4$^{-/-}$). Similar results can be observed for an EphA4 mutant where the cytoplasmic part has been replaced by GFP (EphA4$^{GFP/GFP}$) constituting a "forward signalling" deficient mutant (Dufour et al., 2003; Egea et al., 2005). This elegantly showed that in some axon path-finding situations during development a fine tuning of kinase activity is required to sense a gradient of ephrin (ephrinA5) ligand for correct (thalamocortical) projections since the constitutive active EphA4$^{2E/2E}$ did not rescue the kinase dead phenotype. An additional possibility that cannot completely be ruled out is that SH2 domain containing interactors of EphA4 are needed which can no longer bind to the Y to F or the Y to E mutants. On the other hand though, correct axon guidance of the CST is affected in kinase dead mutants but rescued in constitutively active mutants, arguing that interpretation of the repulsive cue provided by ephrinB3 at the midline is an all-or-nothing decision (Egea et al., 2005).

In addition to the role that Ephs and ephrins play in guidance of thalamocortical and corticospinal axons, they have been shown to be instructive in the projection of retinal axons to the tectum in chick and the superior colliculus in mammals (for a comprehensive review, see (Lemke and Reber, 2005)). There are gradients of Eph receptors in the retina and ephrins in the tectum that set up the map. EphA3 expression is low in nasal and high in temporal neurons and the corresponding ephrins are ephrin A2 and-A5 whose levels are low in the anterior and high in the posterior tectum. This results in nasal to posterior and temporal to anterior projections due to the repulsive action of the receptors and ligands involved (Cheng et al., 1995; Drescher et al., 1997). This rather simple scheme has become more complex since recent evidence points to a cis-interaction between EphA3 on retinal axons with co-expressed ephrinA5 which might serve as a way of desensitising the axons towards ephrins presented in trans (Carvalho et al., 2006). Dorso-ventral mapping is achieved through high levels of EphB2 and-B3 in the ventral retina axons that project to the dorsal tectum, high in ephrinB1 and exemplifying an attractive/growth promoting action rather than repulsion (Braisted et al., 1997; Hindges et al., 2002; Holash and Pasquale, 1995; Mann et al., 2002) although newer evidence also points to an involvement of ephrinB1 as a repulsive cue (McLaughlin et al., 2003).

Reverse signalling by ephrins

Since the first evidence for "reverse" signalling was found 10 years ago (Bruckner et al., 1997; Holland et al., 1996), an increasing number of studies have concentrated on elucidating the molecular events downstream of ephrins. Combining genetic tools such as knock-ins of signalling incapable receptors or ligands with cell-biological assays has clearly demonstrated the biological relevance of ephrin reverse signalling. Studies about reverse signalling include the role of ephrinBs in dorsal retinal axon pathfinding (Birgbauer et al., 2000), requirement of ephrinB2 cytoplasmic domain in proper vascular development (Adams et al., 2001), a cell-autonomous role of ephrinB1 reverse signalling for neural crest cell migration (Davy et al., 2004), requirement of ephrinB reverse signalling for NMDA-independent mossy fiber LTP (Armstrong et al., 2006), and many others (Cowan et al., 2004; Dravis et al., 2004). For a comprehensive overview of reverse signalling, there are several excellent reviews available (Davy and Soriano, 2005; Gauthier and Robbins, 2003; Murai and Pasquale, 2003; Palmer and Klein, 2003).
Although GPI-linked ephrinAs do not contain a cytoplasmic domain, it has been shown in cultured cells that their activation by Eph receptors results in an integrin-dependent adhesion to laminin (Huai and Drescher, 2001) and may involve intracellular kinases such as MAPK and Fyn (Davy et al., 1999; Davy and Robbins, 2000). Furthermore, ephrinAs seem to mediate at least some of the repulsive signalling on the anterior-posterior axis of retino-tectal mapping (Knoll and Drescher, 2002) as well as acting as guidance "receptors" for EphAs on incoming sensory axons in the olfactory system (Cutforth et al., 2003). Frisén and colleagues used mice lacking ephrinA2 to show that EphA7 induces ephrinA2 reverse signaling, which negatively regulates neural progenitor cell proliferation (Holmberg et al., 2005). EphrinA proteins presumably transduce signals by sequestration in raft microdomains and association with transmembrane proteins capable of activating intracellular signalling pathways, although the nature of these postulated ephrinA co-receptors remains to be discovered. Attenuation of ephrinA mediated reverse signalling has been proposed to involve cleavage by the Kuzbanian metalloprotease (Hattori et al., 2000).

EphrinBs, on the other hand, do contain a cytoplasmic domain and considerable effort has been spent to uncover the active roles of the transmembrane ephrins during development and in adult model organisms. The B-class ephrins display a sequence identity of 95% in the last 33 amino acids of their conserved cytoplasmic tail, including five conserved tyrosines, a poly-proline stretch and a C-terminal PDZ binding motif (Figure 2). Among the growing

number of reverse signal transducers, Grb4 has been demonstrated to bind to ephrinB1 in a tyrosine phosphorylation dependent manner via its SH2 domain (Cowan and Henkemeyer, 2001). Furthermore, a group of PDZ domain containing proteins have been shown to interact with ephrinBs, including GRIP (Bruckner et al., 1999), PTP-BL (Palmer et al., 2002), PDZ-RGS3 (Lu et al., 2001), and it has been hypothesized that some of these PDZ proteins take part in assembling higher order clusters. For an overview of ephrinB interactors, please refer to Figure 4.

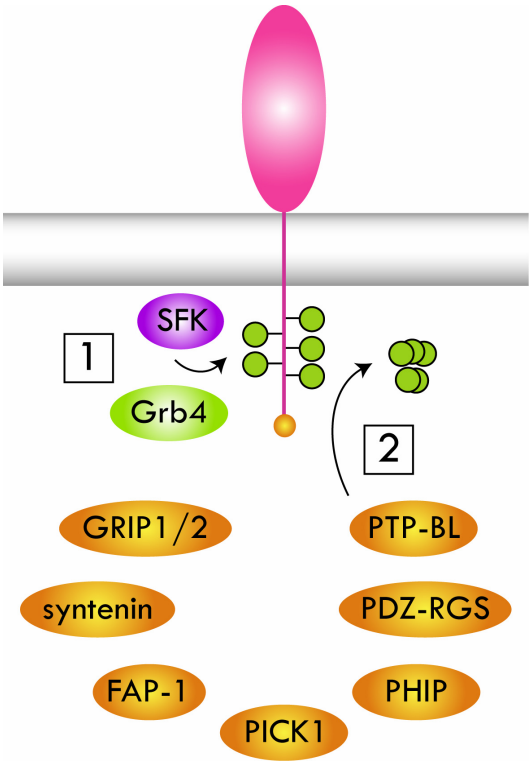

Figure 4 EphrinB reverse signalling

1. *Stimulation and clustering of ephrin by Eph (not depicted) recruit src-family kinases (SFK). Tyrosine phosphorylation by SFKs allows Grb4 to bind via its SH2 domain and link to downstream signalling.*

2. *De-phosphorylation of ephrinB by PTP-BL initiates a switch to PDZ-dependent signalling as proposed by Palmer et al, 2002.*

Phospho-tyrosines represented by green circles, PDZ-binding motif at the very C-term of ephrinB in orange, as are PDZ -interactors.

SFK (src family kinases, cytoplasmic tyrosine kinases), Grb4 (growth-factor receptor-bound 4, a SH2/SH3 adaptor), GRIP1/2 (glutamate receptor interacting protein, a seven PDZ domain scaffolding molecule), Syntenin (a synaptic, membrane-organising molecule), FAP-1 (Fas-associated protein-tyrosine phosphatase 1), PICK1 (protein interacting with C kinase, cytoplasmic adaptor), PHIP (pleckstrin homology domain interacting protein), PDZ-RGS (Regulator of G protein Signaling), PTP-BL (Protein tyrosine phosphatase Burkitts lymphoma).

Similar to the conformational changes undergone by activated Eph receptors, it has also been proposed that upon stimulation, the B-class ephrins succumb to a structural rearrangement induced by tyrosine phosphorylation that serves to recruit interactors (Song, 2003; Song et al., 2002). De-phosphorylation by PTP-BL has been shown by Klein and colleagues and has been speculated to act as a molecular switch mechanism between phospho-tyrosine dependent through SH2 adaptors and PDZ-interactor mediated signalling (Palmer et al., 2002) and Figure 4).

Analysis of the formation of the anterior commissure (AC) in mouse mutants has shown that the ephrinB-expressing commissural axons travel through EphB2 and EphA4 expressing regions. Null mutant mice for receptors and ligands involved in this process all show axon guidance defects. However, a rescue of this misrouting could be demonstrated by knock-ins of a catalytically inactive EphA4 or a C-terminally truncated EphB2. Hence the correct AC formation solely depends on reverse signalling of ephrinBs in the AC axons and in this case, Eph receptors act as "ligands" (Cowan et al., 2004; Kullander et al., 2001b; Orioli et al., 1996).

1.2 Rin1

In my thesis work I have investigated the role of Rin1 (Ras/Rab interactor 1) downstream of Eph receptors. In the following chapter I will review the current knowledge on this protein. Rin1 is cytoplasmic signal transducer composed of several distinct protein domains. The murine Rin1 protein consists of 763 amino acids (aa), including a N-terminal src-homolgy 2 (SH2) domain, followed by a proline-rich region, a conserved 14-3-3 binding motif, a Rab5 guanine nucleotide exchange factor (GEF) domain and a conserved C-terminal Ras association (RA) domain (Figure 5).

Figure 5 Rin1 domain structure

Rin1 consists of a N-terminal (N) src-homology 2 (SH2) domain depicted in blue, multiple poly-proline motives (PxxP) in pink, a conserved 14-3-3 binding motif (a short stretch of aa including p-Serine340) depicted as a light grey bar, a Vps9p-like (Vps9p is a GEF for the yeast ortholog of Rab5, Vps21p) catalytic GEF domain in green and a C-terminal (C) Ras-association (RA) domain in orange

Recent identification of Rin2 (Kimura et al., 2006; Saito et al., 2002) and Rin3 (Kajiho et al., 2003) has made Rin1 only the first of a family of highly similar proteins to be discovered. In a screen for mammalian cDNAs capable of suppressing the $RAS2^{V19}$ phenotype in yeast performed by Wigler and colleagues, Rin1 was originally identified as clone JC99 (Colicelli et al., 1991). $RAS2^{V19}$ is a point mutant of the yeast RAS2 protein, expression of which results in heat shock sensitivity and failure to survive prolonged nutrient survival (Sass et al., 1986; Toda et al., 1985). Further research demonstrated that JC99 can interact directly with human H-Ras protein, hence it was termed Ras interaction/ interference 1, abbreviated Rin1 (Han and Colicelli, 1995), an acronym which is currently listed in NCBI as Ras/Rab interactor 1. The same study also showed that Rin1 interacts most strongly with GTP-bound Ras, whereas it failed to bind to an effector domain mutant of Ras ($H\text{-}Ras^{L35R37}$) and a dominant negative form ($H\text{-}Ras^{A15}$). It directly competes with the known

Ras effector Raf1 in vitro, thus the authors proposed Rin1 as a novel effector or regulator of H-Ras (Figure 6). Research from this laboratory later determined that Rin1 can interfere with transcriptional activation dependent on the Ras-MAPK cascade, that in addition, it interacts with 14-3-3 isoforms epsilon, beta and zeta and that Rin1 binds to and is a substrate for c-ABl (Han et al., 1997). Rin1 is able to rescue BCR-ABL mutants for transformation, a phenomenon which depends on tyrosine phosphorylation of Rin1 and its binding to Abl-SH2 and SH3 domains through its poly-proline motives (Afar et al., 1997), (Figure 6). More recent work revealed that Rin1 is able to induce Abl2 (Arg) catalytic activity, which results in enhanced phosphorylation and thus inhibition of the cytoskeletal regulators CRK (chicken retroviral kinase) and CRKL (Crk-like) and a block of cell migration (Hu et al., 2005).

The focus of Rin1 research however, has become the ability of Rin1 to act as a GEF for the small GTPase Rab5 (for further information about Rab5, please refer to chapter 1.3.1). It had been known previously that activated alleles of Rab5A or Rab5A overexpression can stimulate EGFR internalisation and fluid phase endocytosis (Barbieri et al., 2000) and that also overexpression of Ras can enhance the latter process (Bar-Sagi and Feramisco, 1986). Earlier work had also determined that potentiation of endocytosis by Ras seems to occur upstream of Rab5 (Barbieri et al., 1998), though it had remained unclear how this is achieved. Horazdovsky and colleagues then showed that Rin1 is able to stimulate Rab5 guanine nucleotide exchange, Rab5A dependent endosome fusion and EGFR endocytosis, all of which is potentiated by activated Ras (Tall et al., 2001). Thus, the authors proposed Rin1 as an integrator of cell signalling and endocytosis that physically links the signalling GTPase Ras to the membrane trafficking GTPase Rab5. Further mechanistic insight was provided by a study on the molecular interaction of Rin1 and EGFR. It demonstrated that the SH2 domain of Rin1 mediates direct interaction with the activated, tyrosine-phosphorylated EGFR receptor and that Rin1 was rapidly recruited to the plasma membrane and endosomes upon EGF stimulation (Barbieri et al., 2003).

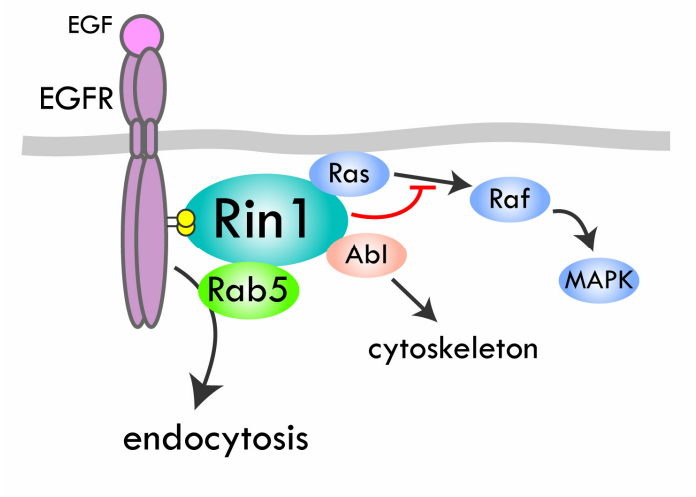

Figure 6 Schematic representation of Rin1 interactions

It has been shown that Rin1 binds via its SH2 domain to the activated EGFR (Epidermal Growth Factor Receptor, phospho-tyrosines as yellow circles), and enhances EGFR endocytosis via activation of Rab5, a feature which is enhanced by concomittant binding of activated Ras (rat sarcoma, GTPase). Rin1competes with Raf (RAF proto-oncogene serine/threonine-protein kinase) for the binding to Ras and thus blocks (or diverts the signalling outcome away from) the canonical Ras-Raf-MAPK (mitogen activated protein kinase) pathway. Rin1 binding to Abl (Abelson kinase) has been shown to affect cytoskeletal regulators Crk and CRKL (chicken retroviral kinase and Crk-like).

Furthermore it was shown that Rin1 can also interact with other RTKs, such as Insulin Receptor (IR), Platelet-Derived Growth Factor Receptor (PDGFR) and Fibroblast Growth Factor Receptor-II (FGFR-II) through its SH2 domain (Barbieri et al., 2003). A recent publication elaborated on the interaction between Rin1 and IR showing that Rin1 can both enhance IR internalisation as well as regulate known IR signal transduction pathways (Hunker et al., 2006b).

The in vivo biological relevance of Rin1 in mice was addressed in a knock-out approach by Colicelli and colleagues (Dhaka et al., 2003). This group described a prominent expression of Rin1 in dendrites of mature forebrain neurons, a place where Rin1 also interacts with endogenous Ras. Rin1$^{-/-}$ mice are viable, fertile and appear to develop normally. When examining plasticity in the adult brain however, they could show elevated amygdala LTP, enhanced fear conditioning and elevated conditioned taste aversion in null mutants compared to wt littermates. Hippocampus-dependent learning and LTP, as well as motor learning, anxiety and exploratory behaviour, on the other hand, were unaffected in knock-out animals (Dhaka et al., 2003).

Rørth and colleagues discovered a homologue of Rin1 in Drosophila in 2001 and called it *sprint*, for SH2, poly-proline containing Ras interactor (Szabo et al., 2001). They described two isoforms, sprint-a and sprint-b with temporally distinct expression patterns suggesting unique functions for the two proteins. The same laboratory recently inplicated Sprint as a

regulator of endocytosis involved in modulating RTK signalling in guided migration (Jekely et al., 2005). Migration of border cells during Drosophila oogenesis is guided by two RTKs, EGFR and PVR (the Drosophila PDGF/VEGF receptor) that respond to their respective oocyte-expressed ligands, Gurken and PVF1 (Duchek and Rorth, 2001; Duchek et al., 2001). It was demonstrated however, that a mere increase in EGFR and PVR signalling did not perturb the correct migration whereas only about 50% of border cells mutant for Cbl (Casitas B-lineage lymphoma) correctly reached their target. This effect was supressed by reducing the amount of the EGFR ligand Gurken and strongly enhanced by overexpression of EGFR and PVR in Cbl mutant background arguing that the Cbl phenotype resulted from excessive misregulated signalling (Jekely et al., 2005). Given the biochemical function of Cbl as an E3 ubiquitin (Ub) ligase involved in endocytosis, downregulation and Ub-mediated degradation of RTKs (Thien and Langdon, 2001), the authors furthermore investigated whether Hrs, an endosome-associated, Ub-binding protein required for degradation of RTKs (Raiborg et al., 2002), would have an effect of border cell migration. Hrs mutant cells showed an accumulation of signalling active EGFR and PVR; in spite of this increase in signalling though, the migration was not significantly impaired, confirming the effect seen in border cells overexpressing EGFR and PVR (Jekely et al., 2005). Since the Cbl phenotype showed incomplete penetrance, the authors investigated the role of Sprint and found that when challenged by overexpression of the relevant RTKs, Sprint mutant border cells displayed significant migration defects. Cells mutant for both Cbl and Sprint rarely reached the oocyte suggesting a synergistic role of the two proteins acting in parallel to regulate the same process. Finally, RTK activity in the migrating border cells was shown to be restricted to the leading edge of the cells (as judged by phospho-tyrosine stainings) where also Sprint localises, an effect that was abolished in Cbl mutants (Jekely et al., 2005). The requirement for Cbl and Sprint suggested that the cellular activity required for signal restriction is RTK endocytosis, which was supported by the result of dominant negative shibire (dynamin) expression which also affected correct migration. Thus in this physiological context of guidance by RTKs, endocytosis serves not to downregulate active receptors but to ensure their correct spatial localisation. Figure 7 shows an explanatory model proposed by the authors that integrates the aforementioned data.

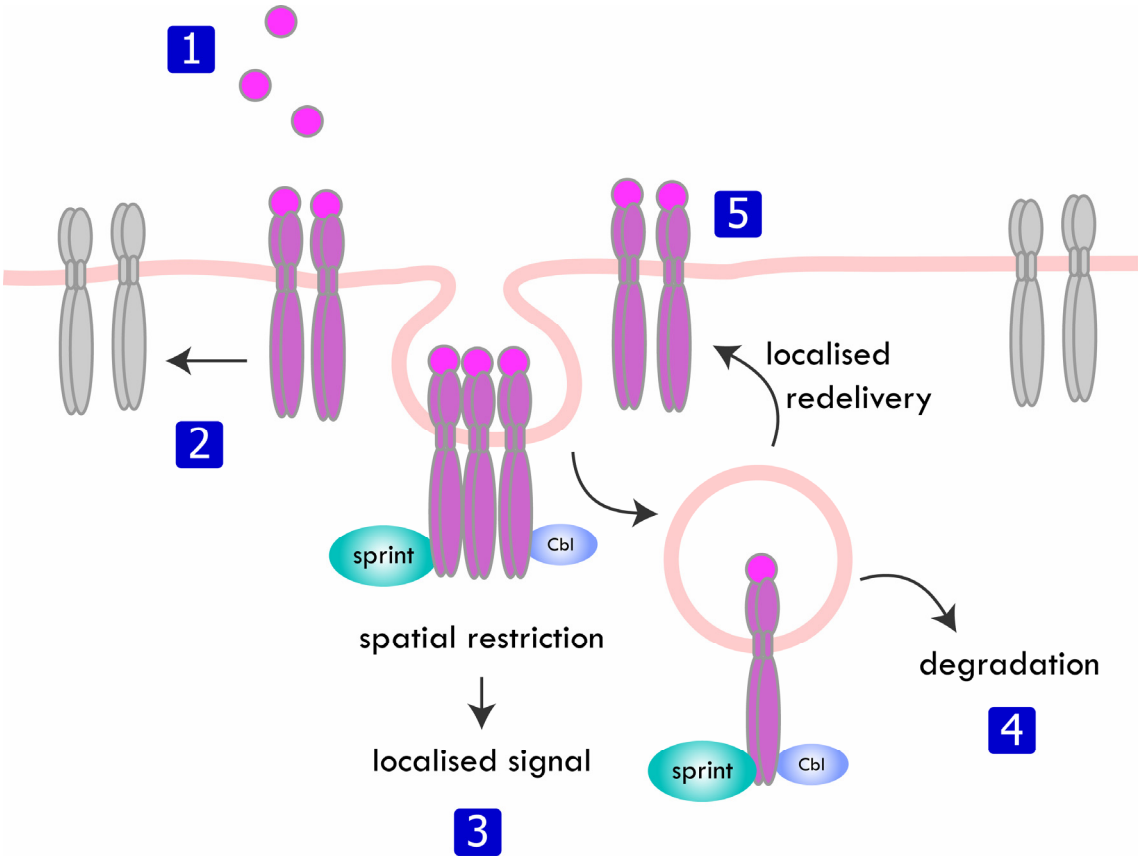

Figure 7 Maintenance of localised EGFR and PVR signalling by Cbl and Sprint in Drosphila border cell migration

1. *The diffusible ligands Gurken and PV1 from the oocyte bind to their respective receptors EGFR and PVR in the migrating border cells and activate them.*

2. *Lateral movement of activated receptors or spreading of RTK activation in the membrane would de-localise the signal as has been described for ErbB1 (Verveer et al., 2000), and thus needs to be prevented for correct guidance.*

3. *Cbl and Sprint could spatially restrict the activated receptors by sequestering them in coated pits which would lead to a localised signalling output at the leading edge of the migrating cells.*

4. *The potential degradation of endocytosed PVR and EGFR does not seem a satisfactory explanation for the phenomena observed as data by Jékely et al. showed that no significantly increased levels of RTK signalling were observed in Cbl or Sprint mutants yet migration was severely perturbed.*

5. *Prior endocytosis of active RTKs proceeds to a local regulated recycling or redelivery leading to in increase in spatially restricted signalling output.*

Inactive RTK are depicted in grey, ligand activated receptors shown in purple. Adapted from Jékely et al., 2005

1.3 Endocytosis

As explained in the previous chapter, one of the most prominent functions of Rin1 is its role in endocytosis as a Rab5 GEF. In the work presented here I studied the role of Rin1 in the endocytosis of EphA4 receptor. Therefore I will point out the basic principles of endocytosis, the most important molecules involved and examples for the biological relevance of endocytosis in the following paragraphs.

Endocytosis (from greek endon meaning within, kytos/cytos meaning hollow vessel = the cell and -osis meaning condition, process or state) is a means by which cells regulate nutrient uptake, plasma membrane composition and signal transduction. However, recent data shows that different endocytic pathways serve to integrate diverse signals, hence contributing to a higher level of cellular organisation (Polo and Di Fiore, 2006). Endocytosis of receptor-ligand complexes was initially thought to serve solely the purpose of attenuating signalling by removing said complexes from the plasma membrane and targeting them for degradation. The cellular machinery however, achieves a high order of regulation by exploiting the compartmentalisation and functional specialisation of the endocytic pathway, going beyond its conventional role in cargo degradation. Endosomes are specialised endocytic organelles that are ideally suited for such regulation as they are organised into a network of physically and biochemically distinct membranous domains, interconnected by a tightly controlled transport system (Gruenberg, 2001; Miaczynska and Zerial, 2002; Pfeffer, 2003; Zerial and McBride, 2001). The dynamic identity and functional diversity of endosomes is driven by finely choreographed mechanisms that rapidly recruit small GTPases, phosphatidylinositol lipids and various secondary effectors to these organelles (Miaczynska et al., 2004). Furthermore they are interconnected with biosynthetic routes and secretory pathways thereby expanding their role beyond endocytic organelles (Perret et al., 2005). The plasma membrane was considered the exclusive location of signalling until Bergeron, Posner and colleagues observed that shortly after ligand addition the majority of activated epidermal growth factor receptors (EGFRs) and their downstream signal transducers such as Shc, Grb2 and mSOS were found on early endosomes instead of the plasma membrane (Di Guglielmo et al., 1994). The same laboratory furthermore suggested that EGFR signalling continues from this compartment (Baass et al., 1995). Subsequent demonstration that nerve growth factor (NGF) was bound to its activated receptor TrkA and phospholipase C-γ1 (PLC-γ1) in endocytic organelles (Grimes et al., 1996) led to the 'signalling endosome' hypothesis. This hypothesis has been further supported recently by two groups investigating the role of retrograde transport of

internalised receptor-ligand complexes in endosomes of sympathetic neurons. Mobley and colleagues could demonstrate that upon nerve growth factor (NGF) treatment of distal neuronal processes, NGF-engaged TrkA, along with activated downstream effectors such as Erk1/2 and Akt, co-localises with Rab5 and EEA1 (early endosome antigen 1) on endosomes in axons and cell bodies (Delcroix et al., 2003). Furthermore, the accumulation of retrogradely transported NGF-TrkA complexes in cell bodies is required for neuronal survival whereas stimulation of the soma with NGF was not sufficient (Riccio et al., 1997; Ye et al., 2003).

It has long been known that there are several different endocytic routes; the biological relevance of this, however, is still poorly understood. Characteristics of the four main routes of endocytosis, namely caveolar/raft mediated endocytosis (CRE), clathrin-mediated endocytosis (CME), phagocytosis (from greek "phagein", to eat) and macropinocytosis (from greek "pinein", to drink) are shown in Figure 8.

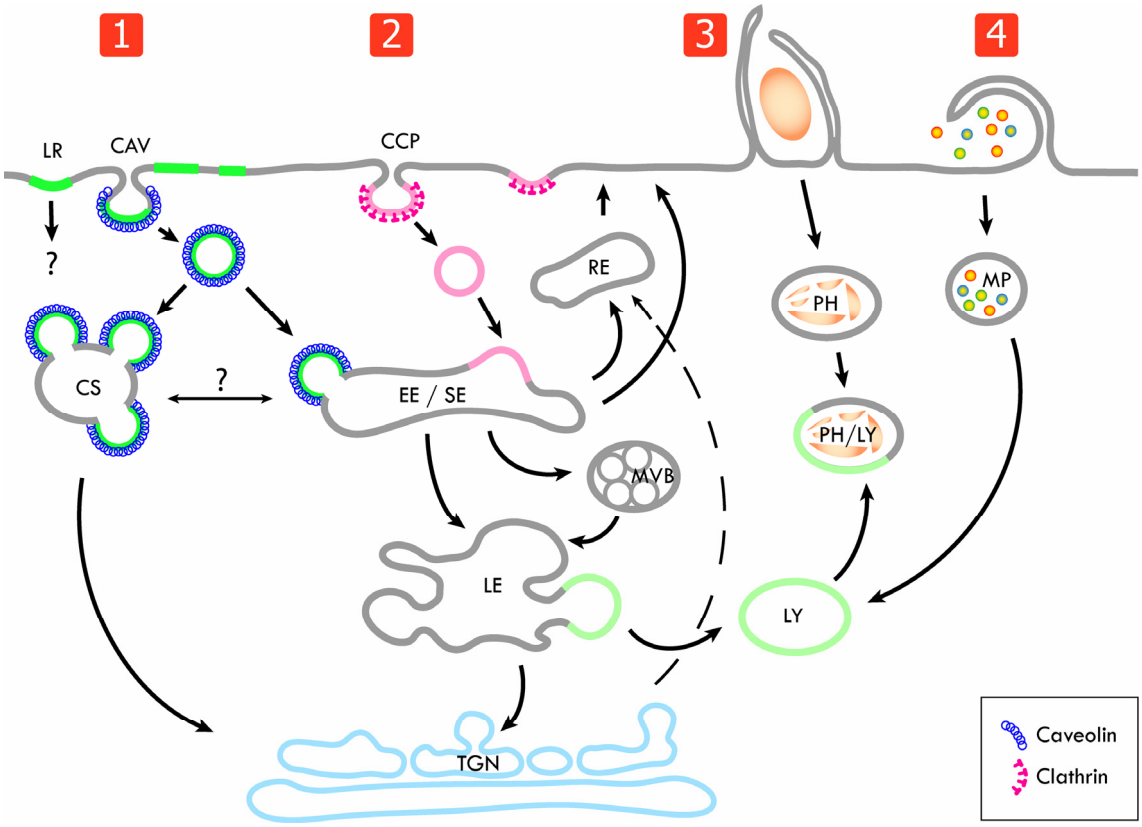

Figure 8 Endocytic routes in eukaryotic cells

1. Caveolar/Raft mediated Endocytosis:

Proteins resident in lipid rafts (LR) like GPI-anchored molecules or membrane receptors recruited to raft microdomains can be internalized in this clathrin-independent pathway. After initial uptake from caveolae (CAV), proteins reach specialised vesicles known as caveosomes

(CS), from which GPI-anchored cargo can traffic to the Golgi complex (trans-Golgi network, TGN). Invaginations are usually characterized by the presence of caveolin1/2 but, in absence of caveolins, internalisation from rafts has also been observed. GPI-linked molecules subject to this clathrin- and caveolin-independent from of endocytosis then traffic to the GPI-anchored protein-enriched early endosomal compartment (GEEC, not depicted in the scheme), from where they can continue to recycling endosomes (RE). Mechanisms regulating this pathway are unclear.

2. Clathrin-Mediated Endocytosis:

Receptor-ligand complexes are internalised to early endosomes (EE) or sorting endosomes (SE), from which they reach either late endosomes (LE), compartments committed to the degradative route to lysosomes (LY), or recycling endosomes (RE), from where they can traffic back to the cell membrane

3. Phagocytosis:

Specialised cells such as macrophages, monocytes and neutrophils clear debris and pathogens by phagocytosis. A rearrangement of the cytoskeleton allows engulfment of the particle. After internalisation, the phagosome (PH) fuses with a lysosome (LY) to form the phago-lysosome (PH/LY) in order to acquire the necessary hydrolytic enzymes for degradation of the cargo.

4. Macropinocytosis:

Stimulation with growth factors or other signals can trigger the actin-driven formation of membrane protrusion that fuse with the plasma membrane to form large endocytic vesicles, known as macropinosomes (MP). These encapsulate large volumes of extracellular fluid and either fuse to lysosomes or recycle back to the cell surface.

EE (early endosome), SE (sorting endosome), LE (late endosome), RE (recycling endosome), MP (macropinosome), CCP (clathrin coated pit), LR (lipid raft), CAV (caveolae), CS (caveosome), PH (phagosome), LY (lysosome), PH/LY (phago-lysosome), TGN (trans-Golgi-network), MVP (multivesicular body) adapted from Miaczynska et al., 2004 and Perret et al., 2005

Clathrin-mediated endocytosis (CME) is the best-studied pathway so far, so named for the clathrin triskelion lattice found on membrane invaginations (Clathrin-coated pit, CCP) and vesicles (clathrin-coated vesicle, CCV) (Bonifacino and Lippincott-Schwartz, 2003; Kirchhausen, 2000). The original concept that CME involves a common mechanism for a variety of receptors has been quickly replaced by a new scenario where different receptors utilize highly individualized endocytic mechanisms. Novel imaging techniques helped reveal the sequential recruitment of accessory and scaffolding proteins (e.g. AP2,

epsin, dynamin, actin and ARP2/3) during CCV formation (Conner and Schmid, 2003; Merrifield, 2004; Rappoport et al., 2004) and receptor-specific requirements for certain molecules of the endocytic machinery have been demonstrated (Motley et al., 2003).

Clathrin-independent forms of endocytosis however, also play important roles. One of these, the **caveolar/ raft endocytosis** (CRE), relies on cholesterol-rich membrane domains, namely lipid rafts and flask-shaped invaginations called caveolae. Although it was initially believed that caveolin, which is found on the caveolae, was an essential structural component in this pathway, it has been demonstrated that a form of lipid-raft endocytosis can occur also in absence of caveolin (Johannes and Lamaze, 2002; Parton, 2003; Sharma et al., 2002). The balance between caveolin-1 and raft lipids influences the rate of caveolar endocytosis (Sharma et al., 2004) and caveolin overexpression can inhibit certain endocytic pathways (Kirkham et al., 2005; Nabi and Le, 2003). Endocytosis from plasma membrane caveolae, which have been shown to be stably anchored by the actin cytoskeleton (Stahlhut and van Deurs, 2000; Thomsen et al., 2002) proceeds to a compartment termed caveosome (Pelkmans and Helenius, 2002) or to the early endosome.

An important insight from recent studies is that the route of entry into the cell may also determine the ultimate fate of the ligand–receptor complex. At low ligand levels, EGFR is internalized as a functional signalling receptor by CME, whereas at high EGF concentrations, EGFR is (mono)-ubiquitinated, after which it is internalized by a lipid raft/caveolar mechanism and subsequently degraded (Chen and De Camilli, 2005; Sigismund et al., 2005). Interestingly, this concept of differential routes affecting functional outcome has also been observed for transforming growth factor-ß receptor (TGF-ß R). Wrana and colleagues could show that internalisation of TGF-ß R via CCPs leads to signal propagation whereas CRE results in signal termination (Di Guglielmo et al., 2003). It has been hypothesised that compartmentalisation, i.e. plasma membrane versus endosomes or CME versus CRE provides an additional means by which cells regulate signalling (Polo and Di Fiore, 2006).

Phosphatidylinositol lipids (PIs) or phosphoinositides are key components of membranes that are distributed along the endocytic pathway in a spatially and temporally restricted manner. As a result of the activities of specific PI kinases and phosphatases, PIs are produced and consumed at regions of high membrane curvature where fusion or fission of vesicles can occur (De Matteis and Godi, 2004). A key role of PIs is to recruit proteins containing PI-binding modules such as the epsin-N-terminal-homology (ENTH) domain,

pleckstrin homology (PH) or PHOX homology (PX) domains and the FYVE motif. Early-endosome antigen 1 (EEA1), for example is recruited to Phosphatidylinositol-3 Phosphate (PtdIns3P) which is highly abundant in and specific to the early endosome membrane via its FYVE domain (Le Roy and Wrana, 2005).

Components of the cytoskeleton, e.g. actin and microtubules, have also been shown to play important roles in endocytosis (Apodaca, 2001; da Costa et al., 2003; Kaksonen et al., 2006) as have cytoskeletal regulators such as Rac (Cowan et al., 2005; Marston et al., 2003). Microtubule-dependent motors function at various stages in the endocytic pathway and dynamic interaction between plus- and minus-end-directed motors influences the steady-state intracellular distribution of endosomes (Fan et al., 2004; Hoepfner et al., 2005).

1.3.1 Rab proteins in endocytosis

Human cells express more than 60 different Rab-GTPases, members of the Ras GTPase family that are involved in transport-vesicle formation, motility, docking and fusion (Pereira-Leal and Seabra, 2001; Pfeffer, 2001; Segev, 2001; Zerial and McBride, 2001). Like all GTPases they shuttle between an active, GTP-bound and an inactive, GDP-bound state. Transition from inactive to active is facilitated by guanine nucleotide exchange factors (GEFs), whereas inactivation is achieved through GTPase-activating proteins (GAPs). Rabs are membrane-associated via their C-terminal prenylations and bind to other membrane-associated proteins there. They are, however, also found in the cytosol, bound to the GDP-dissociation inhibitor GDI (Alory and Balch, 2001). Figure 9 presents a scheme of a few Rab proteins involved in the endocytic pathway. Zerial and colleagues have proposed a model by which Rab proteins act as membrane organizers (Christoforidis et al., 1999b; Sonnichsen et al., 2000; Zerial and McBride, 2001) a concept which shall be exemplified here for Rab5.

Rab5 is regulated by GEFs, such as Rab5-activating protein 6 (RAP6) (Hunker et al., 2006a), Rabex-5 (Horiuchi et al., 1997), Ras/Rab interactor 1 (Rin1, see also chapter 1.2) (Tall et al., 2001), Rin2 and Rin3 (Kajiho et al., 2003; Saito et al., 2002), Alsin (Topp et al., 2004) and GAPs, such as RNtre (Matoskova et al., 1996) . In its active GTP-bound state, Rab5 interacts with a variety of effectors. One of these, the type III PI_3K (hVPS34/p150) is recruited to the Rab5 domain on the early endosome (EE) leading to a local production of

PI_3P in the EE membrane which thus serves as a docking site for Rab effectors that contain a FYVE motif, such as EEA1 (Christoforidis et al., 1999a). In compartments devoid of the type III PI_3K such as clathrin-coated vesicles (CCVs) or the plasma membrane, the FYVE-finger containing Rab5 effectors are not recruited despite the presence of active Rab5 (Rubino et al., 2000). Furthermore, some Rab5 effectors form oligomeric complexes with components of the SNARE machinery, hence the Rab5 domain on EEs seems to be involved mainly in endosome docking and fusion (McBride et al., 1999). The formation of the Rab5 domain depends on the cooperative action of several membrane constituents. In the case of Rab5 and possibly other Rab proteins, the binding of effectors and the presence of exchange factors in the effector complexes (Lippe et al., 2001) may initiate a positive feedback loop that amplifies the recruitment and the activation of the GTPase.

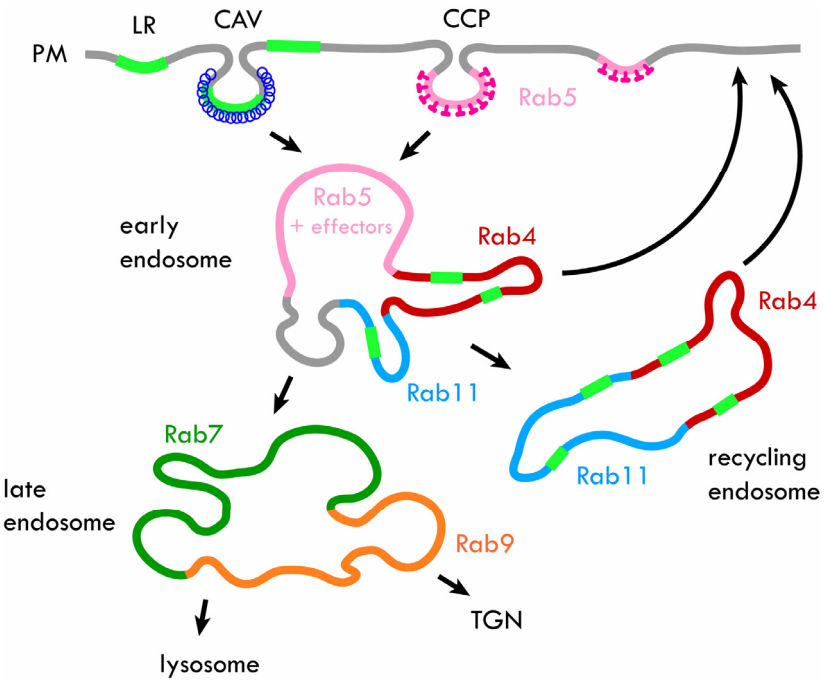

Figure 9 Rab proteins and Rab domains in the endocytic pathway

Intracellular compartments of the endocytic route are characterised by the distinct composition of Rab proteins in their membranes. For details please refer to the text. PM (plasma membrane), LR (lipid raft), CAV (caveloae), CCP (clathrin-coated pit), TGN (trans-Golgi network). Adapted from Miaczynska and Zerial, 2002

The proposal that Rab proteins and their effectors can be restricted to specialized membrane domains received further support from the morphological analysis of the distribution of Rab proteins in early and recycling endosomes (Sonnichsen et al., 2000) (Figure 9). Despite a significant degree of colocalisation within the same organelle,

different Rabs occupy separate areas on the membrane, forming domains that exhibit different pharmacological sensitivity and are in a dynamic equilibrium with each other. Early endosomes appear mainly composed of Rab5 and Rab4 domains, with a smaller proportion of Rab11-positive regions. In contrast, recycling endosomes are enriched in Rab11 and Rab4 domains (Sonnichsen et al., 2000). Several other Rab proteins have also been localized to compartments of the early endocytic pathway, such as Rab15, Rab18, Rab20, Rab22, and Rab25 (Somsel Rodman and Wandinger-Ness, 2000; Zerial and McBride, 2001). Late endosomes are characterized by the presence of Rab7 and Rab9 (Somsel Rodman and Wandinger-Ness, 2000). Rab7 regulates transport between early and late endosomes, whereas Rab9 governs the formation of carriers destined for the TGN (Figure 9).

1.3.2 The biological relevance of endocytosis

Although the phenomenon of endocytosis has been studied for a long time, reports demonstrating its essential contribution during developmental processes in living organisms have only accumulated during recent years. Researchers have tampered with molecules of the endocytic pathway to uncover their important functions *in vivo*.

A number of studies have focussed on the trafficking of the cell adhesion molecule E-cadherin. Eaton and colleagues could show that in Drosophila wing development, the planar cell polarity pathway (PCP) regulates the arrangement of wing epithelial cells by controlling the trafficking of E-cadherin. They found E-cadherin to colocalise with Rab11 in recycling endosomes indicative of its endocytosis and recycling and to accumulate there when a dominant negative form of Rab11 was used. By blocking endocytosis with a temperature sensitive allele of *shibire* (the Drosophila Dynamin homologue), epithelial cell rearrangement was abrogated. The protocadherin Flamingo, which is part of the PCP pathway, is thought to recruit the exocyst component Sec5 to distinct membrane areas to redirect the delivery of E-cadherin. Thus, the authors demonstrated that endocytosis and regulated redelivery of E-cadherin is necessary for the morphological transition undergone by wing disc epithelial cells during metamorphosis (Classen et al., 2005). Similarly, E-cadherin endocytosis was proposed to destabilise certain cell junctions to allow for cell intercalation during Drosophila germband extension, a morphogenetic event in gastrulating embryos during which an epithelial sheet doubles its length and reduces its width by half (Bertet et al., 2004; Lecuit, 2005). Also in Zebrafish gastrulation, E-cadherin endocytosis is

important for the directed migration of mesendodermal cells that lead to the formation of the prechordal plate. *Silberblick*, the Zebrafish wnt11 homologue which is an essential regulator of zebrafish gastrulation (Heisenberg et al., 2000; Ulrich et al., 2003), was recently shown to determine the amount of E-cadherin at the plasma membrane by directing its endocytic trafficking (Ulrich et al., 2005). Interfering with endocytosis by use of a dominant negative form of Dynamin or morpholinos against Rab5 or its GAP, RNtre, resulted in a phenotype which resembles that of *wnt11* mutants, whereas expression of an activated form of Rab5 can rescue the *wnt11* phenotype (Ulrich et al., 2005).

In Drosophila embryos, the distribution of wingless (Wnt-1 homologue) changes from symmetrical to asymmetrical at stage 10 in a regulated fashion (Couso et al., 1993; Sanson et al., 1999). This transition is achieved by endocytosis and lysosomal degradation of wingless at the posterior end of each stripe of its expression domain. This is partly due to the segmental activation of signalling by the EGFR, which accelerates wingless degradation at the posterior end, thus leading to asymmetrical wingless signalling along the anterior-posterior axis (Dubois et al., 2001). Also for Decapentaplegic (Dpp), the Drosophila TGF-ß homologue, it has been shown that endocytosis is integral for generating a gradient in wing imaginal discs (Entchev et al., 2000).

Regulated internalisation has not only been shown to be important for cell adhesion molecules and soluble ligands or morphogens but also for receptor tyrosine kinases. Rørth and colleagues recently demonstrated that Cbl and Sprint, the Drosophila homologue of the Rab5 GEF Rin1, synergistically regulate EGFR and PVR signalling in border cell migration during Drosophila oogenesis (Jekely et al., 2005), an example which is discussed further in chapter 1.2.

1.3.3 Trans-Endocytosis of transmembrane molecules

Endocytosis of protein complexes mediated by trans-interaction of two transmembrane proteins has rarely been documented in the literature (Sorkin and Von Zastrow, 2002). Trans-endocytosis in a unilateral fashion has been described in Drosophila, where the transmembrane ligand Bride of Sevenless (Boss) is internalised via its receptor Sevenless (Sev) into R7 photoreceptor cells (Cagan et al., 1992). Endocytosis of a membrane tethered form of Sonic Hedgehog by its receptor Patched has also been observed, again only in a unidirectional manner (Incardona et al., 2000). One well studied example that bears similarity with the Eph-Ephrin system though is that of the Notch receptor and its ligands,

DSL (for Delta and Serrate from Drosophila and Lag2 from C. elegans; Jagged is the homologue in vertebrates).

The Notch-Delta system

For comprehensive reviews on Notch signalling and Notch in endocytosis please refer to (Le Borgne, 2006; Schweisguth, 2004). Notch is a single-pass transmembrane protein, originally identified in Drosophila that mediates many developmental signalling events, such as lateral inhibition and binary cell fate decisions (Radtke et al., 2005). Signalling by Notch receptor involves three successive cleavages, the last of which is performed by Presenilin and releases the Notch intracellular domain which translocates to the nucleus where it acts as a transcriptional co-activator (Fortini, 2001).

Endocytosis is required for Notch activation in both the receptor-expressing as well as the ligand-expressing cell (Seugnet et al., 1997). Although Dynamin and the ubiquitin ligase Deltex seem to be involved (Hori et al., 2004; Seugnet et al., 1997), endocytosis in the Notch-expressing, signal-receiving cell is not fully understood. Somewhat contradictory results suggest though that Notch endocytosis might also have an inhibitory function. In wt epithelial cells, Notch is endocytosed through a Rab5 -dependent pathway (Lu and Bilder, 2005) and targeted for degradation by the ESCRT complex. However, mutations of the Drosophila homologues of ESCRT-complex members result in accumulation of Notch in endosomes and concomitant overactivation (Moberg et al., 2005; Thompson et al., 2005; Vaccari and Bilder, 2005).

The asymmetric division of Drosophila sensory organ precursors (SOP) has emerged as a successful model for the analysis of Notch signalling in a developmental context. After SOP division, Notch and Delta are present in both daughter cells, but differential regulation of endocytic trafficking ensures that Notch signals in the future pIIa but not the pIIb cell (reviewed in (Emery and Knoblich, 2006)). In the ligand-expressing cell, endocytosis plays an activating role. The ubiquitin ligases Neuralized (Neur) and Mind bomb (Mib) are involved in Delta endocytosis and are required for the ligand to activate Notch on neighbouring cells (Lai et al., 2005; Le Borgne et al., 2005; Wang and Struhl, 2005). Other authors have suggested that Delta needs to be endocytosed and recycled through Rab11 endosomes before it becomes competent to activate Notch (Emery et al., 2005; Wang and Struhl, 2004; Wang and Struhl, 2005). A third way to ensure Notch signalling in the pIIa but not the pIIb cell is achieved through Numb, which after SOP division is specifically

inherited by pIIb. Numb has been shown both to bind to Notch, as well as α-adaptin, an important molecule in early endocytic events (Berdnik et al., 2002). A novel four-transmembrane molecule, Sanpodo (Spdo) has recently been identified as an important regulator of Notch signalling and shown to bind to both Numb and Notch (Hutterer and Knoblich, 2005; O'Connor-Giles and Skeath, 2003). In the pIIb cell and in the presence of Numb, it co-localises with Notch, Rab5 and Rab7 (Hutterer and Knoblich, 2005), indicative of trafficking to the late endosomal, possibly degradative pathway.

Endocytosis of Ephs and ephrins

Despite the fact that Notch and Delta are both transmembrane molecules, can both elicit signalling and are endocytosed in their respective cells, a number of facts still make the Eph-Ephrin system unique. Most importantly, although there is evidence that the Notch extracellular domain can be trans-endocytosed by the delta-expressing cell (Parks et al., 2000), it is not the entire receptor which can be engulfed by the signal-sending cell. Data concerning the endocytosis of Ephs and ephrins has come out of only very few studies (Cowan et al., 2005; Marston et al., 2003; Parker et al., 2004; Zimmer et al., 2003). The EphB2 receptor has recently been linked to clathrin-mediated endocytosis in cultured cells and cultured rat hippocampal neurons. Yamaguchi and colleagues demonstrated that ephrinB2-stimulated EphB2 phosphorylates the phosphatidylinositol 5'-phosphatase synaptojanin 1 and inhibits thus both the interaction with endophilin and the 5'-phosphatase activity of synaptojanin 1 (Irie et al., 2005). They further showed an increase in transferrin uptake in cultured cells as well as GluR1 internalisation in cultured neurons, both of which processes depended on EphB2 kinase activity and Synaptojanin phosphorylation. Even though these results are intriguing they did not elucidate the endocytosis of the Ephs and ephrins themselves.

Greenberg and colleagues demonstrated that during growth cone guidance ephrinA1-mediated activation of EphA4 leads to Vav-dependent endocytosis of the ligand-receptor complex. Vav family proteins are Rho GEFs that induce membrane ruffles and lamellipodia as well as strongly activate Rac family GTPases in mammalian cells (Arthur et al., 2004; Kawakatsu et al., 2005; Liu and Burridge, 2000; Marcoux and Vuori, 2003; Marignani and Carpenter, 2001; Schuebel et al., 1998; Servitja et al., 2003; Tamas et al., 2003). In the absence of Vav proteins, there is no detectable endocytosis of ephrinA1 into Eph-expressing retinal ganglion cells (RGCs) whereas internalisation of transferrin seemed

unaffected (Cowan et al., 2005). They furthermore showed that Vav2/Vav3 double knockout mice display abnormal retinogeniculate projections, indicating an important role for Vav proteins in the formation of the ipsilateral retinogeniculate map, possible due to regulation of ephrin-Eph mediated axon guidance (Cowan et al., 2005).

A few years ago, two groups independently discovered the phenomenon of bi-directional trans-endocytosis in the Eph-ephrin system (Marston et al., 2003; Zimmer et al., 2003). Work from both laboratories proposed the process as an underlying mechanism that mediates repulsion between Eph receptor and ephrin ligand expressing cells. Nobes and colleagues microinjected adjacent rows of fibroblast cells in a confluent culture with EphB4 and its ligand ephrinB2 and analysed their interaction using time-lapse microscopy. Ligand and receptor cells in contact retracted from one another, concomitant with endocytosis of the activated receptor and its bound, full-length ligand into the Eph-expressing cell. Similar results were observed with primary human umbilical vein endothelial cells (HUVECs) that endogenously expressed EphB4 when challenged with ligand expressing cells. Internalisation and retraction were shown to depend on Rac-signalling and elicited actin polymerisation.
EphB4 and ephrinB2 had been shown previously to act as a receptor-ligand pair triggering repulsive cell responses. They are expressed during vascular development in venus and arterial endothelial cells respectively, and are necessary to maintain the boundary between the two types of endothelial cells (Adams and Klein, 2000). Interestingly, Nobes and colleagues could also detect EphB4-positive vesicles in the ligand-expressing cell; this however, was only observed in a small proportion of the examined cases. The trans-endocytosis of EphB4 into ephrinB2 cells could be enhanced by expressing a truncated version lacking the kinase-domain of the receptor from a mean 10% with full-length EphB4 to 37% with the mutant EphB4 (Marston et al., 2003).

Klein and colleagues used fibroblasts expressing the EphB2 receptor or ephrinB1 ligand in cell-cell stimulation assay where the “recipient” cells expressing either the receptor or the ligand were presented with “stimulator” cells seeded on top and expressing the respective counterpart (Zimmer et al., 2003). They could observe both ephrinB1 being internalised as a full-length protein into recipient EphB2 cells as well as the full-length receptor being transferred to recipient ligand-expressing cells. Similar results were obtained by time-lapse imaging of axonal growth cones (of primary cortical neurons) that were challenged with HeLa cells expressing either a fluorescently tagged ephrinB1 or EphB2. Contact by the growth cone resulted in growth cone collapse and retraction concomitant with trans-

endocytosis (Zimmer et al., 2003). To gain insight into the underlying molecular determinants of this process, Klein and colleagues interfered with the cytoplasmic portions of either EphB2 or ephrinB1 and studied ensuing endocytic processes (for an illustration please see Figure 10). When both partners come in contact as full-length proteins, short-term (10 min) trans-endocytosis primarily occurs into the recipient ligand cell, in analogy to "reverse" signalling termed "reverse" endocytosis, after 60 min though ephrinB1 has also been trans-endocytosed to the stimulator EphB2 cell, termed forward endocytosis. Recipient cells expressing a cytoplasmically truncated ephrinB1 (ephrinB1ΔC) were unable to transcytose EphB2 whereas the ephrinB1ΔC was readily transferred to the receptor cell. A truncated receptor was equally incapable of mediating trans-endocytosis and the balance after 60 min was now shifted into the ephrinB1 expressing stimulator cell. Similar results were obtained for a kinase-dead version of EphB2. Figure 10 gives a summary of the bidirectional endocytosis events and subsequent cellular responses obtained with different receptor or ligand mutant proteins.

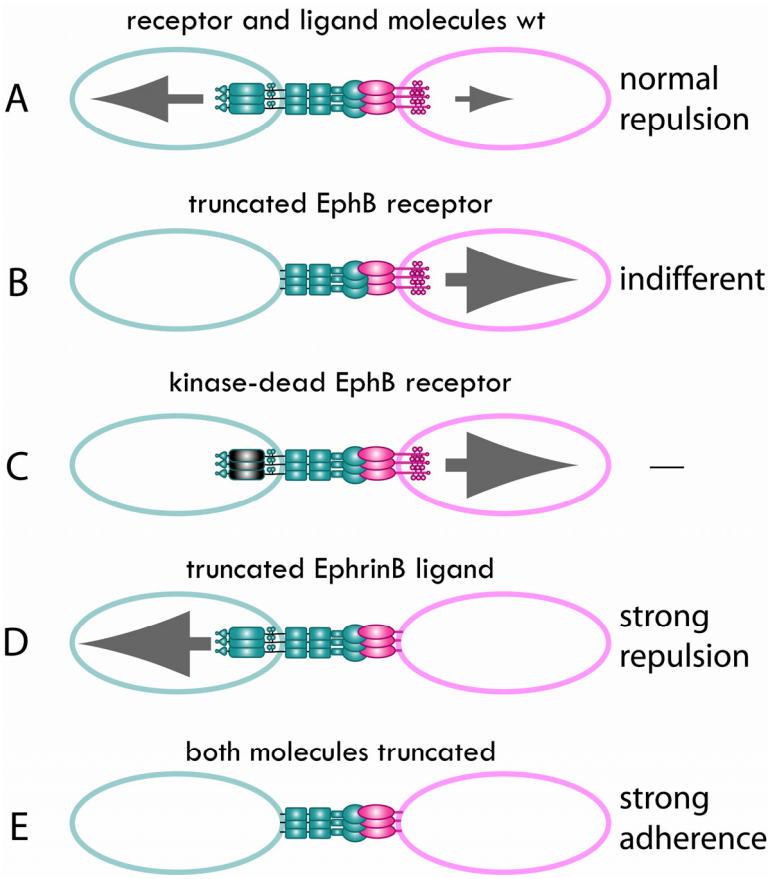

Figure 10 Bidirectional endocytosis of EphB2 receptor and ephrinB1 ligand

*Zimmer et al proposed a "tug-of-war" model for the trans-interaction and ensuing endocytosis of receptor and ligand in which cytoplasmic determinants influence the direction in which the trans-endocytosis occurs. Eph receptor molecules in green, Eph-expressing cells in light green, ephrins depicted in pink, ephrin-expressing cells in light pink; direction of the TE is indicated by arrows, sizes of arrows are indicating the relative strength of the endocytic force of the respective partner cell. (**A**) Wt EphB2 trans-endocytoses wt ephrinB1 more efficiently than vice versa. The cellular response is retraction of the EphB2 cell. (**B**) A cytoplasmically truncated EphB2 receptor cannot endocytose ephrinB1; cells in contact neither show adherence nor repulsion and behave like untransfected controls. (**C**) Like the truncated receptor, a kinase-dead version of EphB2 cannot endocytose ephrinB1. Cellular response was not determined. (**D**) A truncated ephrinB1 was strongly trans-endocytosed into the EphB-expressing cell which responded with an even stronger (than in the case of wt ephrinB1) retraction. (**E**) When both interaction partners are compromised in their signalling capabilities by cytoplasmic truncations, neither side is able to endocytose and cells display strong adherence with prominent fascicles between them.*

1.4 Synaptic Plasticity

Both Rin1 and EphA4 have in implicated in synaptic plasticity (Dhaka et al., 2003; Grunwald et al., 2004), therefore the relevant information on the underlying mechansims and brain regions involved shall be reviewed in this chapter. Neurons are able to change their input-output characteristics as well as alter the morphology of the fine structures with which they are connected, the synapses. These are the underlying mechanisms of plasticity and the basis of all learning processes in the brain. The idea that learning-induced modifications of the connections between neurons establish memory has already been proposed more than 100 years ago (Cajal, 1894; Sherrington, 1906). Neurons are believed to encode memory through activity-dependent changes in the efficacy of their synaptic connections (Bliss and Collingridge, 1993; Martin et al., 2000). Synaptic connections are formed between axonal, pre-synaptic terminals and dendritic, post-synaptic sites (in late embryonic development through postnatal stages), a process which is called synaptogenesis (Constantine-Paton and Cline, 1998). Once formed, a synapse undergoes activity-dependent remodelling (Katz and Shatz, 1996; Nagerl et al., 2004). Presynaptic axon protrusions have been demonstrated to be in contact with long and thin dendrite extensions called filopodia, more mature structures called spines or the shafts of dendrites (Fiala et al., 1998; Miller and Peters, 1981). Filopodia are highly motile structures thought to serve as "probes" that make contact with the axon, and thus implicated in synaptogenesis, and have also been proposed as precursors of mature mushroom-shaped spines (Bonhoeffer and Yuste, 2002; Harris, 1999; Ziv and Smith, 1996).

Spine development is regulated through signals that target rearrangements of the actin cytoskeleton (Bonhoeffer and Yuste, 2002; Matus et al., 2000), such as the EphB2 receptor through activation of the Rho GEFs Kalirin (GEF for Rac1) (Penzes et al., 2003) and Intersectin (GEF for cdc42) (Irie and Yamaguchi, 2002), or by clustering and tyrosine-phosphorylating Syndecan-2 (Ethell et al., 2001), a molecule that had previously been shown to regulate spine maturation (Ethell and Yamaguchi, 1999). Synapses are, through their pre-and post-synaptic changes flexible in both morphology and function and thus make for ideal "gates" that regulate the transmission of information in the brain (Harris and Kater, 1994; Hering and Sheng, 2001; Yuste and Bonhoeffer, 2001). In 1949, Donald Hebb postulated as the cellular basis of learning that simultaneous activation of a pre- and post-synaptic process triggers the reinforcement of the active input and thus strengthens the synaptic contact (Hebb, 1949). However, neuronal plasticity or the changes in efficacy of transmission can either be strengthened or weakened depending on the applied stimulus

(Malenka, 1994). The weakening of a synapse is called Long-Term Depression or LTD and can be elicited by prolonged low-frequency stimulation. The strengthening of synapses though, was demonstrated first by Bliss and Lomo in rabbit hippocampi where they were able to increase basic synaptic transmission for several hours by applying a brief high frequency stimulus (Bliss and Lomo, 1973). Hence, this phenomenon was termed long-term potentiation or LTP. These authors studied the first of the three major excitatory pathways in the hippocampus (Figure 11), the perforant path that connects neurons in the entorhinal cortex with the granule cells in the dentate gyrus (DG). These granule cells in turn send their axons to make connections to pyramidal cells in the CA3 (Cornu ammonis) region, via the mossy fibre pathway. Currently, the Schaffer collateral, which connects the CA3 with the CA1 region, is the place where hippocampal plasticity is most intensely studied.

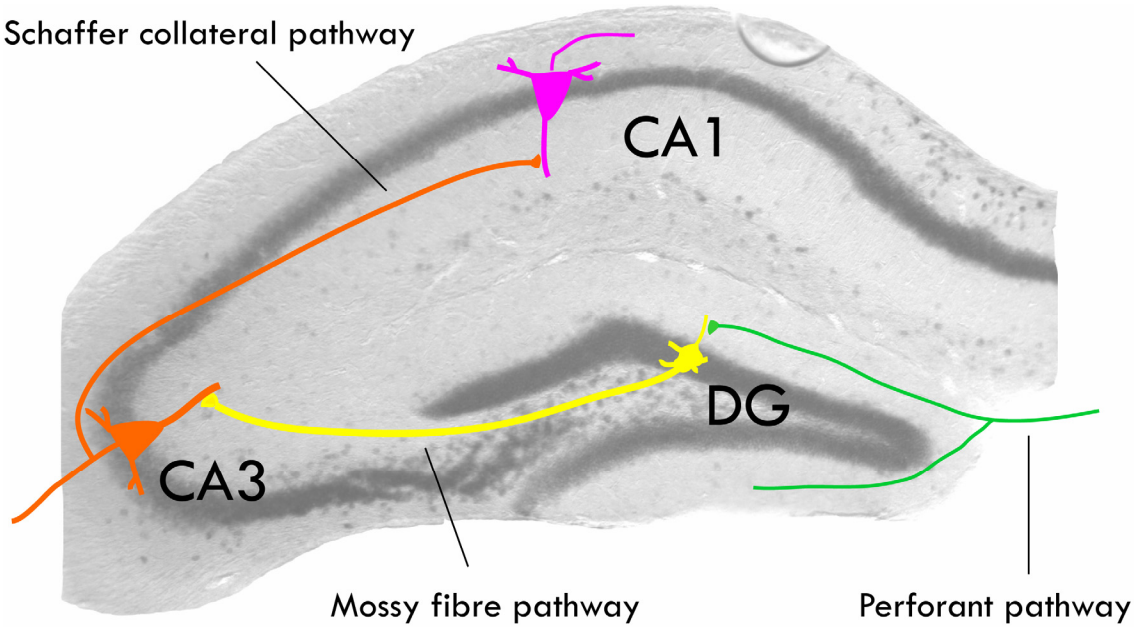

Figure 11 A mouse hippocampal section illustrating the three major pathways

The neurons in the perforant pathway (in green) from the entorhinal cortex synapse on granule cells in the dentate gyrus (DG); the Mossy fibre pathway (in yellow) connects granule cells to pyramidal neurons in the CA3 (Cornu ammonis) region; and CA3 neuron axons (Schaffer collaterals in orange) target CA1 pyramidal cells (in pink)

Eph receptors and ephrins have been shown to be important for LTP and LTD in the hippocampus, therefore i will briefly mention the implication of EphA4 since it is most relevant to this study. Klein and colleagues have shown that at CA3-CA1 synapses, EphA4 only acts as an activating agent for the signalling competent, post-synaptic ephrinBs using

EphA4$^{eGFP/eGFP}$ mutant mice. The EphA4^{eGFP} receptor cannot actively signal itself but nevertheless in these mice both the LTP and LTD defects displayed by EphA4$^{-/-}$ mice were rescued. The authors proceeded to speculate though that the requirement of signalling by either ephrins (reverse signalling) or Ephs (forward signalling) in synaptic plasticity might be specific for each individual pathway (Grunwald et al., 2004).

Although the induction of LTP depends on NMDA receptors, the increase in synaptic efficacy is mainly due to an increase of post-synaptic membrane targeting of AMPA receptors (Hayashi et al., 2000). LTP and LTD, although studied most intensely in the hippocampus, have also been described in other structures in the brain, such as the cortex or the cerebellum (for reviews, please refer to (Malenka and Bear, 2004) and references therein). The amygdala shall be of particular interest for this study.

The amygdala is a subcortical structure in the medial temporal lobe thought to represent an emotional memory system and is essential for fear learning (Fanselow and LeDoux, 1999; LeDoux, 2000; Maren, 2001). It is composed of several nuclei, individual clusters of neurons that are highly interconnected with each other. Figure 12 presents a schematic overview of the amygdala and the pathways underlying fear conditioning. Fear conditioning provides an experimental model that is most commonly used to study fear memory, a learning process that is much simpler and thought to be much older than spatial learning taking place in the hippocampus. During fear conditioning, emotional significance is attached to an initially biologically insignificant conditioned stimulus, e.g. a tone, when such neutral stimulus is paired with an aversive unconditioned stimulus, e.g. a mild foot shock (reviewed in (Dityatev and Bolshakov, 2005)). Projections to the lateral nucleus of the amygdala (LA) from sensory processing areas of the neocortex and the thalamus are involved in coding the emotional significance of sensory stimuli (Rogan and LeDoux, 1996). These sensory-amygdala interactions are best understood for auditory signals. Individual LA neurons are thought to integrate information from both the auditory thalamus and cortex during emotional learning (Li et al., 1996) (LeDoux, 1986). They express both NMDA and AMPA receptors (R) (Farb and Ledoux, 1999), both of which have been shown to be important in vivo for synaptic transmission from afferents onto LA neurons. It was demonstrated by intra- and extracellular recordings and use of inhibitors that NMDA-R and AMPA-R are essential at thalamo-amygdala synapses whereas at cortico-amygdala synapses NMDA receptor blockage did not interfere with synaptic transmission (Li et al., 1996).

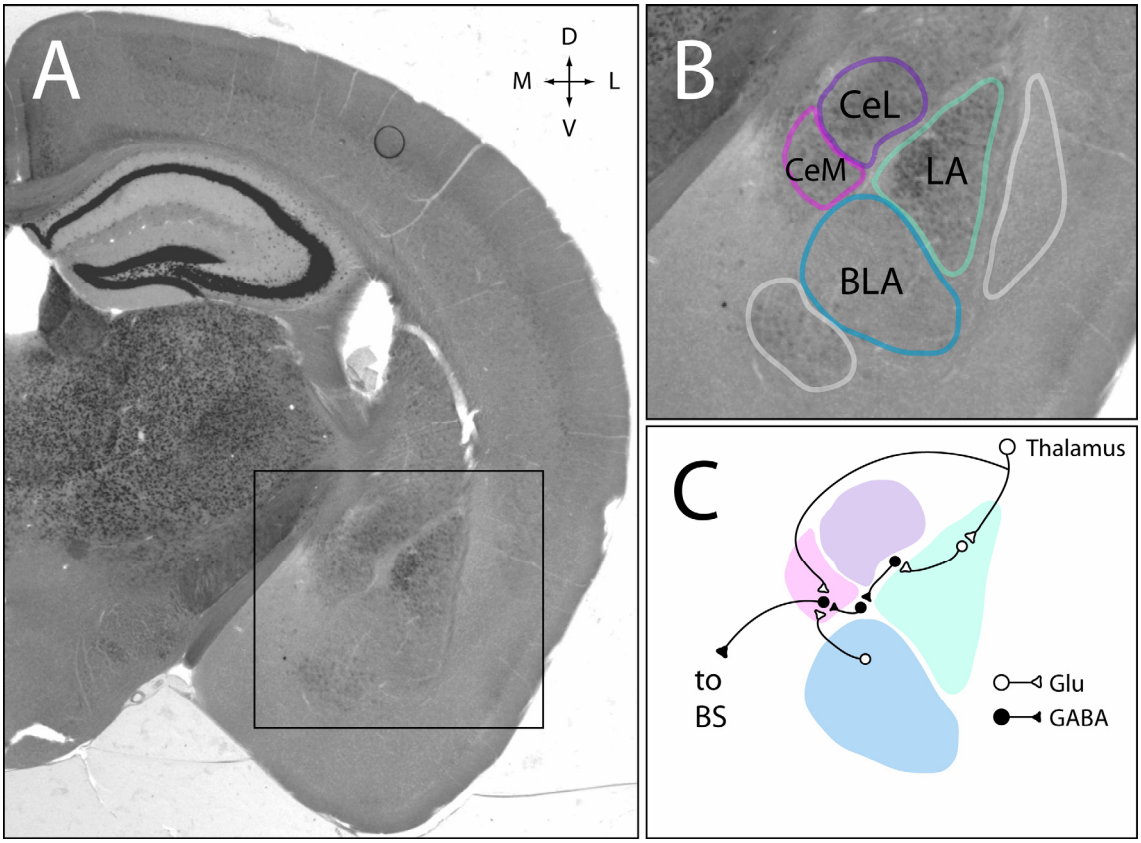

Figure 12 The amygdala and its pathways involved in fear conditioning

*(**A**) Half of a coronal section of an adult mouse brain (in situ for ephA4), boxed area enlarged in B. The orientation of the coronal section is indicated by the cross (D, dorsal; V, ventral; L, lateral; M, medial) Please note that ephA4 expression is particularly high in the LA, see also B. (**B**) Magnification of boxed area in (A). Nuclei of the amygdala are indicated by coloured outlines, (CeL)central nucleus, lateral part, (CeM) central nucleus medial part, (LA) lateral amygdala, (BLA) baso-lateral amygdala. (**C**) Pathways involved in fear conditioning. The LA is currently believed to be the only input station of the amygdala for conditioned stimuli. It is connected to the CeM via intercalated cells positioned between the BLA and the CeM. The CeM is the only significant source of amygdala projections to the brain stem (BS), which in turn mediates the behavioral responses of fear, such as startling and freezing. It has been shown that chemical or electrical excitation of the CeM elicits the behavioral correlates of fear (reviewed in Davis, 2000). Omitted in the scheme are projections from the LA to the BLA, which have been shown to be irrelevant for the acquisition of conditioned fear (Amorapanth et al., 2000; Holahan and White, 2002; Nader et al., 2001) .The BLA projects to all regions in the Central nucleus (CE), not shown. In addition there are projections from the LA to the CeL and from the CeL to the CeM, however, the CeL to CeM projections are GABAergic and would lead to an inhibition of CeM and therefore would decrease rather than augment fear conditioning. There is also direct input in the CeM from the posterior part of the thalamus*

which likely transmits multimodal sensory information. (Glu) Glutamate. Adapted from (Pare et al., 2004).

The analysis of knock-out mice has revealed several molecules that are involved in LTP in the amygdala, such as Ras-GRF or GRF1, a GEF for Ras whose null mutants show reduced amygdala LTP and and impaired memory consolidation in fear conditioning tests (Brambilla et al., 1997) or Rin1, a Rab5-GEF (please also refer to chapter 1.2). Rin1$^{-/-}$ mice in contrast to Ras-GRF$^{-/-}$ show increased amygdala LTP and enhanced fear memory (Dhaka et al., 2003). The authors propose the model shown in Figure 13, wherein Ras signalling is vital for LTP induction, hence Rin1 acting as a negative modulator would prevent Raf from binding to Ras under wt conditions and thereby prevent Ras-Raf-MAPK signalling. This is in accordance with Ras-GRF acting as a positive modulator of Ras-signalling and the respective LTP phenotypes of Rin1$^{-/-}$ and Ras-GRF$^{-/-}$ mice in the amygdala (Brambilla et al., 1997; Dhaka et al., 2003).

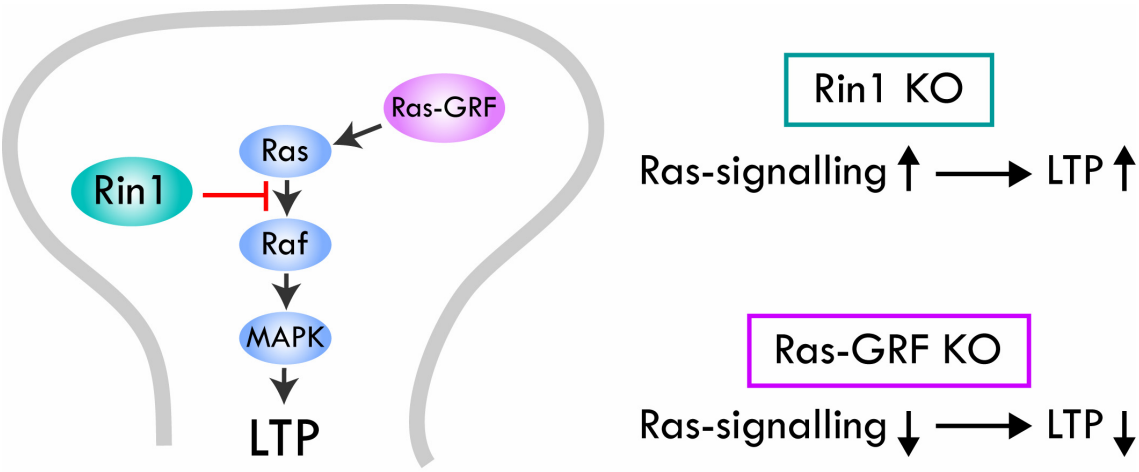

Figure 13 Ras signalling modulation by Rin1 and Ras-GRF in amygdala LTP

(left side) Schematic representation of Ras signalling leading to LTP in the amygdala and its modulation by Rin1 and Ras-GRF. Positive interaction/ induction represented by arrows. Rin1 prevents Raf from binding to Ras, indicated by a red bar.

(right side) Rin1 KO (knock-out) mice show elevated Ras signalling and increased LTP whereas Ras-GRF KO mice display reduced Ras signalling and reduced LTP. Adapted from Dhaka et al, 2003.

1.5 Summary of the thesis project

As outlined in chapter1.2, Rin1 has many interesting properties. It links RTK signalling with endocytosis and the Ras-MAPK pathway. Moreover, Rin1 is almost exclusively expressed in the postnatal brain and there most prominently in regions important for learning and memory, such as the hippocampus and the amygdala. At the start of my thesis work, nothing was known about the function of Rin1 in mature neurons which motivated me to investigate the role of Rin1 with regard to this aspect.

First, I attempted to discover novel interactors of Rin1 using a proteomic approach in a neuronal cell line, as we were convinced that the list of Rin1-binding proteins known until then was far from complete. We succeeded on one hand to purify known interactors of Rin1, such as Ras and on the other hand found a number of novel interactors with intriguing functions in the nervous system or in cellular processes such as endocytosis. Future experiments will be aimed at validating these novel candidates we co-purified with Rin1 and to uncover the role they play in Rin1-mediated events.

The expression pattern of Rin1 in the postnatal brain was strikingly similar to a particular Eph-receptor, EphA4. This prompted me to further investigate a potential relationship between these two molecules. I found Rin1 to be phosphorylated downstream of EphB2 in a neuronal cell line and was able to demonstrate physical interaction between EphA4 and Rin1 in vitro and in synaptic membranes from adult mouse forebrain by co-immunoprecipitations.

Next, I investigated the role of Rin1 in the endocytosis of EphA4 since it was already known that Rin1 plays an important role in early endocytic events in its function as a Rab5GEF (chapter 1.2). Very little mechanistic insight existed about the internalisation of Eph receptors but I was able to show that EphA4 trafficks through endocytic Rab5 compartments in cultured cells and primary neurons. Furthermore, overexpression of Rin1 enhanced the endocytosis of EphA4, a phenomenon that depended on the presence of the catalytic domain of Rin1, as dominant negative mutants of Rin1 blocked the specific, ligand-induced internalisation of EphA4.

Finally, the fact that $Rin1^{-/-}$ mice display an amygdala LTP phenotype, prompted us to investigate whether $EphA4^{-/-}$ mice would show a defect in this aspect as well. We could demonstrate that contrary to Rin1 null mutants, EphA4 knockouts are defective in amygdala LTP. Thus we proposed a model in which reduced endocytosis of EphA4 in amygdala neurons of $Rin1^{-/-}$ mice leads to elevated LTP whereas absence of EphA4 on the other hand would prevent LTP.

2. Results

2.1 TAP purifications

In an attempt to discover novel interactors of Rin1, the Tandem Affinity Purification (TAP) technology was utilized (Rigaut et al., 1999). I generated the Rin1-CtermTAP fusion protein which is schematically outlined in Figure 14.

Figure 14 Schematic representation of the Rin1-cTAP fusion protein

The full-length Rin1 protein was C-terminally fused to the TAP-tag consisting of CBP, the TEV cleavage site and ProtA. Sizes of proteins/ domains not to scale. (N) N-terminus, (C) C-terminus, (CBP) Calmodulin-binding protein, (TEV) tobacco etch virus protease cleavage site (indicated by a yellow star), (ProtA) ProteinA.

The cTAP-fusion protein was expressed in the human neuroblastoma cell line SK-N-BE2 and complexes of Rin1 and interacting proteins were purified from these cells. Purified proteins were identified by mass spectrometry by collaborators at Cellzome, Inc. and analyzed with available databanks online.

Rin1 cells were either not treated (NT) prior to the TAP procedure or treated with vanadate (V). Vanadate is a general phosphatase inhibitor and leads to hyper-phosphorylation on tyrosine residues of cellular proteins since the balance between phosphorylation by kinases and de-phosphorylation by phosphatases is skewed. Vanadate treatment was employed to ensure the stability of possible interactions between phospho-tyrosine and the Rin1 SH2 domain. For a picture of the stained SDS gel please see Figure 15.

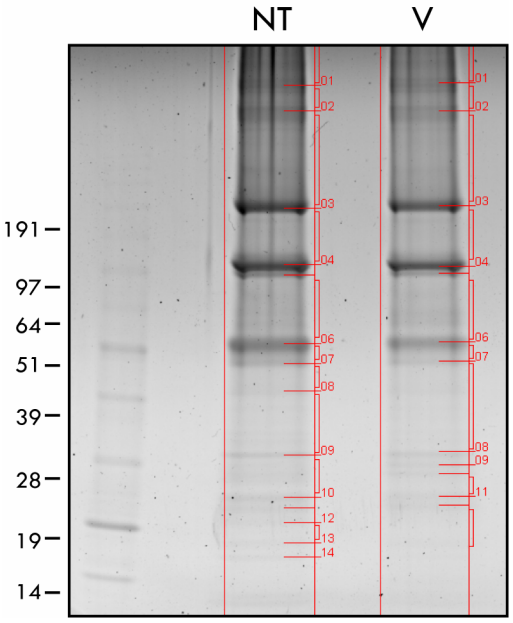

Figure 15

SDS PAGE of Rin1 Tandem Affinity Purification

Coomassie-stained SDS gel with TAP samples from SK-N-BE2-Rin1CtermTAP cells, either untreated (NT) or vanadate-treated (V) and separated by electrophoresis. Indicated in red are the gel fragments that were cut and subjected to mass spectrometry by collaborators at Cellzome, Inc..

Mass spectrometry results were received from Cellzome, Inc. as annotated raw data lists indexing proteins by IPI (International Protein Index) accession number. Descriptions of protein identity and function were obtained from the EMBL-EBI (European Bioinformatics Institute) website by entering the respective IPI number for the protein of interest into the databank search field (http://srs.ebi.ac.uk/srsbin/cgi-bin/wgetz?-page+top) and following the link to the UniProtKB/Swiss-Prot databanks if available to obtain more detailed information. The list presented in Figure 16 shows all interactors purified from SK-N-BE2-Rin1-CtermTAP cells except proteins that have been classified as "sticky" by Cellzome. These proteins have been identified in virtually all complex purifications performed and are therefore most likely unspecific interactors. They have been omitted from the table shown here except for 14-3-3 proteins alpha/beta, zeta/delta and epsilon since they have previously been shown to be interactors of Rin1 (Han et al., 1997; Wang et al., 2002).

Figure 16

Rin1 interactors identified with Tandem Affinity Purification and Mass Spectrometry

For Figure legend please refer to page 42.

accession nr.	description	NT	V
IPI00023064.1	UPF0240 protein C6orf66	x	-
IPI00033598.1	14-3-3 protein gamma, *YWHAG* (psp!)	x	x

IPI00021263.1	14-3-3 protein zeta/delta, *YWHAZ* (psp!)	x	x
IPI00163495.1	14-3-3 protein beta/alpha, *YWHAB*, Protein kinase C (PKC) inhibitor protein-1, KCIP-1 (Cytoplasmic)	x	-
IPI00000816.1	14-3-3 protein epsilon, *YWHAE* (psp!)	x	x
IPI00030286.1	14-3-3 protein eta, *YWHAH* (activates tyrosine and tryptophan hydroxylases in the presence of CAMKII, strongly activates PKC; potential multifunctional regulator of the cell signaling processes mediated by both kinases)	x	x
IPI00018146.1	14-3-3 protein theta, 14-3-3 protein tau, HS1 protein, *YWHAQ* (cytoplasmic, in neurons, axonally transported to the nerve terminals)	x	x
IPI00157362.1	40S RIBOSOMAL PROTEIN S10	x	-
IPI00026593.1	60S ribosomal protein	x	-
IPI00022891.1	ANT1, ADP/ATP translocase 1, SLC25A4 (Catalyzes the exchange of ADP and ATP across the mitochondrial inner membrane)	x	x
IPI00018198.1	Centrosomal protein of 27 kDa, Cep27 protein	x	-
IPI00027839.1	CRH, corticoliberin precursor	x	x
IPI00018289.1	DNA-DIRECTED RNA POLYMERASE II 23 KDA POLYPEPTIDE	x	-
IPI00022018.1	DPM1, Dolichol-phosphate mannosyltransferase (ER)	x	-
IPI00001022.1	FKSG19 (Myofibrillogenesis regulator MR-1), hypothetical protein	x	-
IPI00101627.1	GRP75, HSPA9 (stress-70 protein, mitochondrial precursor (75 kDa glucose regulated protein) (GRP 75) (Peptide-binding protein 74) (PBP74) (Mortalin) (MOT))	x	-
IPI00025512.2	heat-shock protein beta-1 (HspB1)	x	x
IPI00155062.1	heterogeneous nuclear ribonucleoprotein H1, hnRNP H (Part of a ternary complex containing FUBP2, PTBP1, PTBP2)	x	-
IPI00031701.1	hnRNP A1, heterogeneous nuclear ribonucleoprotein A1	-	x
IPI00000006.1	HRas	x	x
IPI00010440.4	HS1-BINDING PROTEIN, HAX1, may function in promoting cell survival, may also associate with cortactin (endocytosis and golgi, scaffold for actin assembly and organisation)/EMS1 in nonlymphoid cells	x	x
IPI00103303.1	hypothetical protein FLJ22555	x	-
IPI00151354.2	hypothetical protein FLJ37183	x	-
IPI00026593.1	hypothetical protein XP_016822	x	-
IPI00089349.1	hypothetical protein XP_088787	x	-
IPI00031821.1	ITM2b, integral membrane protein 2B, Transmembrane protein BRI (may be associated with familial British dementia (FBD) characterized by progressive dementia, spasticity, and cerebellar ataxia)	x	x
P01116	KRas2	x	x

(swissprot)			
IPI00009650.1	LCN1, lipocalin1	x	x
IPI00012369.1	MAD2A, mitotic spindle assembly checkpoint protein (nuclear)	x	x
IPI00008868.1	MAP1B, Microtubule-associated protein 1B (phosphorylated MAP1B may play a role in the cytoskeletal changes that accompany neurite extension)	x	-
IPI00003968.1	NDUFA9, (NADH-ubiquinone oxidoreductase 39 kDa subunit, mitochondrial precursor; transfer of electrons from NADH to the respiratory chain)	x	x
IPI00025796.1	NDUFS3 (NADH-ubiquinone oxidoreductase 30 kDa SU, mitochondrial precursor)	x	x
IPI00142462.3	no entry	x	x
IPI00178653.1	no entry	x	-
IPI00180803.1	no entry	x	-
IPI00000005.1	NRas	x	x
IPI00003174.1	P4HA1, Prolyl 4-hydroxylase alpha-1 subunit precursor (catalyzes the posttranslational formation of 4- hydroxyproline in -Xaa-Pro-Gly- sequences in collagens and other proteins)	x	-
IPI00006052.1	PFDN2, Prefoldin subunit 2 (binds to nascent polypeptide chain and promotes folding in an environment with many competing pathways for nonnative proteins)	x	-
IPI00002567.1	Phosphate carrier protein, mitochondrial precursor (PTP), SLC25A3 (transport of phosphate groups from the cytosol to the mitochondrial matrix)	x	x
IPI00022974.1	PIP, Prolactin-inducible protein precursor (secretory actin-binding protein)	-	x
IPI00002412.1	PPT1, PALMITOYL-PROTEIN THIOESTERASE 1 PRECURSOR (removes thioester-linked fatty acyl groups such as palmitate from modified cysteine residues in proteins or peptides during lysosomal degradation)	x	-
IPI00144171.1	predicted: similar to 60S ribosomal protein L7	x	-
IPI00085960.1	predicted: similar to immunoglobulin binding protein 1(CD79A-BINDING PROTEIN 1, B Cell Signal Transduction molecule alpha 4, ALPHA 4 PROTEIN)	x	-
IPI00052113.3	predicted: similar to POTE2A, similar to FKSG30	x	-
IPI00032183.1	PRO1472, HSP DnaJ	-	x
IPI00028077.1	PSEN1 FAD mutant M146V, presenilin 1, PS1, PS-1, Psnl1 (catalytic subunit of the gamma-secretase complex, an endoprotease complex that catalyzes the intramembrane cleavage of integral membrane proteins such as Notch receptors and APP (beta-amyloid precursor protein), integral membrane protein, Golgi and endoplasmic reticulum, bound to Notch also at the cell surface)	x	-
IPI00016833.1	PSMA2, proteasome subunit alpha type 2	x	-
IPI00000788.1	PSMA5, proteasome subunit alpha type 5	x	-
IPI00024175.1	PSMA7, proteasome subunit alpha type 7	x	-
IPI00000814.1	PSMB5, proteasome subunit beta type	x	-

IPI00023919.4	PSMC5, 26S PROTEASE REGULATORY SUBUNIT 8	-	x
IPI00008527.1	RPLP1, 60S acidic ribosomal protein P1	x	-
IPI00029750.1	RPS24, 40S ribosomal protein S24	x	-
IPI00014458.1	SCO2 protein homolog, mitochondrial precursor (a copper chaperone, transporting copper to the Cu(A) site on the cytochrome c oxidase subunit II (COX2))	x	-
IPI00009693.1	SDHA (succinate dehydrogenase [ubiquinone] flavoprotein SU, mitochondrial precursor)	x	-
IPI00069475.1	similar to 40S ribosomal protein S18	x	-
IPI00060803.1	similar to discoidin I-gamma	x	x
IPI00047765.3	similar to tubulin alpha chain	x	-
IPI00029744.1	SSBP1 (single-stranded DNA-binding protein, mitochondrial precursor (Mt-SSB) (MtSSB) (PWP1-interacting protein 17))	x	-
IPI00017897.2	SSR1, Splice Isoform 1 of Translocon-associated protein alpha SU precursor (TRAP proteins are part of a complex whose function is to bind calcium to the ER membrane and thereby regulate the retention of ER resident proteins)	x	-
IPI00164305.1	stomatin-like2, SLP-2, EPB72-like 2 (peripheral membrane protein and associated with the cytoskeleton, belongs to the band 7/mec-2 family)	x	-
IPI00012795.1	TRIP-1, TGF-beta receptor interacting protein 1, EIF3S2, (binds to the 40S ribosome and promotes the binding of methionyl-tRNAi and mRNA, phosphorylated by TGF-beta type II receptor)	x	-
IPI00027284.2	UQCRC2, Ubiquinol-cytochrome-c reductase complex core protein 2, mitochondrial precursor	x	-
IPI00002646.1	UXT protein,	x	-
IPI00004537.2	ZW10 INTERACTOR, Zwint-1 (nuclear, associated with the kinetochore)	x	-

Figure 16

Rin1 interactors identified with Tandem Affinity Purification and Mass Spectrometry

SK-N-BE2 cells stably expressing TAP-tagged Rin1 were left untreated or treated with vanadate prior to harvesting of cells. Lysates were analysed by mass spectrometry, identified proteins indexed with IPI accession numbers and further information about expression and function was obtained through NCBI databases online. Proteins, previously published to be interactors of Rin1 are highlighted in orange, interesting candidates in the nervous system are highlighted in green. If proteins are known by several aliases, the most common name is listed and alternate names are mentioned additionally. (NT) not treated, (V) vanadate-treated, (psp!) potentially sticky protein.

One of the first known interactors of Rin1 to be identified by Colicelli and colleagues was Ras (Colicelli et al., 1991; Han and Colicelli, 1995). We found all three Ras isoforms, namely Hras (Harvey rat sarcoma virus oncogene), Kras (Kirsten rat sarcoma viral oncogene homolog) and Nras (neuroblastoma ras oncogene) present in our TAP purifications in untreated as well as vanadate-treated conditions. In preliminary experiments, we confirmed the interaction between Rin1 and Nras (Figure 17). GST-pulldowns were performed by Ben Short, PhD using Nras-GST fusion proteins incubated with total forebrain lysate from adult mice as a source of Rin1. We found a strong interaction of Rin1 with the GTP-bound Nras and a concomitant depletion of Rin1 in the lysate after the pulldown. The GDP-bound Nras only precipitated a very small amount of Rin1. Equal amounts of the forebrain lysate used as input in the pulldowns were loaded for comparison. Furthermore, we transiently expressed Nras-Q61L (GTPase-deficient, GTP bound Nras) and Rin1 in HeLa cells and could show co-immunoprecipitations in both directions (data not shown). An enhancement of the Rin1 – Ras interaction due to GTP loading of Ras was already shown previously (Han and Colicelli, 1995)

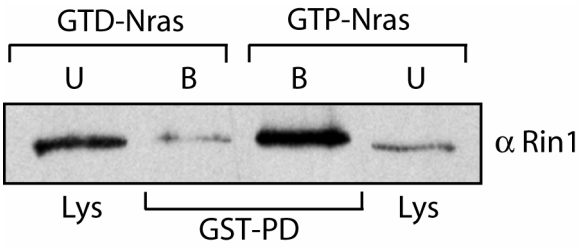

Figure 17 Rin1 interacts with Nras in a GST-pulldown

Constitutive active and inactive forms of Nras-GST fusion proteins, GTP-Nras and GDP-Nras, respectively, were incubated with total forebrain lysate from adult wt mice. Equal amounts of the lysates after the pulldowns were loaded for comparison and show a depletion of Rin1 in the GTP-Nras sample. U: unbound, B: bound, PD: pulldown

2.2 Rin1 expression

2.2.1 Generation and validation of Rin1-specific antibodies

To study Rin1 in neurons and intact brain tissue, we considered the generation of antibodies against mouse Rin1 to be of high priority since the only commercially available antibody was directed against human Rin1 and failed to recognize the murine homologue. I cloned a C-terminally $(His)_6$-tagged expression construct, confirmed induction of protein expression and the functionality of the $(His)_6$-tag. Rodrigo Sanchez in our laboratory performed the large scale antigen purification from bacterial lysates and prepared the serum obtained from the immunised animals. Immunisation of two rabbits (#1203 and #1204) and one goat (#113) were carried out by the in-house facility of the MPI for Biochemistry/ Neurobiology. The antibody from rabbit #1203 yielded the best results hence data shown in this study was obtained with this serum.

To confirm specificity of the polyclonal rabbit anti-Rin1 antibody generated in our laboratory, control experiments were performed. As can be seen in Figure 18, panel A, HeLa cells transiently transfected with Rin1-FL (full-length protein) show a strong cytoplasmic staining when stained with anti-Rin1 as revealed by anti-rabbit*Cy2. A nuclear stain (HOECHST) marks all cells in the field. In the merged images, the presence of additional, untransfected cells can be seen that do not show any Rin1 signal.

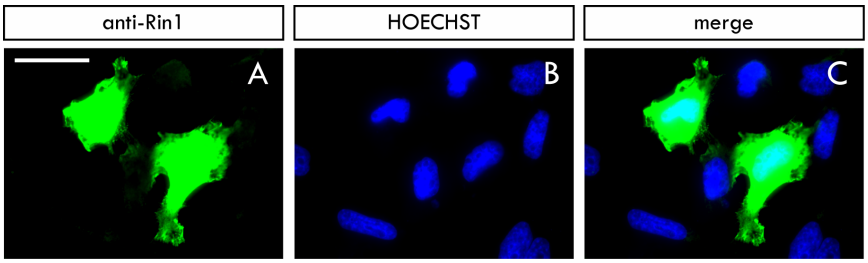

Figure 18 Polyclonal anti-Rin1 antibody detects overexpressed Rin1

HeLa cells were transiently transfected with Rin1-FL and stained for Rin1 (dilution 1:500) in green (A, C). A nuclear stain shows all cells present in the selected field in blue (B, C). Untransfected cells show no staining. Scale bar represents 50µm.

Western blots performed with lysates from wild type adult mouse forebrain show a strong band at approximately 90kDa, which appears weaker in Rin1 heterozygous mice and is completely absent in Rin1 k.o. animals which were kindly provided by the Collicelli laboratory (Figure 19).

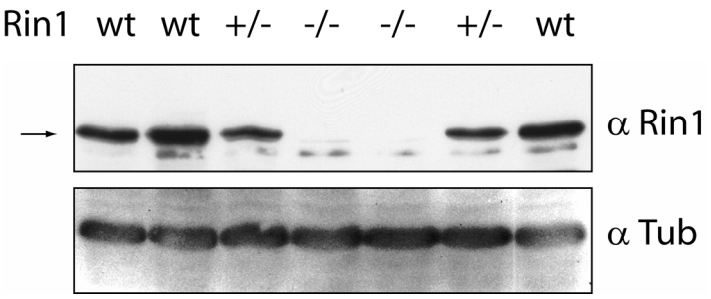

Figure 19 Rin1 expression in adult mouse forebrain

Total lysates from adult mouse forebrains, either Rin1$^{wt/\ wt}$ (lanes 1, 2, 7), Rin1$^{+/-}$ (lanes 3, 6), or Rin1$^{-/-}$ (lanes 4 and 5) were immunoblotted against Rin1. Anti-Tubulin antibody was used as loading control (α Tub), 50μg protein per lane.

Next, the antibody was used on wild type forebrain (cortex and hippocampus) or hippocampal neurons dissected from E18.5 embryos and plated on poly-lysine/laminin coated glass coverslips. Neurons were cultured for different lengths of time (9 days in vitro (DIV), 13 DIV) to monitor Rin1 expression since Rin1 protein was undetectable by western blot at E18.5 (Figure 23). Immunofluorescence stainings were performed using aforementioned rabbit polyclonal Rin1 antibody (#1203) and pre-immunisation serum of the same rabbit at the same dilution as a control (see Figure 20). Images were acquired with equal exposure times to compare staining results. Already at 9 DIV there is a clear difference between the pre-immune serum and the anti-Rin1 antibody staining and Rin1 positive puncta could be observed along neurites in addition to a strong cytoplasmic staining.

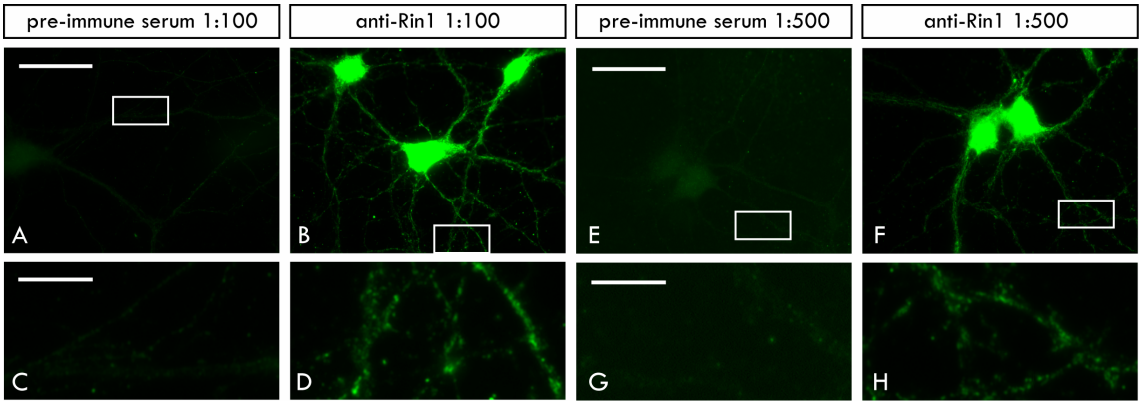

Figure 20 Immunofluorescence staining of cultured forebrain neurons

Mouse forebrain neurons were cultured for 9 DIV (A-D) or 13 DIV (E-H) and stained with a 1:100 (9 DIV) or 1:500 dilution (13 DIV) of either pre-immune serum (A, E) or anti-Rin1 polyclonal antibody (B, F). Higher magnification of boxed areas in A, B, E, F can be seen in C,

D, G and H, respectively. Pictures were acquired with exposure times of 0.5sec (A-D) or 2sec (E-H). Scale bars represent 50µm (A, B, E, F) and 10µm (C, D, G, H).

Pre-immune serum and Rin1 antibody were furthermore applied to coronal sections to localise endogenous Rin1 protein in the adult brain. As can be seen in Figure 21, pre-immune serum showed no detectable staining in CA1 neurons. In contrast, Rin1 antibody showed high levels of Rin1 in cell bodies and dendrites.

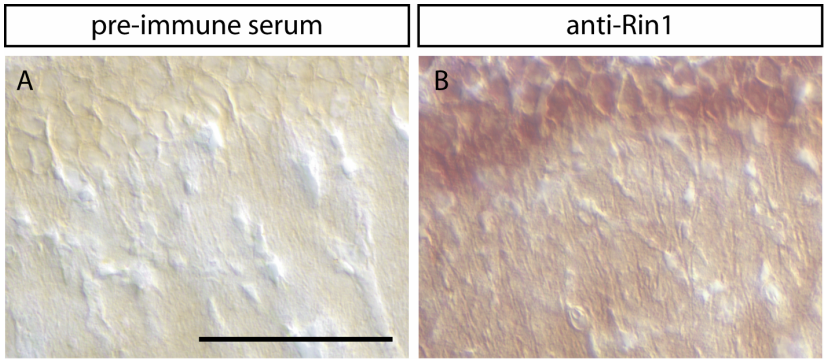

Figure 21 Rin1 expression in CA1 neurons

*(**A**) preimmune serum used as control. (**B**) Staining with anti-Rin1 antibody, both samples processed identically, dilution 1:500, magnification 40x, scale bar 100µm.*

2.2.2 Rin1 expression in primary neurons

In order to address a potential synaptic localisation of Rin1 protein, co-stainings with anti-Synaptophysin and anti-PSD-95 were performed on dissociated cultured hippocampal neurons. Synaptophysin is a 38 kDa transmembrane protein associated with synaptic vesicles often used as a presynaptic marker. PSD-95 (SAP90, Synapse-associated protein 90) is a 95 kDA multi-PDZ domain scaffold molecule associated with the post-synaptic density (PSD) and used as a post-synaptic marker. Rin1 protein, abundantly present in dendritic shafts, can also be found in dendritic protrusions and co-localises partly with PSD-95. Co-staining with PSD-95 was observed as early as 9 DIV (Figure 22, panels A-F) yet PSD-95 immunoreactivity remained relatively faint and clusters observed were much smaller than at later culture time points (data not shown). A more pronounced punctuated pattern of Rin1 localisation could be found along the processes of older neurons in culture (21 DIV) in addition to the strong cytoplasmic signal. Especially clusters of strong Rin1

immunoreactivity showed a striking co-staining with Synaptophysin (see Figure 22, panels G-L).

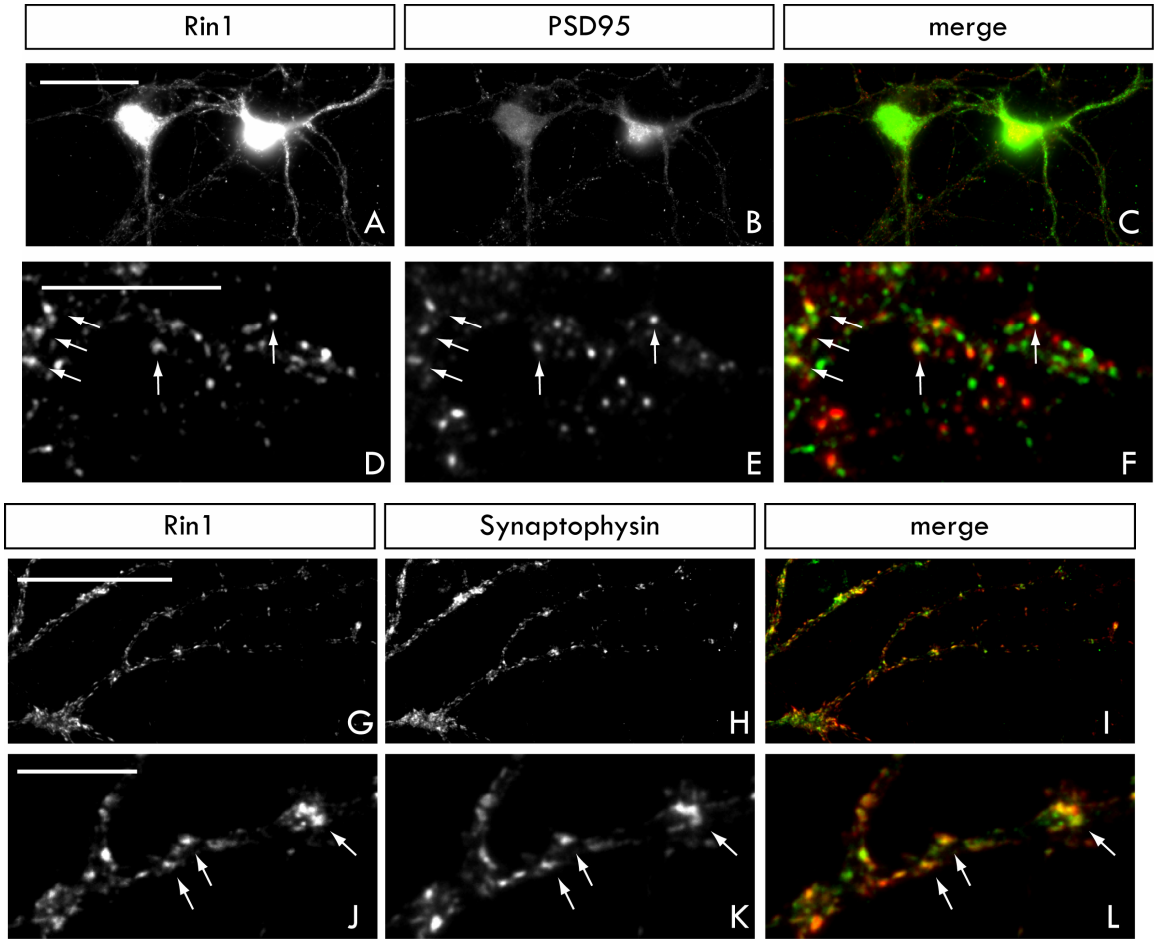

Figure 22 Rin1 protein localisation in cultured hippocampal neurons

Hippocampal neurons (E18.5) were cultured for 9 DIV and stained for Rin1 (green) and PSD-95 (red) (A-F), or 21 DIV and stained for Rin1 (green) and Synaptophysin (red), (G-L). D-F are magnifications of pictures shown in A-C, J-L are magnifications of pictures shown in G-I. Arrows indicate examples of co-localisation of the two respective proteins. Scale bars represent 50μm (A to C and G-I), and 10μm (D-F and J-L).

2.2.3 Rin1 expression in vivo

It has been previously published that rin1 mRNA is undetectable in embryonic brain, expressed at extremely low levels at P0 and is still weak at P6 (Dhaka et al., 2003). These findings were supported by a developmental expression profile I did by Western blot (Figure 23). Forebrain lysates of mice ranging in age from E13.5 (lysate from whole head)

to adult showed no Rin1 expression before P6. Rin1 knock-out forebrain lysate revealed no signal at the expected size (97kDa). EphA4 expression increases only slightly during development whereas the presynaptic marker Synaptophysin is virtually undetectable before E13.5 but shows a marked increase in expression over time paralleling the establishment of synapses.

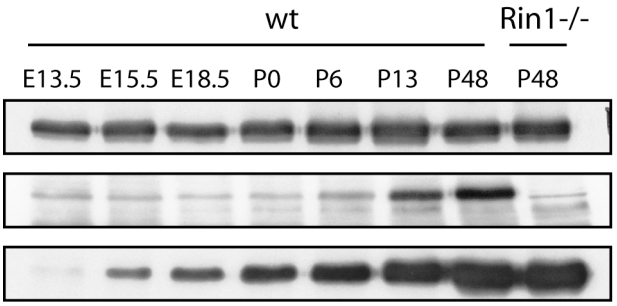

Figure 23 Developmental expression profile of Rin1

Mouse forebrain protein samples (E13.5 –P48) were subjected to immunoblotting with the antibodies indicated

I used immunhistochemistry with anti-Rin1 antibody and in-situ hybridisation to further characterise the expression pattern of Rin1 in the adult brain. Coronal sections of adult mouse brain were stained with anti-Rin1 antibody or subjected to in-situ hybridisation with rin1 antisense probe. As can be seen in Figure 24, panel A, most Rin1-immunoreactive neurons in the cortex were found in layers II-III and layerV; weaker staining could be also observed in other layers. Panel B shows individual neurons at a high magnification, taken from the same section as shown in A. Panels C and D show localisation of Rin1 protein and mRNA, respectively, in the hippocampus. We observed that Rin1 not only localises to cell bodies but also to the apical and basal dendrites, especially in the CA1 region of the hippocampus (see Figure 24, C).

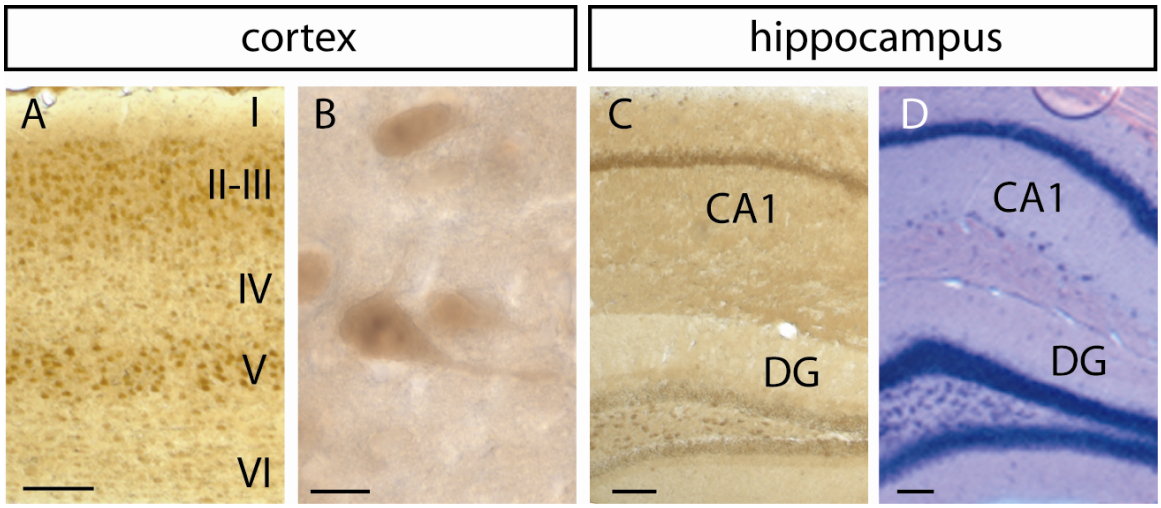

Figure 24 Localisation of Rin1protein (A-C) and mRNA (D) in the adult mouse brain

Coronal sections of adult mouse brain, stained with anti Rin1-antibody (A-C) or subjected to in-situ hybridisation (D) with rin1 antisense probe. Scale bars 100µm in A, C, E, 10µm in B.

I further set out to determine the specific sublocalisation of Rin1 in neurons in vivo, in particular whether Rin1 is present at synapses as suggested by the stainings performed on cultured hippocampal neurons (Figure 22). To address this question, immunofluorescence stainings were performed on adult brain tissue. For technical reasons, the antibody against PSD-95 could not be used for stainings on tissue sections. Stacks of confocal images were acquired and analysed for localisation of Rin1-positive puncta with regard to the localisation of Synaptophysin-positive puncta. Visual examination of these stainings showed a remarkable degree of Synaptophysin-Rin1 juxtaposition indicative of an at least partly, postsynaptic localisation of Rin1. Therefore, a quantitative analysis was performed in such a way that all Synaptophysin positive puncta in single optical sections were marked with a mask of circles around the spots of staining and counted. Then this mask was overlaid on the merged double staining of both Rin1 and Synaptophysin and the number of circles that also encompassed a juxtaposed Rin1-positive spot was counted. The average number of Synaptophysin-positive puncta in a 512 by 512 pixel quadrant at 63x magnification was 340, a mean of 133 had a juxtaposed Rin1-immunoreactive spot, which corresponds to 39%. For pictures of the staining and the quantitative analysis, please see Figure 25.

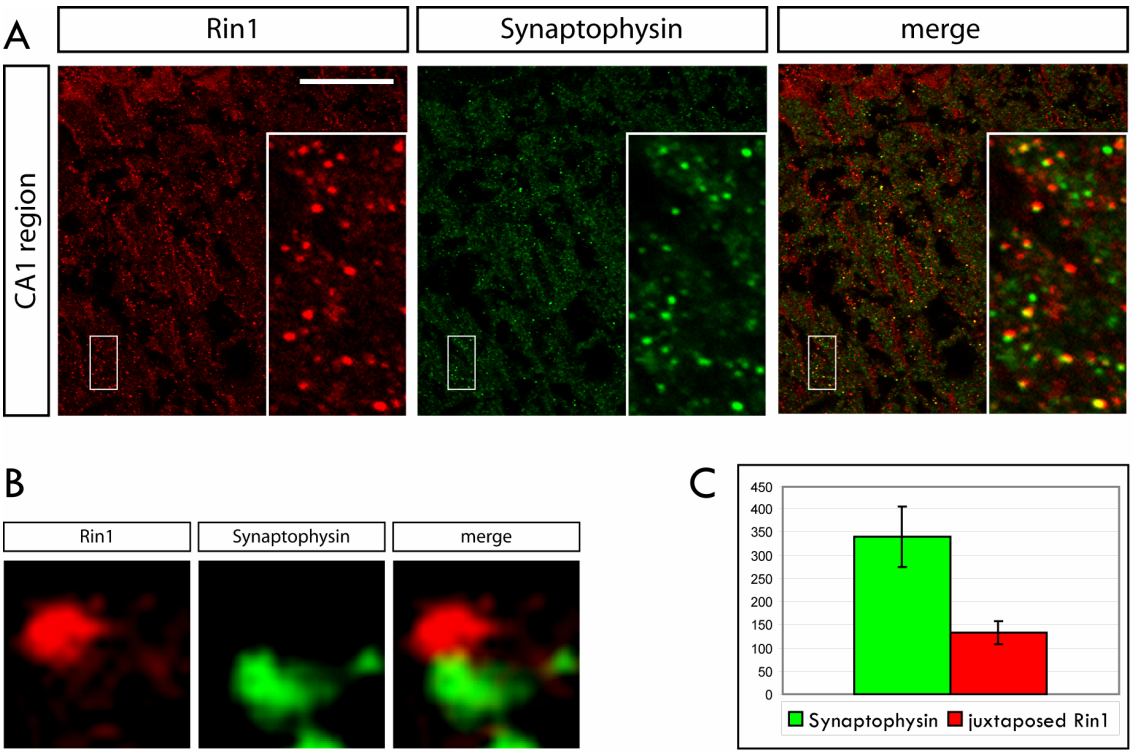

Figure 25 Synaptic localisation of Rin1

*Rin1 staining in red, Synaptophysin staining in green. (**A**) Rin1 localisation at synapses in the CA1 region of the hippocampus. Insets show boxed areas in the single and merged channels at high magnification. Images were acquired at 63x magnification with a confocal microscope.*

*Scale bar 50μm. (**B**) High magnification of a single synaptophysin punctum (left panel, red) and Rin1 punctum (middle panel, green) and the merged image suggesting a synaptic structure. The close juxtaposition of the two puncta is indicative of a partly post-synaptic localisation of Rin1. (**C**) Average number of puncta counted in 512 by 512 pixel fields of single optical confocal planes at 63x magnification. Error bars represent STDEV. On average, 133 of the mean total 340 Synaptophysin puncta had juxtaposed Rin1 puncta (t-test, 1 tailed, 2 sample equal variance: 0,0005) corresponding to 39%.*

2.2.3.1Rin1 and EphA4 – a comparison of expression patterns

When investigating Rin1 distribution in the adult brain, I found striking similarities in the pattern when comparing it to the expression of Eph-receptors, in particular EphA4. I used in-situ hybridisation on coronal slices of adult mouse brain for the comparison. In the hippocampus, both messages were expressed at high levels throughout all regions, namely CA1-CA3 and dentate gyrus (see Figure 26, B and F). In cingulate cortical neurons their expression patterns were nearly indistinguishable (see Figure 26, C and G). In contrast to the findings of Dhaka et al., I detected a strong signal of rin1 mRNA in the thalamus, distributed in a "salt-and-pepper" fashion strongly reminiscent of ephA4 (see Figure 26, D and H). In the amygdala I could observe differences, since ephA4 message was most pronounced in the lateral nucleus (LA) and weak in the basolateral nucleus (BLA) whereas rin1 was detected at more equal levels throughout these nuclei and also detectable in other regions of the amygdala (see Figure 26, A and E and for a scheme of amygdaloid nuclei, please refer to chapter 1.4, Figure 12).

The similarity of expression patterns of rin1 and epha4 were intriguing and prompted me to further investigate the possible functions of Rin1 in postnatal neurons, possibly downstream of Epha4 signalling.

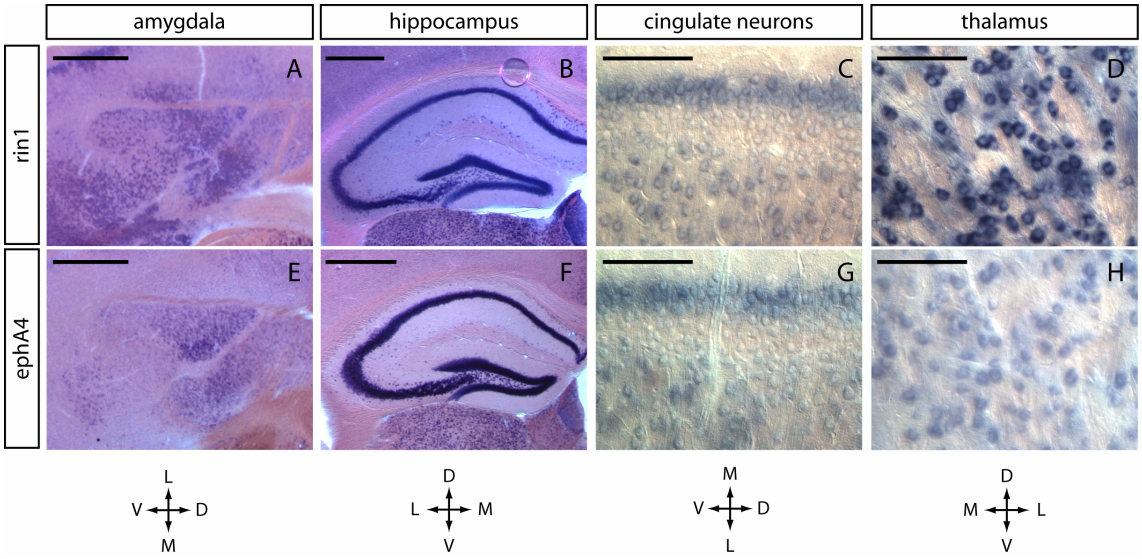

Figure 26 Comparison of rin1 and ephA4 expression in the adult mouse brain

Coronal sections of adult mouse brain were subjected to in-situ hybridisation with rin1 and ephA4 antisense riboprobes. Scale bars equal 500µm in A, B, E and F and 100µm in C, D, G and H. Orientation indicated by crosses. (L) lateral, (D) dorsal, (M) medial, (V) ventral.

2.3 Tyrosine phosphorylation of Rin1

Rin1 was previously shown in non-neuronal and immortalised cells to facilitate transforming growth mediated by BCR/Abl, a process which depended on Rin1 tyrosine-phosphorylation. I therefore asked, if Rin1 could be tyrosine phosphorylated in neuronal cell types in response to neurotrophic factors. As a model system, I employed the human neuroblastoma cell line SK-N-BE2 (for reference see www.atcc.org). I determined the expression of the receptors TrkAand TrkB for nerve growth factor (NGF), Brain-derived neurotrophic factor (BDNF), respectively and the receptor cMet for hepatocyte growth factor (HGF). As can be seen in Figure 27, SK-N-BE2 were tested by Western blot for TrkA and TrkB, which both show moderate expression levels. In addition, high levels of cMet, as well as the human Rin1 were detected.

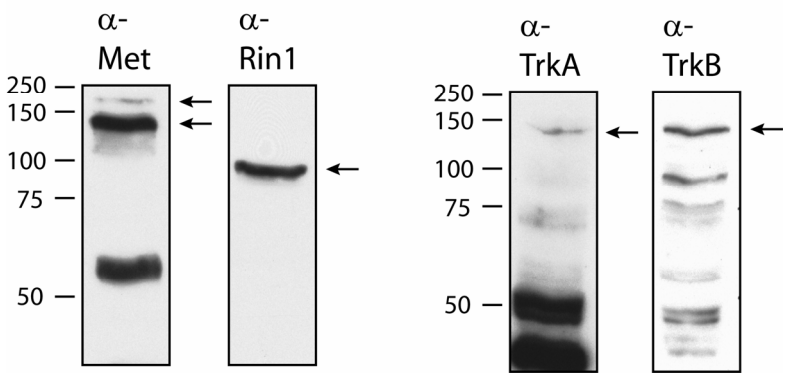

Figure 27 Human neuroblastoma cell line SK-N-BE2

Total protein lysates (50μg/lane) of SK-N-BE2 were immunoblotted against the indicated proteins and found to be expressing cMet, TrkA, TrkB and Rin1.

Starved cells were stimulated with the respective ligands for these RTKs and tyrosine phosphorylation of Rin1 analysed along with MAPK activation to address the different kinetics of pathway activation downstream of the different receptors. The time course of Rin1 phosphorylation downstream TrkA and TrkB after stimulation with NGF and BDNF, respectively, can be seen in Figure 28.

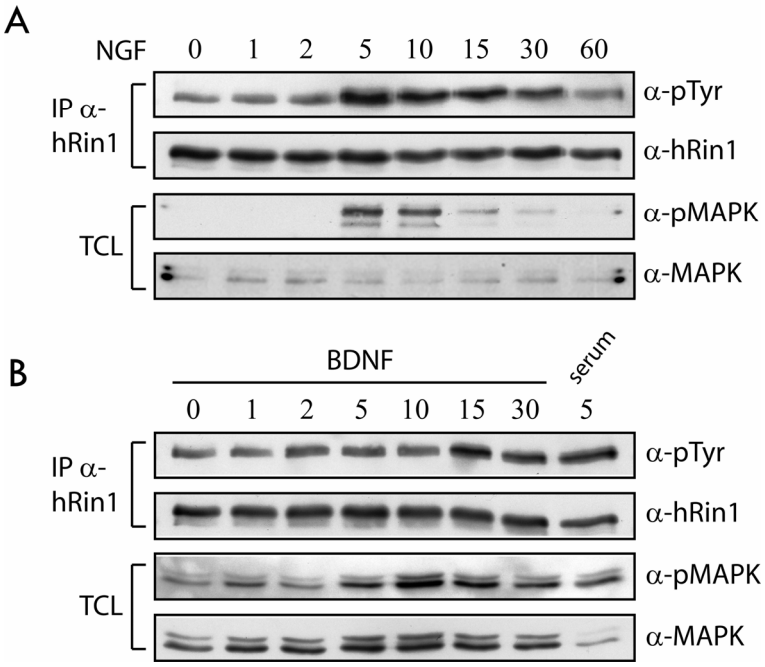

Figure 28 Rin1 tyrosine phosphorylation downstream NGF and BDNF in SK-N-BE2 *SK-N-BE2 were starved for 24h in 0.5% serum, then stimulated with either (A) NGF or (B) BDNF. IP α-Rin1 from 1mg, total lysates (TCL) 50μg per lane. Immunoblots against the indicated proteins. Time course in minutes.*

Rin1 showed a high induction of phosphorylation in response to NGF at the 5 minute time point, in total remained high for 30 minutes and showed a decline back to baseline levels at the 60 minute time point. In SK-N-BE2, MAPK was phosphorylated robustly but very transiently from 5 to 10 minutes after NGF stimulation and decreased to a baseline level after 15 minutes. Rin1 phosphorylation downstream TrkB happened with different kinetics and was comparatively low. A slight elevation of tyrosine phosphorylation of Rin1 could be observed at the two minute time point, and again at 15min but decreased shortly thereafter. In contrast to the NGF stimulation, Rin1 phosphorylation seemed delayed when compared to MAPK activation, which occured transiently between the 5- and 15 minute intervals (Figure 28).

A very different time course was found downstream HGF and its receptor cMet. As can be seen in Figure 29, the onset of Rin1 tyrosine phosphorylation was very rapid (1 minute time point) and maintained for 15 minutes. The kinetics of MAPK activation paralleled that during NGF stimulation.

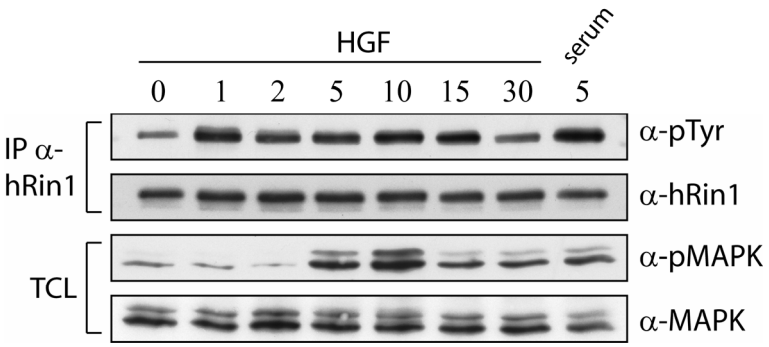

Figure 29 Rin1 phosphorylation downstream cMet
SK-N-BE2 were starved for 24h and stimulated with HGF (time course in minutes) Immunoblot against proteins as indicated

Next, I investigated whether Rin1 becomes tyrosine phosphorylated downstream Eph receptors. Since I wanted to address this question in a system where both the Eph receptor and Rin1 were endogenously expressed I had to resort to looking at another receptor than EphA4. No suitable in vitro system could be found where EphA4 and Rin1 were both expressed and it is known that overexpression of Eph receptors leads to their constitutive activation. SK-N-BE2 strongly express Rin1 (Figure 27) but no EphA4 (data not shown), as assessed both by immunofluorescence staining and Western blot. Therefore we checked for expression of related Eph receptors and found strong levels of EphB2 receptor present in these cells. Results obtained with EphB2 may be of particular interest since this receptor responds to the same group of ligands as EphA4, namely ephrinB2 and B3. I observed a strong but transient phosphorylation of Rin1 on tyrosine residues upon treatment of the cells with pre-clustered ephrinB2. The level of this phosphorylation is similar to that after serum stimulation for 5 minutes, used here as a positive control. Control samples mock-stimulated with pre-clustered Fc show only residual background phosphorylation, present even after starvation of the cells (Figure 30, see also Figure 28, panels A and B and Figure 29). These results suggest that Rin1 can be tyrosine phosphorylated in neuronal cell types and may be a direct substrate of Eph receptors.

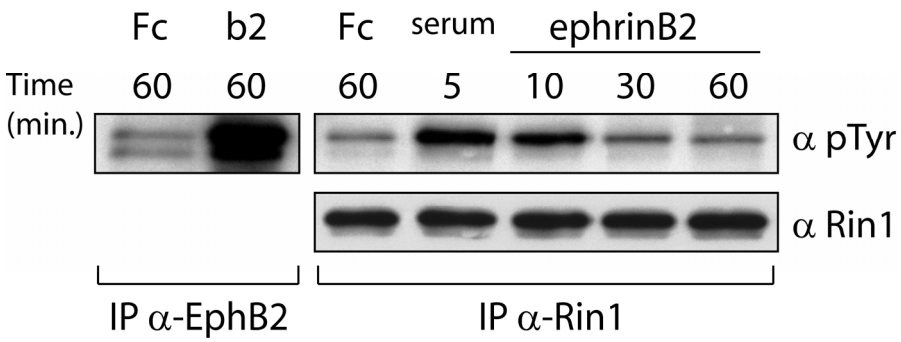

Figure 30 Rin1 tyrosine phosphorylation downstream EphB2 receptor

SK-N-BE2 cells were starved for 24h, then stimulated with either pre-clustered Fc alone (control) or ephrinB2-Fc. Immuno-precipitations and –blots against proteins indicated. IPs from 1mg protein, total lysates 50µg per lane.

2.4 Rin1 interacts with the EphA4 receptor

To determine whether Rin1 and EphA4 Receptor can physically interact in mammalian cells, both proteins were transiently transfected into HeLa cells and co-immunoprecipitations (co-IPs) were performed. Full length Rin1 can be detected in an anti-EphA4 Receptor immunoprecipitation (IP) as shown in Figure 31, A and B whereas controls of receptor-only or Rin1-only samples showed no signal after IP when probed for Rin1. We hypothesised a SH2 domain dependent interaction between Rin1 and EphA4 and therefore created a point mutation in Rin1 (R93E). The arginine at position 93 is part of the highly conserved FLVR motif in SH2 domains and has been shown to be the critical residue to make direct contact with a phosphorylated tyrosine. The mutation to a glutamic acid should abrogate the interaction (Marengere and Pawson, 1992). However, the Rin1-R93E mutant protein co-immunoprecipitated with EphA4 just as well as the wt full length protein (Figure 31, A). In order to confirm that the Rin1 SH2 domain is indeed dispensable for the interaction with the Eph receptor, we tested a Rin1 protein lacking the first 169aa including the SH2 domain (Rin1ΔSH2) in the same assay. As shown in Figure 31, panel B, the Rin1ΔSH2 mutant protein was readily detected in EphA4 IPs at comparable levels to the wt full length Rin1 indicating that the SH2 domain of Rin1 is unnecessary for the interaction with EphA4.

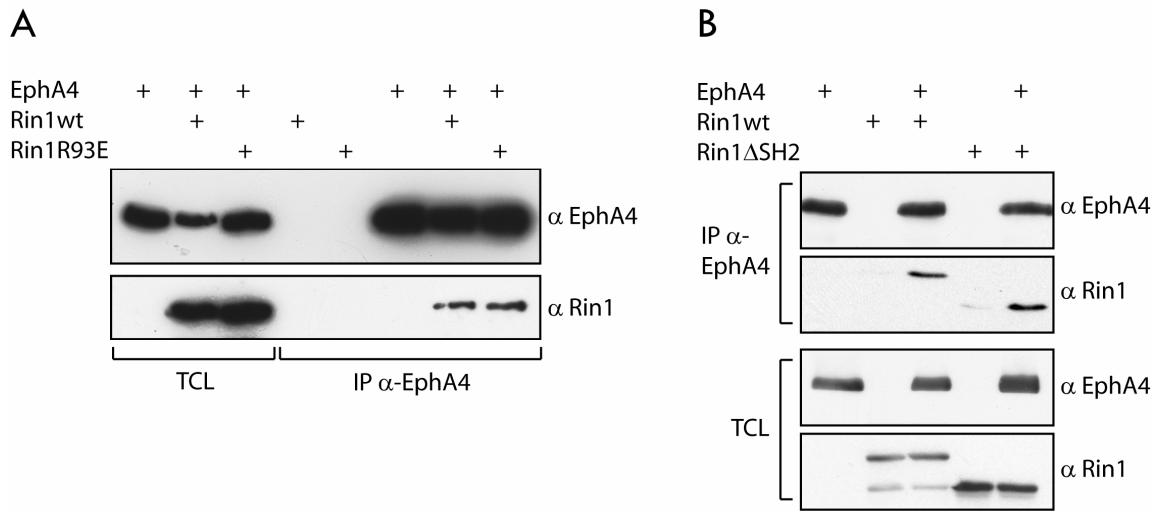

Figure 31 Co-immunoprecipitation of EphA4 and Rin1

(A) Rin1-wt or Rin1-R93E and (B) Rin1-wt or Rin1-ΔSH2 were expressed in HeLa cells together with EphA4. Immunoprecipitations (IP) and immunoblots against proteins indicated. Toyal lysates (TCL) 50 μg per lane, IP from (A) 1mg, (B) 200μg total protein. For a

schematic representation of expression constructs used, please refer to Material and Methods, chapter 4.1.3, Figure 45.

Next, I tested whether I could also observe this interaction in vivo. I tried to co-IP EphA4 and Rin1 from total forebrain lysates of wt adult mice but failed to do so (data not shown). In order to increase the probability of detecting the interaction I prepared synaptosome fractions from adult forebrain. As shown in Figure 32, Rin1 was only slightly enriched in synaptosome fractions when compared to non-synaptosome fractions, whereas PSD95, used as a control for fraction purity was almost exlusively detected in the synaptosome sample.

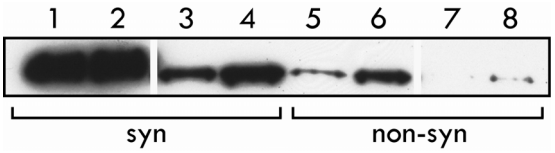

Figure 32 Rin1 is present in synaptosome preparations from adult mouse forebrain

Lanes 1, 3, 5 and 7: 25μg total protein, lanes 2, 4, 6 and 8: 50μg total protein. Syn: synaptosome fraction, non-syn: non-synaptic fraction. Lanes 1, 2, 7, 8 immunoblotted against PSD-95, lanes 3, 4, 5, and 6 immunoblotted against Rin1

I furthermore prepared post-synaptic-density (PSD) fractionations and found Rin1 to be present in PSD fractions, as shown in Figure 33. The distribution of EphA4 Receptor in non-synaptosomal and PSD fractions has previously been determined. EphA4 was shown to be present in all fractions at comparable levels (Grunwald et al., 2004).

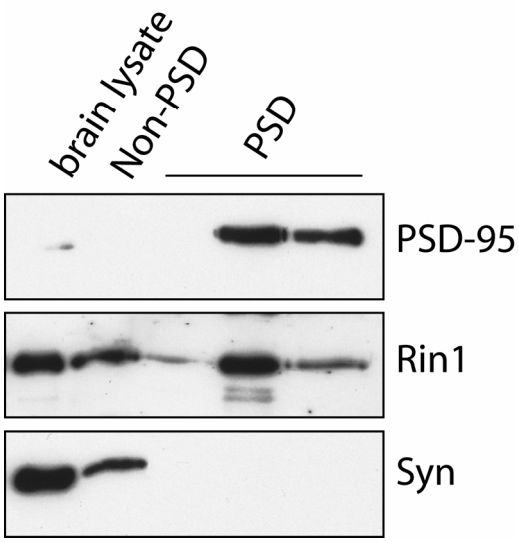

Figure 33 Rin1 is present in PSD fractions prepared from adult mouse forebrain

Total forebrain lysate (10μg), non-PSD and PSD fractions (30μg each) were immunoblotted for the indicated proteins. Syn (Synaptophysin) and PSD-95 are shown as markers of fraction purity. As expected, Synaptophysin is undetectable in PSD fractions, whereas PSD-95 is highly enriched there but hardly detectable in total forebrain lysate.

I immunoprecipitated EphA4 from synaptosomal and non-synaptosomal material prepared from adult mouse forebrain and tested these samples for the presence of Rin1. I found Rin1

to co-immunoprecipitate from the synaptic membrane material but not from a total brain lysate nor the non-synaptosomal fraction (Figure 34), indicative of a specific interaction of the two proteins at synaptic membranes in the adult brain.

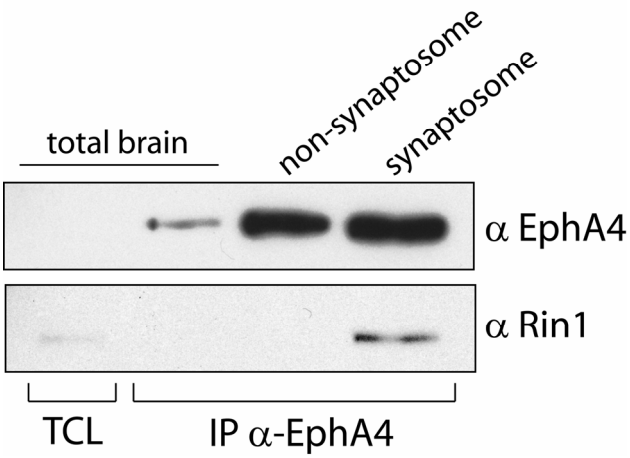

Figure 34 Rin1 interacts with EphA4 in synaptosome fractions

Rin1 was specifically co-immuno-precipitated with EphA4 from synaptic membranes prepared from adult mouse forebrains. IPs of comparable amounts of EphA4 from non-synaptosomal fractions did not reveal the presence of Rin1. TCL: total cell lysate

2.5 Internalised EphA4 trafficks through Rab5 compartments

Since it has been published that Rin1 is a GEF for the small GTPase Rab5 (Tall et al., 2001), which is involved in the early steps of endocytosis (please refer to chapter 1.3 for more information on endocytosis, endosomes and Rab5), we sought to establish whether internalised EphA4 reaches Rab5 endosomes. It has been shown previously that Eph receptors get internalised upon stimulation with soluble pre-clustered ephrin-Fc fusion proteins (Zimmer et al., 2003). The route of endocytosis taken by internalised Ephs and the regulation of this event however, are unknown. As described in chapter 1.3, Figure 8, there are many different pathways that internalised molecules take inside the cell, some of which converge on Rab5-positive endosomes, others that do not. Since several experts on Rab5 agree that stainings for the endogenous molecule cannot be achieved (Marino Zerial, Martha Miaczynska personal communication), I used a constitutively active Rab5-GFP (GFP-Rab5Q79L) fusion protein which allows visualisation of enlarged early endosomes. I transfected HeLa-EphA4 (for details on this line stably expressing EphA4, please see chapter 2.6 and Figure 38) with GFP-Rab5Q79L and found EphA4 to accumulate in Rab5 positive endosomes (Figure 35) after stimulation with ephrinB3-Fc (for details about pre- and post-permeabilisation staining, please refer to the methods section and see chapter 2.6 and Figure 39). Stimulation with Fc alone did not induce endocytosis and no Eph-ephrin complexes were found in Rab5 endosomes (data not shown). To verify that expression of the Rab5 construct did not affect the size of receptor-ligand clusters per se, I performed controls using a GFP-tagged wt Rab5 construct or transfecting only GFP, which gave comparable results (data not shown).

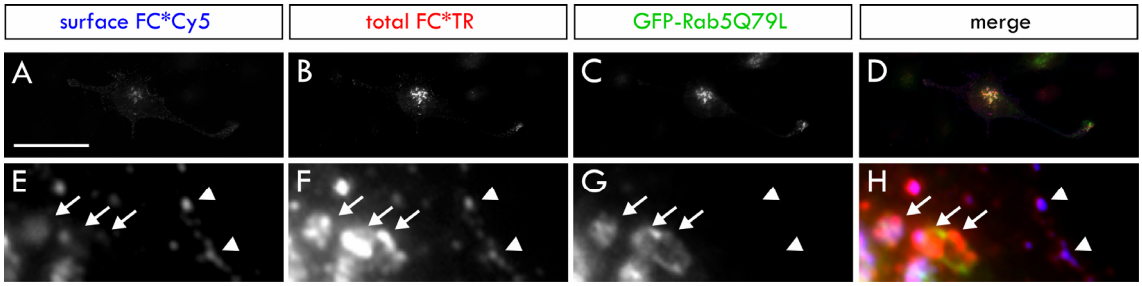

Figure 35 Internalised EphA4 reaches Rab5 compartments in stable HeLa-EphA4 cells

HeLa cells stably expressing EphA4 were transfected with Rab5Q79L and stimulated with pre-clustered ephrinB3-Fc for 30 min. Cells were stained for surface receptor-ligand-complexes with an anti-Fc antibody conjugated to Cy5 (false colour blue in the merged images) and total receptor-ligand-complexes with an anti-Fc antibody conjugated to TexasRed (false colour red). In the merged images, surface receptor clusters appear in purple, indicated by arrowheads. Internalised clusters are stained in red and complexes that have reached Rab5-positive endosomes appear orange, indicated by arrows. Scale bar (A) 50μm

I was interested to see whether endogenous EphA4 would behave the same way. To address this question I used primary cultured hippocampal neurons as a model and could show that they express high levels of EphA4 in the first week in culture. Furthermore I confirmed that when stimulated with ephrinB3-Fc and subsequently stained against Fc and with a specific antibody against EphA4, virtually all clusters detected with the anti-Fc antibody were also positive for EphA4 (data not shown, see also (Egea et al., 2005)). Thus I proceeded to use only the anti-Fc staining to follow clustered EphA4, which in addition only visualises receptor molecules engaged by the ligand. As can be seen in Figure 36, 30 minutes after addition of preclustered ephrinB3-Fc, clustered receptor can be detected on the surface of neurons as well as inside the processes and the soma (panels A, B and magnifications in E and F). Large clusters of internalised receptor ligand complexes co-localised with Rab5 positive endosomes (panels D and H, indicated by arrows). Similar results were observed in glia cells also present in the culture (see panels I to P). Thus I concluded that EphA4 trafficks through Rab5 endosomes after ligand-induced endocytosis.

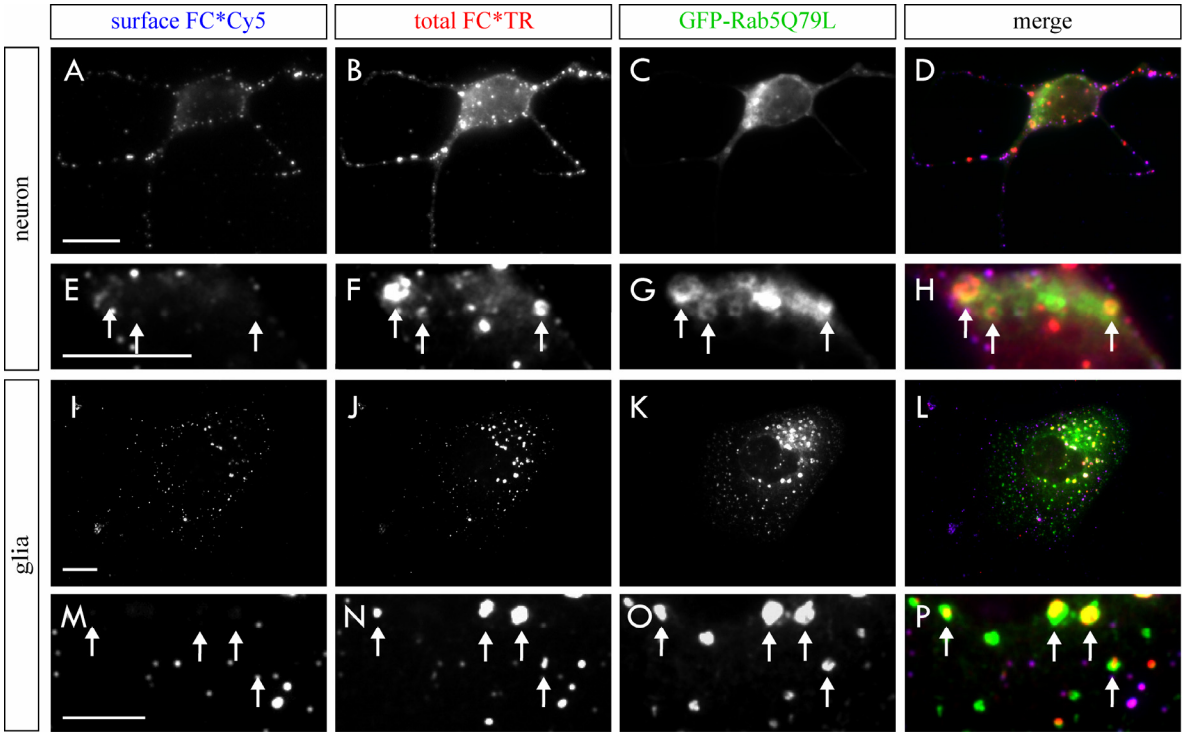

Figure 36 Internalised EphA4 reaches Rab5 positive endosomes in primary cultures

Hippocampal neurons were transfected with GFP-Rab5Q79L at 2 DIV and cultured for an additional 48h before stimulation with pre-clustered ephrinB3-Fc for 30 min. Cells were stained for surface receptor-ligand-complexes with an anti-Fc antibody conjugated to Cy5 (false colour blue) and total receptor-ligand-complexes with an anti-Fc antibody conjugated to TexasRed (false colour red). Examples show a transfected neuron (A-D and magnifications in E-H) and a transfected glia cell (I-L and magnifications in M-P). In the merged images, surface receptor clusters appear in purple, internalised clusters in red and complexes that have reached Rab5-positive endosomes appear yellow or orange, indicated by arrows. Scale bars in A-D and I-L 10µm, E-H and M-P 5 µm.

2.6 Rin1 enhances the internalisation of EphA4

Next, I asked if and how Rin1 interferes with the internalisation of EphA4-receptor. I addressed this question in two different experimental setups. First a biochemical approach was taken using surface biotinylation assays. For a brief description of experimental procedures, please see legend in Figure 37, for details, please refer to the methods section. In control samples (eGFP transfected), a clear increase of internalisation could be observed over the time course of stimulation with pre-clustered ephrinB3Fc when compared to the stimulation control with pre-clustered Fc alone. Samples in which Rin1-FL was expressed show a marked increase of internalisation when compared with control samples (eGFP). Already at 20 minutes of ephrinB3-Fc stimulation, the amount of endocytosed EphA4 was markedly enhanced, a trend which was even more dramatic at the 60 minute time point (Figure 37).

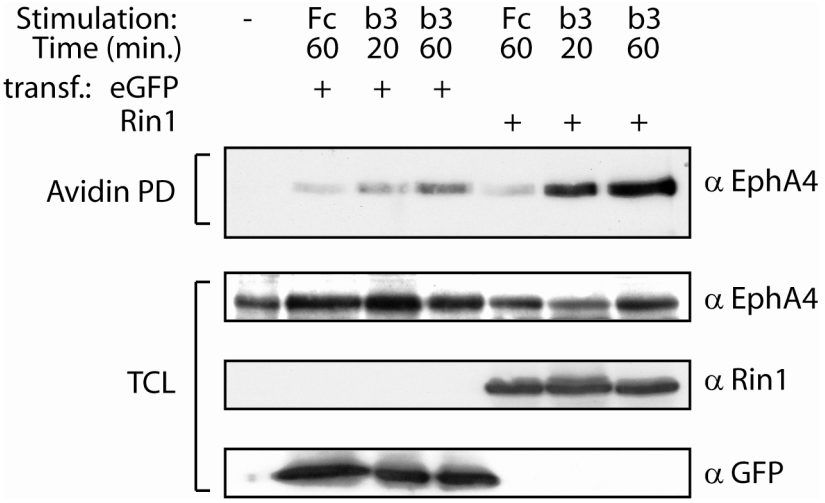

Figure 37
Rin1 enhances internalisation of EphA4
HeLa cells stably expressing EphA4 Receptor were trans-fected with eGFP as a control or Rin1-FL and subjected to a surface biotinylation assay. Surface molecules were biotinylated and then internalisation initiated by stimulation with ligands, pre-clustered Fc (control) or ephrinB3-Fc. After indicated timepoints, cells were placed on ice and biotin was stripped from remaining surface molecules. Avidin pulldown (PD) is a readout for internalised proteins. Total amount of protein present is shown in total cell lysates (TCL), Immunoblots against indicated proteins. (b3) ephrinB3-Fc.

In a second approach, a pre- and post-permeabilisation staining procedure on the stable Hela-EphA4 cells was employed to quantify the number of internalised EphA4-receptor clusters. Native HeLa cells did not show surface clusters when stimulated with ephrinB3-Fc, thus all receptor molecules identified in the staining were indicative of EphA4. Since the population of generated HeLa-EphA4 were heterogeneous in their expression levels even

though originating from a single cell clone, there were cells with no detectable receptor expression when stained with anti-Fc antibody after stimulation (see Figure 38, panel B).
It has been established before that stimulation with clustered Fc alone does not lead to any detectable staining since there is no binding of Fc alone to any surface molecules (see Figure 38, panel A).

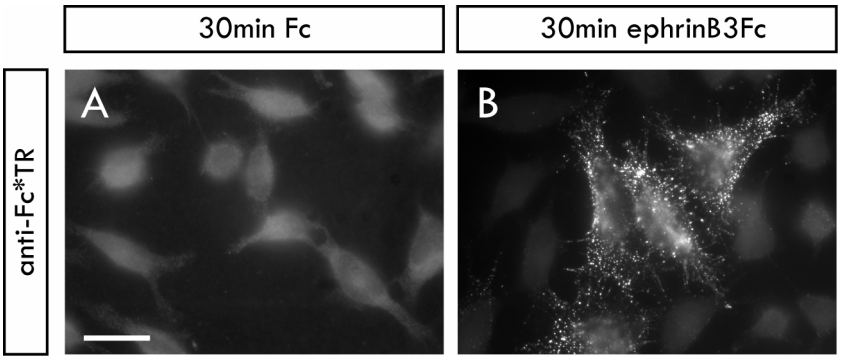

Figure 38
HeLa cells stably expressing EphA4 receptor
Stable HeLa-EphA4 cells were stimulated for 40 min with either pre-clustered Fc (control, panel A) or ephrinB3-Fc. (B) and stained with TR-conjugated anti-Fc antibody. Note that there are many cells with undetectable levels of receptor expression in the population of this stable clone (B: faint shadows of EphA4 negative cells around the cells with clear receptor clusters). Scale bar 50μm

In Figure 39, an example of surface and total anti-Fc staining is shown. Clusters shown in red in the merged image (panel C and blowup in F) are indicative of internalised receptor-ligand complexes.

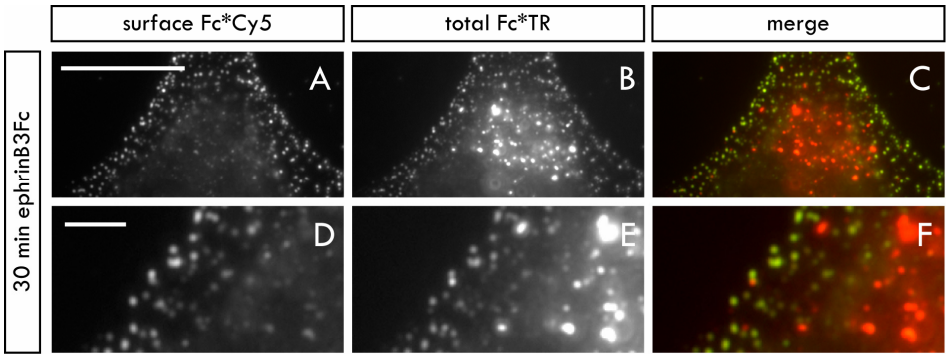

Figure 39 Pre-post-permeabilisation staining for Eph-ephrin complexes
HeLa cells stably expressing EphA4 were stimulated for 30min with pre-clustered ephrinB3-Fc. Shown are EphA4-ephrinB3 complexes identified on the surface of the cells (pre-permeabilisation staining in A, D, green or yellow clusters in merged image C and F) and total number of complexes (post-permeabilisation staining in B, E). Internalised clusters appear red in the merged image. Scale bars 50μm in A-C and 10μm in D-F.

The number of internal receptor-ligand clusters counted after permeabilisation of the cells was divided by the total number of clusters thus resulting in a percentage of EphA4-receptor internalisation for each individual cell analysed. Cells transfected with eGFP show an average internalisation rate of 19%, cells transfected with Rin1 show a highly significant increase of internalisation to 29% (Figure 40).

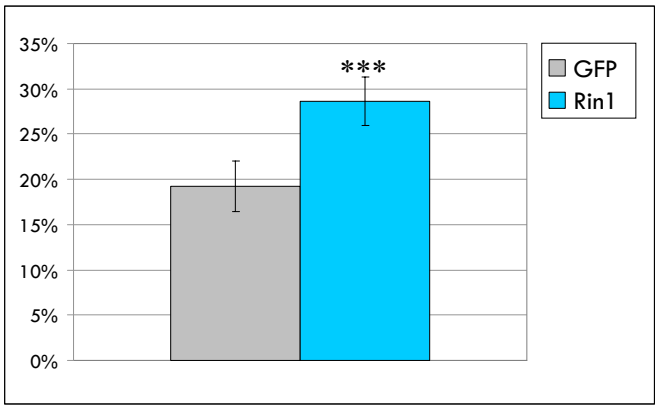

Figure 40 Enhancement of EphA4 internalisation in the presence of Rin1
HeLa stably expressing EphA4 were transfected with either eGFP (control) or Rin1 and eGFP (ratio 5:1) By pre- and post-permeabilisation staining for receptor-ligand complexes and calculation of ratio of internalisation, an increase in the amount of internalised receptor from 19% in control samples to 29% in Rin1 transfected samples was observed. Error bars represent standard deviations. T-test (2-tailed, equal variance) 1,28E-12

We next examined whether the positive effect of Rin1 expression on the internalisation of EphA4 is due to Rin1 guanine nucleotide exchange factor (GEF) activity. It has been described previously that Rin1 includes a Vps9p-like GEF domain in the C-terminal half of the protein with which it acts as an exchange factor for the small GTPase Rab5 (Tall et al., 2001). We designed two putative dominant negative constructs, in which either the entire GEF domain was deleted or only the first 48aa, termed Rin1-ΔGEF and Rin1-splice, respectively. Rin1-splice corresponds in sequence to a naturally occurring splice variant of Rin1 (Han et al., 1997) that has been shown to be unable to stimulate GDP release from Rab5 (Tall et al., 2001). As shown in Figure 41, there was a moderate increase in EphA4 internalisation after 60min stimulation with ephrinB3 when compared to Fc control in the eGFP and an enhanced endocytosis in the Rin1-FL transfected samples. Rin1-ΔGEF and Rin1-splice only showed internalisation levels comparable to the Fc-stimulated eGFP sample but no induction of endocytosis after specific stimulation with pre-clustered ephrinB3. This indicates that the specific increase observed in Rin1-FL-transfected samples was due to the catalytic activity of Rin1 and that remaining, low-level endocytosis of EphA4 still seen with

the Rin1 dominant negative constructs and in Fc-stimulated samples is a residual, ligand-independent form of internalisation.

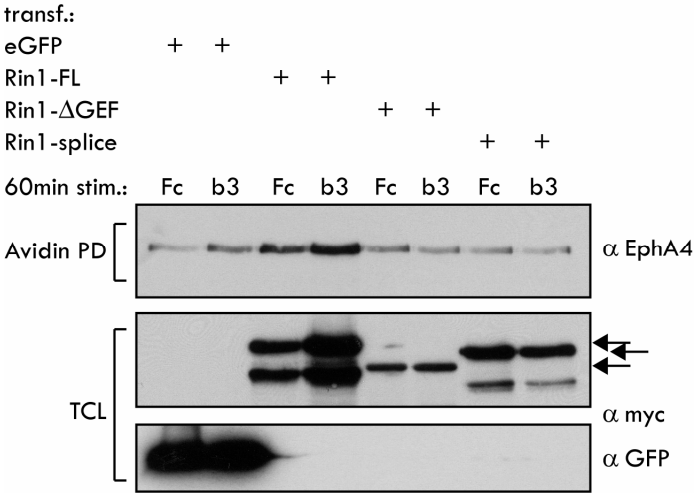

Figure 41 GEF-deficient Rin1 blocks EphA4 internalisation induced by stimulation with ephrinB3

HeLa cells stably expressing EphA4 were transiently transfected with eGFP (control), Rin1-FL, Rin1-ΔGEF or Rin1-splice, stimulated for 60min with either Fc alone or ephrinB3-Fc and subjected to a surface biotinylation assay. Avidin Pulldown (PD) is a readout of internalised proteins. Arrows indicate from top to bottom Rin1-FL, Rin1-splice and Rin1-ΔGEF, lower bands are most likely degradation products of the overexpressed proteins. TCL: total cell lysate.

2.7 EphA4$^{-/-}$ mice have a LTP defect in the amygdala

The relationship between Rin1 and EphA4 I have established so far involves physical (albeit possibly indirect) interaction of the two molecules, an induction of tyrosine phosphorylation in Rin1 downstream Eph receptors and a necessary and sufficient role for Rin1 in the endocytosis of EphA4. Therefore I was interested to see whether EphA4 mutant mice had any defects in amygdala LTP, since Rin1 knockouts have been shown to have elevated amygdala LTP (Dhaka et al., 2003). To see the expression pattern of Rin1 and EphA4 in amygdala, please refer to Figure 26. Coronal slices were sectioned at the level where the external capsule is visible encompassing the lateral (LA) and basolateral (BLA) nuclei of the amygdala (for an example and a schematic overview of amygdaloid nuclei, please refer to chapter 1.4, Figure 12).

Slices were stimulated using a high frequency stimulus (HFS, 2sec 50Hz), placing the stimulating electrode in the external capsule and the recording electrode in the LA (Figure 42, panel A). EphA4$^{-/-}$ (n=21 slices from 9 animals) and EphA4$^{wt/wt}$ (n=17 slices from 7 animals) control littermates were subjected to this protocol. When compared to wt littermates, EphA4 null mice show an initial (first ten min after HFS), weak rise in the normalised field potential (FP) amplitude but then fail to display LTP induction (Figure 42, panel B). Electrophysiological recordings were performed by Dr. Matthias Eder, MPI for Psychiatry, Munich.

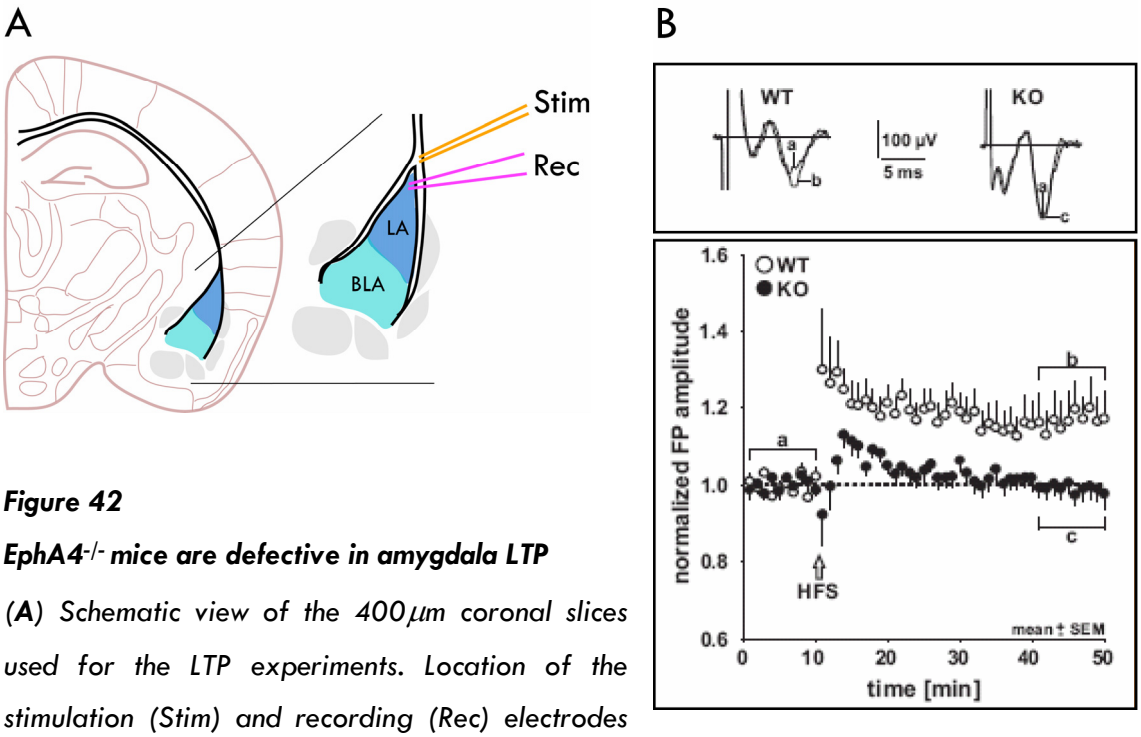

Figure 42

EphA4$^{-/-}$ mice are defective in amygdala LTP

*(**A**) Schematic view of the 400µm coronal slices used for the LTP experiments. Location of the stimulation (Stim) and recording (Rec) electrodes are indicated. (LA) lateral amygdala, (BLA) basolateral amygdala. (**B**) EphA4 knockout mice*

(ko, black circles, n=21 slices from 9 animals, 2-3 slices per animal) fail to display long term potentiation (LTP) after high frequency stimulation (HFS), EphA4$^{wt/wt}$ littermates (wt, open circles, n=17 slices, 2-3 slices per animal) are shown as control. Paired student´s t-test: b vs. a, p= 0.038 c vs. a, p= 0.73; unpaired student´s t-test: b vs. c, p= 0.018. Experiments performed by Dr. Matthias Eder, MPI for Psychiatry, Munich.

3. Discussion

3.1 Rin1 interactors identified by TAP

The tandem affinity purification (TAP) technology (Gavin et al., 2002; Rigaut et al., 1999) has emerged as a useful tool to purify whole complexes of interacting proteins from cells or transgenic organisms. The general picture of protein-protein interaction and their importance for intracellular events has changed since it has become clear that most likely, proteins are engaged not only with one or two binding partners but instead take part in large signalling complexes. These may vary in their composition depending on cellular context or the combination of signals received by the cell. Hence a method was in demand that would allow retrieval of such multimeric complexes from cells or ideally from transgenic animals, which would identify interactors from a more physiological context. TAP is ideally suited for such an endeavour. We employed the TAP technology in this study to obtain more information about proteins that interact with our protein of interest, Rin1. We designed a TAP-tagged Rin1 construct as the bait (Figure 14) which was integrated into the SK-N-BE2 human neuroblastoma cell line by retroviral infection. We chose a neuroblastoma cell line since Rin1 shows strong expression in the nervous system and we anticipated the presence of at least some neuron-specific interactors in the SK-N-BE2 line. The purification of complexes was performed twice, once in untreated conditions and once in the presence of vanadate, a tyrosine-phosphatase inhibitor to ensure phospho-tyrosine dependent interactions. In collaboration with cellzome, the company which performed the mass-spectrometry analysis of the purified proteins, we were able to identify a list of proteins which was further annotated with information obtained from bioinformatical databanks online (NCBI, UniProtKB/Swiss-Prot and see Figure 16). Among the proteins identified are published interactors of Rin1, such as H-Ras and 14-3-3 proteins (Han and Colicelli, 1995; Han et al., 1997) strengthening the relevance of molecules identified with this technology. K-Ras and N-Ras, two other members of the Ras family of GTPases were also discovered and in a preliminary experiment (GST-pulldown) we confirmed that N-Ras is able to precipitate Rin1 from adult mouse forebrain (Figure 17). Recent evidence points to diverse roles of different Ras isoforms at different subcellular locations (Hancock, 2003; Rocks et al., 2006; Silvius, 2002). N-ras for example has been shown to localise to the Trans-Golgi-Network (TGN) where it potently activates the MAPK-pathway (Chiu et al., 2002; Goodwin et al., 2005; Rocks et al., 2005). Our unpublished observations elucidated that at least a

pool of Rin1 is also found at the Golgi where it co-localises with markers such as GM130 and GM97 and N-Ras (data not shown). It will be interesting to uncover the physiological role of the potential interaction of Rin1 and N-Ras at the Golgi.

Among the remaining proteins obtained, we found a number of molecules involved in the protein transcription, translation and folding machinery, such as a RNA-Pol II subunit, RPLP1 (60S acidic ribosomal protein P1), the heat shock protein HSPB1 and PFDN2 (Prefoldin subunit 2), respectively which could be artefacts due to the exogenous overexpression of TAP-tagged Rin1. Furthermore we found a number of proteins involved in the degradative machinery of the cell, such as proteasome subunits PSMA2, PSMA5 and PSMA7, also possibly artefacts due to aforementioned reason.

Potentially relevant candidates however, were also identified. ITM2b, an integral membrane protein has been associated with familial British dementia (FBD), and in addition binds to and modulates APP (amyloid precursor protein) processing (Choi et al., 2004; Fotinopoulou et al., 2005; Matsuda et al., 2005). Intriguingly, another identified interactor, Presenilin 1 (Koo and Kopan, 2004), is an endoprotease that also plays an important role in processing APP and Notch receptor (Selkoe and Kopan, 2003). It localises to the Golgi apparatus but is also found associated with Notch at the plasma membrane. It is possible that both Presenilin 1 and ITM2b bind directly to Rin1 or this could be an example where a tertiary, indirect interactor has been purified.

HAX1 (Suzuki et al., 1997) may function in promoting cell survival and is in addition thought to interact with cortactin, a molecule involved in endocytosis and golgi organisation (Radhika et al., 2004). 14-3-3 isoform eta has been shown to activate tyrosine and tryptophan hydroxylases in the presence of Ca^{2+}/calmodulin-dependent protein kinase II (CAMKII), and strongly activates protein kinase C (Davare et al., 2004; Skoulakis and Davis, 1998). 14-3-3 isoform tau is also present in neurons and gets axonally transported to nerve terminals (UniProtKB/Swiss-Prot). Microtubule-associated protein 1B (MAP1B), has been implicated in cytoskeletal rearrangement during neurite extension among many other roles in the nervous system (Gonzalez-Billault et al., 2004). Stomatin-like2 (SLP-2) is also a cytoskeleton-associated protein that was found in a mass spectrometry analysis of activity-dependent changes in PSD composition (Satoh et al., 2002) and has recently been isolated from caveolin-rich fractions of endothelial membranes (Sprenger et al., 2004).

Further experiments will be needed to confirm the specificity of the interactions between Rin1 and these potentially interesting candidates and to elucidate the role that Rin1 plays in the diverse processes that these interactors have been implicated in.

3.2 Rin1 expression

Several control experiments confirmed the specificity of the rabbit polyclonal antibody against murine Rin1 generated in our laboratory. These included stainings on overexpressed and endogenous Rin1 in cell lines and primary hippocampal neurons using pre-immune serum as a negative control (Figures 18 and 20). Furthermore we performed Western blots on Rin1wt and knockout forebrain lysates (Figure 19) and observed a strong similarity between expression patterns obtained by in situ and antibody staining methods (data not shown). We could show that compared to controls, the serum of rabbit #1203 used throughout this study revealed specific staining and detected a clear band in Western blot corresponding to the expected size of Rin1. Further experiments allowed us to localise Rin1 to synaptic structures in primary hippocampal cultures and in coronal slices of adult mouse brain through co-localisation of Rin1 protein with synaptic markers Synaptophysin and PSD-95 (Figure 22, Figure 25) as well as detection of Rin1 in synaptosome and PSD preparations from adult mouse forebrain (Figure 32, Figure 33). As described before (Dhaka et al., 2003), we found no Rin1 expression during embryonic development (Figure 23) and with the exception of the thalamus where we observed rin1 mRNA distributed in a "salt-and pepper" fashion (Figure 26, panel D), our expression data corresponded to published patterns (Dhaka et al., 2003). The riboprobe used in this study was of a different design than the one used in the study by Dhaka et al, thus we hypothesise that the discrepancy in detection of rin1 in the thalamus could be due to the sequence differences and regions covered by the different probes. In situs on adult mouse brain revealed a striking similarity between the expression patterns of rin1 and ephA4 which lead us to investigate the potential interaction between these two molecules. Additional in situs were performed with specific riboprobes against the other two Rin family members, Rin2 and Rin3 (Kajiho et al., 2003; Kimura et al., 2006; Saito et al., 2002). In contrast to published expression patterns on commercially available northern blot membranes for these two molecules we found expression of both in the adult brain (data not shown). We detected very weak expression of both in all regions of the hippocampus and in some areas of the cortex. In addition, rin3 mRNA was localised in the thalamus but neither rin2 nor rin3 messages could be detected in the amygdala. We hypothesise that the absence of other Rin family members in the amygdala is the reason for the published enhanced LTP seen in Rin1 knockout mice, since the Rin1 null mutation cannot be compensated. In other regions of the nervous system and possibly other parts of the organism, however, absence of Rin1

might be compensated by Rin2 and/or Rin3 and thus no obvious phenotypes could be observed.

3.3 Tyrosine phosphorylation of Rin1

It has been proposed many years ago that signalling initiated by external stimuli is propagated inside cells through cascades of sequentially interacting signal transducers. Tyrosine phosphorylation and subsequent phospho-tyrosine dependent protein-protein interaction has emerged as one of the most important means through which this is achieved. In addition, although this is not a general rule, tyrosine-phosphorylation is commonly thought to be an activating modification of proteins, whereas de-phosphorylation by phosphatases is thought to be inactivating (Cohen, 1992; Koch et al., 1991; Pawson and Schlessingert, 1993; Posada and Cooper, 1992).

The role and nature of tyrosine phosphorylation has been previously addressed by Colicelli and colleagues for the human Rin1 (Afar et al., 1997). These authors employed an assay in Rat-1 cell fibroblasts which showed anchorage-independent growth in soft agar upon transformation with the P185 isoform of BCR/Abl. A mutant of BCR/Abl (Y793F) no longer had transforming capabilities but this could be rescued by overexpression of Rin1 and depended on three phosphorylatable tyrosines in Rin1. Furthermore the authors suggested that tyrosine phosphorylation of Rin1 stabilises its interaction with BCR/Abl by binding to the SH2 domain of BCR/Abl (Afar et al., 1997).

Intrigued by the mapping of phosphorylatable tyrosines shown by these authors, we expressed (in preliminary experiments) murine Rin1 Y to F point mutants of tyrosines predicted to be phosphorylated (http://www.cbs.dtu.dk/services/NetPhos/) in HeLa cells in the presence of the phosphatase inhibitor sodium-ortho-vanadate and found Y35 to show the strongest reduction in overall phospho-tyrosine signal (data not shown). However, we were more interested in the upstream signals that can induce Rin1 phosphorylation and found Rin1 to be phosphorylated in response to activation of endogenously expressed RTKs such as TrkA, TrkB and cMet in the human neuroblastoma cell line SK-N-BE2 (Figure 28, Figure 29), albeit with slightly different kinetics. Differences in the time courses of Rin1 phosphorylation possibly reflect the distance of Rin1 in the signalling cascade from the activated RTK. For future experiments it will be of great interest to determine the function

of Rin1 in signalling events initiated by the growth factors shown here to induce Rin1 phosphorylation.

Since we were interested in the relationship between Rin1 and EphA4, we investigated Rin1 phosphorylation downstream of a related Eph receptor, EphB2, which is endogenously expressed in SK-N-BE2. We could not find a system in which both EphA4 and Rin1 were endogenously expressed and deemed it unsuitable to exogenously express EphA4 since it has been shown before that overexpression of Eph receptors leads to their constitutive activation as assessed by their phosphorylation state. By stimulating EphB2 with one of its ligands, ephrinB2, we detected a strong but transient phosphorylation of Rin1 on tyrosine (Figure 30). Since we could observe this inducible, Eph-mediated modification of Rin1, we propose to place Rin1 downstream activated Eph receptors.

3.4 Rin1 interaction with EphA4 receptor

It has been previously shown that human Rin1 and the Drosophila homologue Sprint are able to interact with several RTKs, such as EGFR, FGFRII, PDGFR, IR and PVR, respectively, by co-immunoprecipitations from cells, GST-pulldowns and yeast two-hybrid assays (Barbieri et al., 2003; Jekely et al., 2005). In all of these experiments the interaction was shown to be phospho-tyrosine dependent and mediated by the SH2 domain of Rin1. Most intensely studied was the binding of Rin1 to the EGFR (Barbieri et al., 2003).

I found endogenously expressed human Rin1 to co-immunoprecipitate with endogenous cMet from SK-N-BE2 cells in a stimulation dependent manner (data not shown), an interaction which has not been reported before in the literature. More experiments will follow this observation in the future, especially with regard to the findings of Colicelli and colleagues who showed that Rin1 is a negative regulator of HGF mediated migration in mammary epithelial cells (Hu et al., 2005). So far, we did not further pursue the involvement of Rin1 downstream cMet as we wanted to concentrate on the relationship between Rin1 and EphA4 in this study.

I found Rin1 to co-immunoprecipitate with EphA4 from transfected HeLa cells (Figure 31). Taking previous findings into consideration, I tried to determine whether the interaction of Rin1 and EphA4 was also mediated by phosphorylated tyrosines (potentially in the cytoplasmic tail of the receptor) and the SH2 domain of Rin1. We approached this question by mutating a critical arginine residue in the conserved FLVR motif of the SH2 domain of

Rin1 (R93E) but found that Rin1R93E co-precipitated with EphA4 just as well as the wt Rin1 protein (Figure 31, panel A). Even a Rin1 mutant protein lacking the entire SH2 domain showed no impaired interaction with EphA4 (Figure 31, panel B). Preliminary data also suggests that EphA4^{2E} is still able to bind to Rin1 (data not shown) although it lacks the two JM tyrosines that upon phosphorylation constitute docking sites for SH2 interactors. As already described in chapter 1.1, there are several features that distinguish Eph receptors from other RTKs. Although so far we cannot base our predictions on experimental data, one can envision that Rin1 could directly interact with EphA4 through a SH2-independent mechanism. Possibilities include protein-protein interactions with the SAM domain, the kinase domain, the PDZ-binding motif or higher order clustering of the receptor that might recruit adapters that link EphA4 to Rin1.

I was furthermore able to demonstrate an interaction between these two molecules in co-immunoprecipitations from synaptic membrane material obtained from adult mouse forebrains (Figure 34). Since my in vitro experiments showed that the SH2 domain of Rin1 is dispensable and I observed a binding of Rin1 to EphA4 in vivo, we speculate that the interaction between the two proteins occurs through a mechanism different to the one previously published for other RTKs.

3.5 Endocytosis of EphA4 is regulated by Rin1

Only recently has endocytosis been appreciated as a process that is tightly linked and probably inseparable from signalling events taking place inside cells (Cavalli et al., 2001; Clague and Urbe, 2001; Sorkin and Von Zastrow, 2002) . Endocytosis itself is modulated by signalling pathways but the endocytic machinery in turn provides an architectural framework in which spatial and temporal control over signal prolongation or attenuation can be exerted (Hoeller et al., 2005; Polo and Di Fiore, 2006). As already discussed in chapter 1.3, the route as well as the purpose of endocytosis can vary even when examining the internalisation of only a single RTK. Studies on RTK endocytosis include work on numerous growth factor receptors, such as TrkA (Delcroix et al., 2003; Shang et al., 2004), cMet (Hammond et al., 2003; Kamei et al., 1999), TGFß-R (Di Guglielmo et al., 2003) and especially EGF-R (Barbieri et al., 2003; Barbieri et al., 2000; Sigismund et al., 2005).

Very little however, is known about regulation or function of Eph receptor internalisation. Eph receptor endocytosis was recently proposed as a means to achieve disruption of cell-

cell contact initiating Eph-ephrin mediated repulsion (Cowan et al., 2005; Marston et al., 2003; Zimmer et al., 2003). Although there is evidence that Rac-mediated rearrangement of the actin cytoskeleton is required in the Eph receptor expressing cell (Marston et al., 2003), it remains unclear what route the internalised receptor takes, how this process is controlled and what purpose it serves.

In this study I could show that stimulation with ephrinB3 leads to endocytosis of EphA4 and subsequent appearance in Rab5 positive endosomes. I observed this phenomenon in HeLa cells stably expressing EphA4 (Figure 35), as well as in primary hippocampal neurons and glia cells (Figure 36). Preliminary data obtained through immunofluorescence stainings in primary neurons and glia also showed co-localisation of the internalised Eph receptor with strong phospho-tyrosine signals (anti-phospho-tyrosine antibody, data not shown). This finding is indicative of still active receptor-ligand complexes, which correlates with the observations of Nobes and colleagues in fibroblasts (Marston et al., 2003). Furthermore, upon stimulation of neurons with ephrinB3-expressing HeLa cells, we found the GTPase Dynamin (responsible for the fission of invaginated pits) present on the receptor side of the formed complexes (using an antibody against the neuron-specific isoform of Dynamin), indicative of an involvement of Dynamin in the endocytosis of Eph receptors (data not shown). Further experiments are in preparation to characterise the Eph internalisation pathway in more detail. These include staining procedures using markers for components of the endocytic machinery and biochemical analysis of the Eph receptor for modifications involved in endocytosis such as ubiquitination. It will also be worthwhile to dissect the possibly diverse routes of EphA4 internalisation initiated through binding of either ephrinA or ephrinB ligands.

Since I have successfully established an interaction of Rin1 and EphA4 (Figures 31 and 34) and have observed trafficking of EphA4 through Rab5 endosomes (Figures 35 and 36), I investigated whether Rin1 regulates the internalisation of EphA4. It has been shown previously that Rin1 exerts a positive influence on EGFR endocytosis through its action as a Rab5GEF (Barbieri et al., 2003; Tall et al., 2001). Our data provides evidence that Rin1 also positively regulates EphA4 endocytosis. Using a surface biotinylation assay, I observed enhanced EphA4 internalisation in HeLa cells stably expressing this receptor when transfected with full-length Rin1 as compared to control (eGFP) transfected cells (Figure37). Further support for this finding was obtained through a quantitative analysis of internalised receptor-ligand clusters in the same cells by immunofluorescence stainings. We observed an average increase of EphA4 endocytosis from 19% in control cells (eGFP transfected) to 29% in cells expressing the Rin1 full-length construct (Figure 40). In addition to this

promising gain-of-function data, we designed dominant negative versions of Rin1, either lacking the entire catalytic (GEF) domain (Rin1ΔGEF) or the C-terminal end of the GEF domain (Rin1-splice), a deletion that corresponds to a naturally occurring splice variant of Rin1 shown to be catalytically inactive (Han et al., 1997; Tall et al., 2001). When applied in the surface biotinylation experiment, I could demonstrate that overexpression of either Rin1ΔGEF or Rin1-splice reduced the amount of endocytosed EphA4 to control levels (Fc stimulated). No specific induction of ephrinB3 induced internalisation that also occurs in eGFP transfected samples could be seen in case of the dominant-negative constructs (Figure 41). Thus we conclude that Rin1 is an important positive regulator of EphA4 endocytosis. For a schematic model incorporating the aforementioned data, please refer to Figure 43.

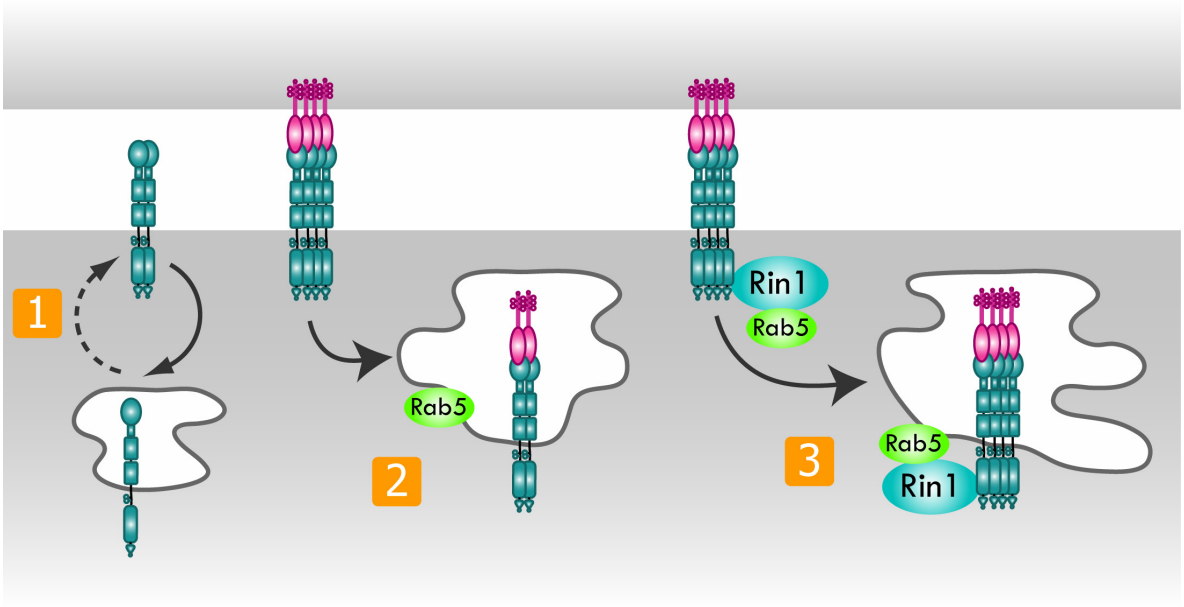

Figure 43 Rin1 is an essential regulator of EphA4 endocytosis

*(**1**) In the absence of ligand stimulation there appears to be a constitutive internalisation of EphA4 since even mock (Fc) stimulated samples in the surface biotinylation show very low levels of internalised receptor. Comparable residual levels were observed when GEF-deficient, dominant-negative forms of Rin1 were used in this assay.*

*(**2**) In untransfected conditions or when expressing a control protein (eGFP) we observed a ligand-dependent induction of EphA4 endocytosis and found EphA4 in Rab5 endosomes*

*(**3**) Expression of full-length Rin1 results in increased EphA4 endocytosis when compared to eGFP transfected control samples in surface biotinylation assays or when quantifying internalisation rates in immunofluorescence experiments*

It is intriguing to speculate that internalisation of Eph receptors might in some contexts lead to signal attenuation, especially since very little is known about negative regulation of Eph receptors. Elegant work from Noda and colleagues recently provided evidence that Phospho-tyrosine phosphatase receptor type O (Ptpro) can specifically de-phosphorylate Ephs (including EphA4) thus reducing the activity state of the receptors. The authors furthermore showed that Ptpro controls the sensitivity of Eph expressing retinal axons towards ephrins and has a crucial role in the establishment of topographic projections in vivo (Shintani et al., 2006). These findings however, do not exclude the existence of additional mechanisms such as endocytosis that might downregulate the activity of Eph receptors and it is even possible that regulation of the phosphorylation state of the receptor is involved in the events necessary for internalisation (Han et al., 2006; Levkowitz et al., 1999).

3.6 EphA4$^{-/-}$ mice have a LTP defect in the amygdala

Plasticity and memory formation involves many of the molecules and cellular processes described in chapter 1, their specific roles in modulating synaptic transmission shall be made clear in the following paragraph to help the appreciation of our current data.

In analogy to the hippocampal system, amygdala LTP is believed to be a cellular model for the acquisition of fear conditioning or learning. It involves the convergence of neural inputs from the conditional and unconditional stimulus (CS and US, respectively) onto lateral amygdala (LA) neurons during training (Blair et al., 2001; LeDoux, 2000; Maren, 2001). In protocols used to elicit LTP it involves a high frequency stimulus (HFS) applied to input pathways to the LA. LA neurons have been shown to increase their firing rates to the CS when paired with the US (reviewed in (Maren and Quirk, 2004)).

NMDA receptors (NMDARs), as well as delivery of (GluR1 containing) AMPA receptors (AMPARs) into synapses have been shown to be essential for acquisition of fear memory (Goosens and Maren, 2004; Maren, 2005; Rodrigues et al., 2004; Rumpel et al., 2005). Ca^{2+} influx through NMDARs and additionally, through voltage gated Ca^{2+}channels (VGCCs) induces a second messenger cascade that converges on Ras-MAPK pathway and ultimately ends in CREB-induced transcription necessary for fear consolidation or long-term memory (Rodrigues et al., 2004). Malinow and colleagues provided evidence that at excitatory synapses in the hippocampus, Ras mediates NMDAR (and CAMKII) signalling that

drives synaptic delivery of AMPARs during LTP (Zhu et al., 2002) but studies in the amygdala have also implicated Ras-Erk signalling in memory formation (Atkins et al., 1998; Brambilla et al., 1997; Schafe et al., 2000).

Eph receptors and ephrins regulate synaptic plasticity through both forward and reverse signalling and mouse mutants have been analysed for their plasticity defects in the hippocampus ((Armstrong et al., 2006; Contractor et al., 2002; Grunwald et al., 2004) and reviewed in (Klein, 2004; Yamaguchi and Pasquale, 2004). Eph(B2) receptor signalling, for example has been suggested to potentiate NMDAR-dependent Ca^{2+} currents and transcription factor activation (Battaglia et al., 2003) and absence of EphB2 leads to a reduction of synaptic NMDARs (Henderson et al., 2001). To our knowledge, the role of Eph receptors in synaptic plasticity in the amygdala has not been addressed prior to the study presented here.

Recent work has emphasised the role of Rab GTPases in synaptic plasticity. Rab8, a GTPase associated with the TGN and the PSD has been shown by Esteban and colleagues to be involved in local delivery of AMPARs to the spine-surface at the post-synapse and a dominant negative Rab8 blocked LTP expression (Gerges et al., 2004). NMDAR-dependent activation of Rab5 on the other hand drives the removal of synaptic AMPARs at excitatory CA3-CA1 synapses in the hippocampus, a process that is both necessary and sufficient for LTD (Brown et al., 2005). Although Colicelli and colleagues could not detect LTP defects in Rin1 mutant mice in the hippocampus (Dhaka et al., 2003), preliminary results from our laboratory suggest that $Rin1^{-/-}$ mice display LTD defects in Schaffer collateral synapses. We hypothesise that this is due to the same mechanisms described for Rab5 in removing AMPARs from the PSD (Brown et al., 2005).

Rin1 has previously been suggested to act as a negative regulator of learning and memory in the amygdala as Rin1 mutant mice show enhanced fear memory and increased LTP (Dhaka et al., 2003). The authors speculate that this is achieved through competition with the Ras effector Raf, thus diverting from the Ras-Raf-MAPK pathway involved in memory and plasticity of excitatory neurons (reviewed in (Weeber and Sweatt, 2002) and refer to Figure 13) or away from other Ras effectors, such as PI3K, also shown to play a role in amygdala plasticity (Lin et al., 2001). Other possibilities considered in this publication concern the enhancement of Abl1 and Abl2 signalling by Rin1, potentially involved in cytoskeletal modification of synapses. The last hypothesis brought forward by these authors states that Rin1 through its role as a Rab5GEF might lead to internalisation of a yet unknown receptor that positively regulates LTP in the amygdala.

Since our current data show that EphA4 null mutant mice are defective in amygdala LTP (Figure 42, panel B), we favour the latter hypothesis. One logical conclusion of reduced receptor endocytosis would be increased levels of receptors in the postsynaptic membrane of LA neurons leading to prolonged signalling, and concomitant increased LTP. We are at present trying to evaluate whether we can observe increased levels of EphA4 at the membrane of LA neurons in Rin1$^{-/-}$ mice. A system in which this question can be addressed has proven to be of great technical complexity. However, we have developed an explant system for the lateral amygdala from mice (two to three weeks of age) in which we can observe single neurons. We plan to challenge wt and Rin1$^{-/-}$ explants with ephrin ligands and assess the internalisation rate of EphA4 by quantification of pre- and post-permeabilisation stainings (described in chapter 2.6 and in the Methods section).

Our data suggest that EphA4 fits the requirements of a receptor that positively regulates plasticity in the amygdala as indeed its absence prevents LTP. It remains to be elucidated how EphA4 signalling influences known molecular events important for LTP expression. One can envision that EphA4 in analogy to EphB2 in the hippocampus (see above) might be involved in enhancing NMDAR signals. Integrating also our results that advocate Rin1 as a positive regulator of EphA4 endocytosis, the complementary phenotypes of Rin1 and EphA4 mutant mice suggest the model presented in Figure 44 that incorporates the results obtained in our current study.

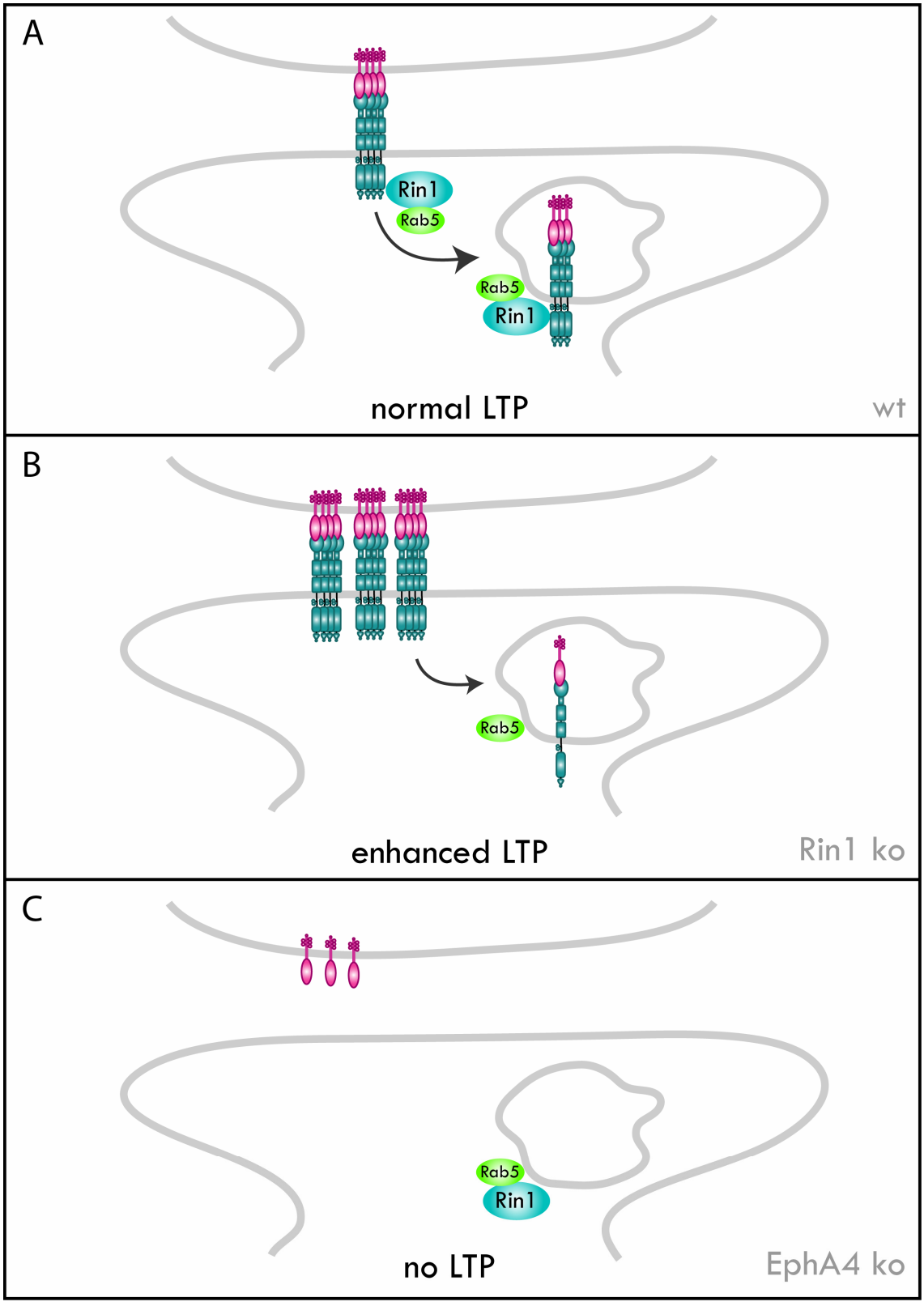

Figure 44 Involvement of Rin1 and EphA4 in amygdala LTP

*(**A**) Under wt conditions, both EphA4 and Rin1 are present in neurons of the lateral amygdala and normal LTP can be induced in these animals.*

*(**B**) Rin1 knockout mice have been shown to display elevated LTP in the amygdala (Dhaka et al., 2003). We propose in this model that the absence of Rin1 leads to reduced internalisation of EphA4, potentially a concomitant increase of EphA4 at the membrane. We hypothesise that increased signalling downstream EphA4 is responsible for the elevated amygdala LTP.*
*(**C**) Mice lacking the EphA4 receptor are deficient in amygdala LTP as shown in this study. We propose that the lack of EphA4 mediated signalling is responsible for the plasticity defect.*

4 Materials and Methods

4.1 Materials

4.1.1 Mouse lines

EphA4-/- (ephA4TAC) were generated by Klas Kullander (Neuron 2001 and Science 2003) and maintained in a mixed 129xC57Bl/6 background. For experiments, offspring of heterozygous intercrosses was used.

Rin1-/- mice were generated by Dhaka et al, J Neurosci., 2003 and maintained in a C57Bl/6 background. For experiments, offspring of heterozygous intercrosses was used.

4.1.2 Bacteria

XL2-blue, chemically competent cells (Stratagene)
Genotype: recA1 endA1 gyrA96 thi-1 hsdR17 supE44 relA1 lac [F'proAB $lacI^qZ\ddot{A}M15$ Tn10 (Tet^r) Amy Cam^r]^a
TOP10 (Invitrogen)
DH5α (Invitrogen)
BL21 (Invitrogen)

4.1.3 Plasmids

Backbone/ Insert	Comments	Reference
mammalian expression		
Rin1-CTAP	Cterm TAPtag (CBP, TEV, ProtA) for proteomics	Cellzome/ K.Deininger
pcDNA3.1		
EphA4-wt	FL wt EphA4-Receptor	K. Kullander
EphA4-KD	Kinase dead EphA4-Receptor	K. Kullander
EphA4-2E	2 juxta-membrane Y's mutated	K. Kullander
EphA4-eGFP	Cytopl. tail replaced by eGFP	K. Kullander
pcDNA3.1mycHis		
Rin1-FL	complete cds	K. Deininger
Rin1-$SH2_{aa1-166}$	SH2 domain	K. Deininger
Rin1 $Cterm_{aa477-763}$	GEF, RA domains	K. Deininger
Rin1-$\Delta SH2_{aa170-763}$	poly-P, GEF, RA	K. Deininger
Rin1-splice	≅ nat. occ. splice variant delta aa 418-479	K. Deininger
Rin1-$\Delta aa_{431-615}$	delta GEF domain	K. Deininger
Rin1-$Nterm_{aa1-430}$	delta GEF, RA domains	K. Deininger
Rin1-R93E	SH2 domain point mutant	K. Deininger
Rin1-Y35F	Tyr 35 to Phe point mutant	K. Deininger
Rin1-Y283F	Tyr 283 to Phe point mutant	K. Deininger
Rin1-Y670F	Tyr 670 to Phe point mutant	K. Deininger

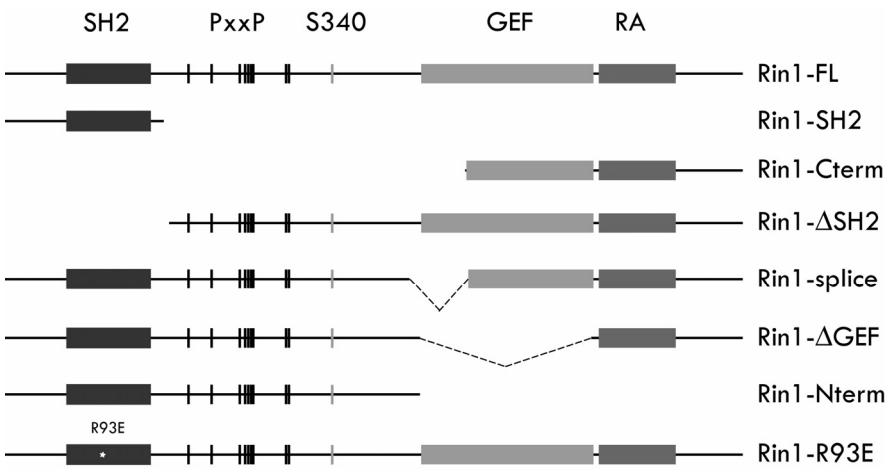

Figure 45 Rin1 overexpression constructs

Shown is a schematic representation of Rin1 overexpression constructs in the pcDNA3.1mycHis backbone. Domains from left to right (N-term to C-term):

(SH2, dark grey box) src homology 2 domain, (PxxP, dark grey bars) poly-proline motif involved in SH3 domain binding, (S340, light grey bar), 14-3-3 binding motif including the crucial serine 340, (GEF, light grey box) guanine nucleotide exchange factor domain, (RA, grey box) conserved Ras association domain.

pEGFP_C1

Rin1-Cterm$_{aa268-763}$	Nterm.GFPtag	K. Deininger
Rin1-SH2$_{aa60-151}$	Nterm.GFPtag	K. Deininger

pEGFP_C3

Rab5-Q79L	Nterm.GFPtag	M. Zerial
Rab5a-wt	Nterm.GFPtag	M. Zerial

pEGFP_C2

Rab5-S34N	Nterm.GFPtag	M. Zerial

Nras-wt	GFP- or myc-tagged	B. Short / F. Barr
Nras-Q61L	GFP- or myc-tagged	B. Short / F. Barr
Hras-wt	GFP- or myc-tagged	B. Short / F. Barr
Hras-Q61L	GFP- or myc-tagged	B. Short / F. Barr

bacterial expression

pDEST15

Rin1FL	Nterminal GST fusion protein	K. Deininger

pDEST17

Rin1FL	Nterminal His_6 fusion protein	K. Deininger

in situ probes

pCR2.1-TOPO

Rin13'UTR	5'-3' insertion, digested EcoNI = antisense probe	K. Deininger
	3'-5' insertion = sense probe	K. Deininger

pCMV-SPORT6

Rin2	digested AccI or BglII	K. Deininger

pCMV-SPORT2

Rin3	digested DrdI	K. Deininger

pBSKS

EphA4	digested XhoI	F. Helmbacher

4.1.4 Chemicals, kits, enzymes and other reagents

All chemicals were purchased from Sigma, Merck, Serva, and Roth unless specified otherwise in the Methods section. All water used in solutions and reaction mixes was filtered through a "Milli-Q-WaterSystem" (Millipore). Restriction and modifying enzymes were obtained from New England Biolabs (NEB). Plasmid Mini- and Maxi-preparations were done using the QIAGEN QIAprep Spin Miniprep or the Plasmid Maxi Kits, respectively. QIAquick PCR Purification and Gel Extraction kits were used in cloning procedures when necessary. Mutations were introduced using the QuikChange Site-directed Mutagenesis Kit (Stratagene).

4.1.5 Media

4.1.5.1 Media and Antibiotics for bacterial culture

LB (Luria-Bertani) media	10g Bacto-Trypton 5g Yeast extract 5g NaCl Add H_2O to 1L, pH to 7.5
SOC	10g Bacto-Tryptone 2.5g Bacto-Yeast extract 0.25g NaCl 5ml 250mM KCl 2.5 ml 2M $MgCl_2$ Add H_2O to 500ml, pH to 7.0 Add 10ml 1M sterile Glucose solution
LB plates	supplement with 15g/L agar
<u>Antibiotics</u>	diluted 1:1000 from stock solutions:

Ampicillin	100mg/ml in H_2O
Kanamycin	50mg/ml in H_2O
Tetracyclin	5mg/ml in Ethanol

4.1.5.2 Primary culture media, reagents, growth factors and stimulants

HBSS	Gibco
Dissociation media	500ml HBSS, supplemented with 1% Penicillin/ Streptomycin (Gibco), 3.5ml HEPES (1M, pH7.5) and 5ml MgCl2 (1M)
Neurobasal media/B27	Gibco, 500ml supplemented with 10ml B27 supplement (Gibco)
Poly-D- or L-Lysine	Sigma, dissolved 1mg/ml in borate buffer
Mouse-Laminin	Gibco, dissolved 5µg/ml in PBS (Sigma)
Papain	Sigma, dissolved 10mg/ml in H_2O
Inhibitor solution	Trypsin inhibitor (Roche), diluted 10mg/ml in dissociation media, neutralized with NaOH
Growth factors	NGF (R&D), used at 100ng/µl BDNF (R&D), used at 20ng/ml HGF (R&D), used at 40ng/ml PDGF (Sigma), used at 30ng/ml
Stimulants	Fc, Eph-Fc and ephrin-Fc fusion proteins were purchased from R&D and used at 1µg/ml

4.1.5.3 Media for cell lines

HeLa	DMEM, 10% FBS, 1% Glutamine, 1% pen/strep
Stable HeLa	DMEM, 10% FBS, 1% Glutamine, 1% pen/strep, 400ng/ml Geneticin (Gibco)
Cos	DMEM, 10% CS, 1% Glutamine, 1% pen/strep
NIH/3T3	DMEM, 10% CS, 1% Glutamine, 1% pen/strep
SK-N-BE2	OptiMEM with Glutamax, 10% ISCS (iron-supplemented calf serum), 1% pen/strep

4.1.6 Buffers and solutions

All buffers and solutions not described in detail were prepared according to standard protocols as described in "Short Protocols in Molecular Biology", John Wiley & Sons, Inc., 1999

Borate buffer	1.2g boric acid 1.9g sodium borate (Borax) Add H_2O to 500ml and pH to 8.5
Cell lysis buffer	50mM Tris·HCl, pH 7.5 150mM NaCl 0.5% TritonX·100 per 50ml: 1 tablet "complete" protease inhibitor cocktail (Roche), 0.22g NaPPi, 0.04g NaF, 1mM Vanadate

Solutions for postsynaptic density fractionation

Solution A	0.32M sucrose, 20mM HEPES (pH 7.4), 10mM NaF, 1mM Na3VO4, 1mM PMSF, protein inhibitor cocktail (Roche)
Solution B	0.32M sucrose, 20mM HEPES (pH 7.4)
Solution C	12mM Tris (pH 8.0), 1% TritonX-100

Solution D	40mM Tris (pH 8.0)
Solution E	12mM Tris (pH 8.0), 6% sarcosyl (N-lauryl-sarcosine)

Reducing sample buffer for SDS PAGE	300mM Tris·HCl pH 6.8
	12% SDS
	600mM DTT
	0.6% (w/v) BromoPhenolBlue
	60% glycerol

Tandem Affinity Purification (TAP) solutions

Lysis buffer	50mM Tris-HCl, pH 7.5
	5% Glycerol
	0.2% NP-40
	1.5mM $MgCl_2$
	1mM DTT
	100mM NaCl
	Add fresh:
	50mM NaF
	1mM Na_3VO_4
	2µM microcystine-LR
	Protease inhibitor cocktail tablet (complete), EDTA-free
TEV Cleavage buffer	10mM Tris-HCl, pH 7.5
	100mM NaCl
	0.1% NP-40
	0.5mM EDTA
	1mM DTT
CBP wash buffer	10mM Tris-HCl, pH 7.5
	100mM NaCl
	0.1% NP-40
	1mM MgAc
	1mM Imidazole
	2mM $CaCl_2$
	1mM DTT

2x CBP dilution buffer (TAP)	10mM Tris-HCl, pH 7.5
	100mM NaCl
	0.1% NP-40
	2mM MgAc
	2mM Imidazole
	4mM $CaCl_2$
	1mM DTT
CBP elution buffer (TAP)	10mM Tris-HCl, pH 8.0
	5mM EGTA

4.1.7 Antibodies

Primary antibodies

antibody	**species**	**company**	**appl.**	**dilution**
anti-phosphoMAPK	mouse monoclonal clone E10	Cell Signaling	WB	1:2000
anti-MAPK	rabbit polyclonal	Cell Signaling	WB	1:1000
anti-Tubulin	mouse monoclonal	Sigma	WB	1:10000
anti-eXFP	mouse monoclonal	BD Clontech	WB	1:1000
anti-pan-ras	mouse monoclonal	Calbiochem	WB	1:1000
	Ab3	Oncogene Res.	IP	1µg
anti-Nras	mouse monoclonal clone F155-227	Calbiochem Oncogene Res.	WB	1:1000
anti-Rab5a	mouse monoclonal clone15	BD Pharmingen	WB	1:500
anti-Rin1	rabbit polyclonal	BD Pharmingen	WB	1:500
			IP	1µg
			IF	1:100
	rabbit polyclonal	In house	WB	1:1000
			IP	2µl

			IF	1:100
			IHC	1:1000
anti-phospho-	mouse monoclonal	Upstate	IF	1:100
Tyrosine	clone 4G10		WB	1:1000
anti-myc	mouse monoclonal	Ascites, in house	WB	1:1000
	conjugated to Cy3		IF	1:100
anti-Clathrin HC	goat polyclonal	Santa Cruz	IF	1:100
anti-PSD95	mouse monoclonal	Sigma	WB	1:2000
	clone 7E3-IB8		IF	1:100
anti-Synaptophysin	mouse monoclonal	Chemicon?	IF	1:100
	MAB5258		WB	1:1000
anti-Synapsin	mouse monoclonal	SySy	IF	1:500
	clone 46.1		WB	1:10000
anti-GluR2	mouse monoclonal	Chemicon	WB	1:1000
	MAB397		IF	1:100
anti-GluR2&3	rabbit polyclonal	Chemicon	IP	2μg
anti-LAMP1	mouse monoclonal	Abcam	IF	1:100
	LY1C6			
anti-Dynamin1	mouse monoclonal	Abcam	IF	1:100
	clone 4E67			
anti-Caveolin	rabbit polyclonal	Abcam (ab2910)	IF	1:100
anti-γAdaptin	mouse monoclonal	BD Pharmingen	IF	1:100
	clone 88			
anti-TGN38	mouse monoclonal	BD Pharmingen	IF	1:200
	clone 2			
anti-GM130	sheep polyclonal	from Francis Barr	IF	1:1000
anti-EphB2				
anti-EEA1	mouse monoclonal	BD Pharmingen	IF	1:100
	clone E41120			
anti-PKCμ (D-20)	rabbit polyclonal	Santa Cruz	IF	1:100
anti-EphA4	mouse monoclonal	BD Pharmingen	WB	1:2000
	(anti-Sek)			
	rabbit polyclonal	In house	IP	1μl
			WB	1:2000
	rabbit polyclonal	Santa Cruz	IF	1:100

	(S-20)		
anti-hFc	goat polyclonal		
	conjugated to Cy5	IF	1:50
	conjugated to TR	IF	1:50

Secondary antibodies

antibody	**conjugate**	**species**	**company**	**appl.**	**dilution**
anti-mouse	HRP	sheep polyclonal	Amersham	WB	1:3000
	Cy3	donkey	Jackson	IF	1:300
	Cy5	donkey	Jackson	IF	1:300
anti-rabbit	HRP	goat polyclonal	Amersham	WB	1:5000
	Cy3	donkey	Jackson	IF	1:300
	Cy5	donkey	Jackson	IF	1:200
anti-goat	HRP	rabbit polyclonal	DAKO	WB	1:4000

4.2 Methods

4.2.1 Tandem Affinity Purification and mass spectrometry

A retroviral transduction vector was generated by cloning the Rin1 open reading frame, amplified by polymerase chain reaction, into a Moloney-based vector with the Gateway site-specific recombination system (Invitrogen) to obtain a C-terminal TAP fusion. Virus stocks were generated in a HEK293 Gag–Pol packaging cell line. SK-N-BE2 cells were infected and complexes were purified by using a modified TAP protocol (Gavin et al., 2002; Rigaut et al., 1999). 40 15cm-dishes of SK-N-BE2-Rin1-CTAP cells were harvested by mechanical detachment, washed with excess PBS on ice and lysed in 10ml lysis buffer each using a glass Teflon dounce homogenizer. Subsequently, lysates were incubated on a rotating wheel for 30min at 4°C and then centrifuged for 10min at 13000rpm, 4°C. The supernatant was added to 200µl rabbit IgG agarose (Roche) and rotated for 2h at 4°C. Beads were saved by centrifugation for 1min (1300rpm, 4°C, Varifuge 3.0R), transferred into a small column (0.8ml Mobicol M1002, MoBiTec) and washed with 10ml lysis buffer followed by a wash with 5ml TEV cleavage buffer. Beads were resuspended in 150µl TEV cleavage buffer and incubated upon addition of 4µl TEV protease (recombinant, Invitrogen) for 3h at 16°C in a thermoshaker (900rpm). The TEV eluate was directly applied to a Calmodulin affinity resin (214303-52, Stratagene) in a new column, mixed with 200µl CBP binding buffer and incubated for 1h at 4°C. Calmodulin beads were washed with 5ml CBP wash buffer and the protein complexes eluted with 600µl CBP elution buffer for 5min at 37°C. Both the CBP beads after elution and the lyophilized protein samples were boiled for 5min with 50µl 4x sample buffer (containing 20mM DTT) and separated by SDS–PAGE. Complete gel lanes were systematically cut into slices and proteins were digested in-gel with trypsin as described (Shevchenko et al., 1996). Protein identification was performed by LC–MS/MS at Cellzome AG, Heidelberg. MS data were searched against an in-house version of the International Protein Index (IPI), maintained at the EBI (Hinxton, UK). Results of database searches were subjected to further bioinformatical analysis. Proteins found repeatedly in complex purifications regardless of nature of the bait were classified as “sticky” and removed from the data list.

4.2.2 Cloning

4.2.2.1 Rin1 cDNA

Mouse Rin1 cDNA was obtained from RZPD (Clone IMAG p998O078934Q2) and correct sequence was verified by sequencing with the following primers:

seq1	5'-GGA GGG CTC AGA GCT CAT GTT CC-3'
seq2	5'-CCA GCC AAA CGG AAA GAC TGC CC-3'
seq3	5'-CCG CCA GGC CCT AAG TCG GGC CC-3'
seq4	5'-GCT GAT GAG TTC CTG CCT CTG C-3'
seq5	5'-CCG AGT GAC CCA ACC AGA TGC G-3'

Rin2 and Rin3 cDNA was also obtained from RZPD, the clone identification numbers were IMAG p998n117646Q and IMAG p998G121372Q3, respectively. Commercially available primers flanking the multiple cloning sites of pCMV-SPORT6 and pCMV-SPORT2, the plasmid containing the Rin2 and Rin3 cDNAs, were used to sequence the respective inserts.

4.2.2.2 Rin1 overexpression constructs

All constructs were generated by PCR-amplifying specific regions of the rin1 gene with primers that usually contained convenient restriction sites for subcloning using the PFUultra DNA Polymerase (Stratagene) following vendor's instructions. Details about the regions of rin1 gene covered in the various deletion constructs are described in the results section. All constructs were verified by sequencing with aforementioned sequencing primers. Mutations were introduced using the QuickChange Site-Directed Mutagenesis Kit (Stratagene), following vendor's instructions. Primers used to amplify regions of the rin1 gene or to mutate specific sequences are as follows.

construct	primer sequences
Rin1-cTAP	
sense	5'-GGGG ACA AGT TTG TAC AAA AAA GCA GGC TAG ACT GCC ATG GAA GAC CCT GGT GAG ACC GGA GCA CAC-3'
antisense	5'-GGG GAC CAC TTT GTA CAA GAA AGC TGG GTA CTC TTC CAA AGC CTG GCT TCC TTC TGC-3'
Rin1FL	
sense	5'-GTG GTC GGA TCC GCC GCC ATG GAA GAC CCT GGT GAG-3'
antisense	5'-GGT TCT TCC TCT AGA CTC TTC CAA AGC C-3'
Rin1FL-R93E	
sense	5'-CCG GGG ACC TTC CTG GTG GAG AAA TCT AAC ACT CGC-3'
antisense	5'-GCG AGT GTT AGA TTT CTC CAC CAG GAA GGT CCC CGG-3'
Rin1FL-Y35F	
sense	5'-CCA TCT ACA GAC CCA CTG TTT GAC ACA CCT GAT ACC-3'
antisense	5'-GGT ATC AGG TGT GTC AAA CAG TGG GTC TGT AGA TGG-3'
Rin1FL-Y283F	
sense	5'-GGA GAG CTC AGT GGG ATT TCG TGT GCC AGG-3'
antisense	5'-CCT GGC ACA CGA AAT CCC ACT GAG CTC TCC-3'
Rin1FL-Y670F	
sense	5'-AGG ACC AGG GCT TCC ATC GCC TGC CCC-3'
antisense	5'-GGG GCA GGC GAT GGA AGC CCT GGT CCT-3'
Rin1- $SH2_{aa\ 1-166}$	
sense	5'-CGG GGT ACC AGG CCG CCA TGG AAG ACC CTG GTG-3'
antisense	5'-CGG AAT TCG GAG ATG GCC TCC AGC TC-3'
Rin1- $Cterm_{aa\ 477-763}$	
sense	5'-CGG GGT ACC AGG CCG CCA TGG CCC CAG TGG AGA CAG AAC AG-3'
antisense	5'-CGG AAT TCC TCT TCC AAA GCC TGG CTT CC-3'
Rin1- $\Delta SH2_{aa\ 170-763}$	
sense	5'-CGG GGT ACC AGG CCG CCA TGG AGT TCT GGA GCT CCT CAC-3'
antisense	5'-CGG AAT TCC TCT TCC AAA GCC TGG CTT CC-3'
Rin1- splice	

(Δaa 418-479)

sense for 5'- part	5'-GCT GGT ACC GCC GCC ATG GAA GAC C-3'
antisense for 5'- part	5'-GCT GAA TTC CAG CCG CTC TGG TGG-3'
sense for 3'- part	5'-GAT GAA TTC GAG ACA GAA CAG GTG C-3'
antisense for 3'- part	5'-CCA CTC GAG CTC TTC CAA AGC CTG G-3'

Rin1- ΔGEF

sense for 5'- part	5'-GCT GGT ACC GCC GCC ATG GAA GAC C-3'
antisense for 5'- part	5'-CCA GAA TTC GAG AAC AGA GCG ATG C-3'
sense for 3'- part	5'-GGT GAA TTC CTC CTC CGA GTA GCC-3'
antisense for 3'- part	5'-CCA CTC GAG CTC TTC CAA AGC CTG G-3'

Rin1- Nterm$_{aa\ 1-430}$

sense	5'-GCT GGT ACC GCC GCC ATG GAA GAC C-3'
antisense	5'-CCA CTC GAG AAC AGA GCG ATG CAG G-3'

For internal deletions (Rin1-splice and Rin1-ΔGEF), a 5' piece upstream of the deletion and a 3' piece downstream of the deletion were generated by PCR. Junction of the pieces was mediated via a EcoRI restriction site contained in the antisense primer for the 5' part and the sense primer for the 3' part. Two amino acids (Glutamic acid [E] and Phenylalanine [F]) were introduced which are coded by the two triplets comprising the EcoRI site.

4.2.2.3 In situ probes

For information about plasmids used for transcribing the in situ probes, please refer to the Materials section. All antisense RNA probes were transcribed with T7 RNA polymerase.
Rin1 antisense RNA was generated as follows. The last 300bp of *rin1* coding sequence followed by 160bp of 3'UTR were amplified from IMAG p998O078934Q2 with the following primers:

sense:	5'-TTG GCC TCT TCC TCT ACA AGG-3'
antisense:	5'-CCA GCT CCC TGT TCC CTA GC-3'

and subcloned into pCR2.1-TOPO vector. Bacterial clones were screened by restriction digestion to determine direction of insertion. Inverse orientation was used as template to transcribe a sense RNA probe, to be used as a control.

4.2.3 Antibody generation

The purification of the recombinant protein used for generation of the anti-Rin1 antibody and the immunization of the rabbits and the goat were conducted in collaboration with Rodrigo Sanchez in our laboratory.

For purification of the Rin1 recombinant protein, BL21 E.Coli were transformed with the expression plasmid pDEST17-His_6-Rin1 containing the FL Rin1 cDNA by the heat shock method. Colonies were selected on an ampicillin supplemented LB agar plate, single clones inoculated into LB media and grown at 37°C to the absorbance of 0.4 at OD_{750}. Protein expression was then induced by adding 1mM isopropyl-D-1-thiogalactopyranoside (IPTG) to the culture and incubation for 2 hours at 30°C with constant agitation. The bacteria were pelleted at 4000 rpm in a 4°C centrifuge. The bacterial pellet was washed twice in cold PBS and resuspended in 20mM TRIS·HCl (pH 8) containing a cocktail of protease inhibitors (Roche) and 1mM DTT. The bacteria were mechanically lysed by passing the bacterial suspension 4 times through a French press. The sample was then centrifuged at 10.000 rpm for 10 min at 4°C and resuspended in binding buffer (6M guanidine hydrochloride, 20mM TRIS·HCl pH 8, 0.5M NaCl, 5mM imidazole, 1mM 2-mercaptoethanol) and kept stirring at RT for 60min before centrifugation at 10.000rpm for 15min at 4°C. Remaining particles were removed by filtration through a 0.45μm filter. The recombinant protein used for antibody production was then purified by Fast Protein Liquid Chromatography (FPLC) using the ÄKTA EXPLORER FPLC device. In brief, a 1ml HITrap Chelating HP column was washed with 5ml distilled H_2O, loaded with 0.5ml 0.1M $NiSO_4$ solution and washed with 5ml distilled H_2O again. The filtered sample was added to the affinity chromatography column at a speed of 1ml per minute and washed first with 10ml of binding buffer, then with 10ml wash buffer (6M urea, 20mM TRIS·HCl pH 8, 0.5M NaCl, 5mM imidazole, 1mM 2-mercaptoethanol). The recombinant protein was eluted with 10ml 50mM TRIS·HCl (pH 8)/10mM glutathione. The eluate was collected into 10 separate fractions of 1ml. The fractions containing the highest concentration of recombinant Rin1 protein were then dialyzed in PBS and concentrated to approximately 1mg/ml using CENTRIPLUS YM10 centrifugal filter device (Millipore Corporation) with an exclusion molecular weight of 30.000 Dalton. Rabbits were immunised and boosted at regular intervals. First bleeds were collected, crude serum extracted and tested in Western blot until satisfactory results were achieved.

4.2.4 Tail DNA preparation and PCR-based genotyping

Mice were genotyped by PCR. Tail samples of mice, usually 4 weeks of age unless needed younger, were collected and heated three times for 15 minutes at 95°C in 100µl 50mM NaOH with vigorous vortexing between heating steps. After cooling, samples were neutralized with 10µl 1.5M Tris·HCl, pH 8.8 and remaining debris was pelleted. 1µl of the DNA solution was used as template in PCRs. PCRs were carried out with 50pmol of each specific primer, PCR buffer (500mM KCl, 15mM $MgCl_2$, 100mM Tris·HCl, pH 8.8, 0.8% Nonidet), dNTPs (25mM each) and Taq polymerase (in house preparation) in a total reaction volume of 50 µl. 25 µl of the PCR reaction were separated on an agarose gel containing ethidium bromide and analyzed under UV light.

Primers used for PCR analysis

gene	primer	sequence
rin1	exon7.5prC	5'-AAG TCC CTG CAT CGC TCT GTT CTC A-3'
	mRINintr7C	5'-ACA GGG CAC AAA GGC ACT ATT C-3'
	mRINneo	5'-TAT TGG CCG CTG CCC CAA AG-3'
ephA4	wt sense	5'-CAA TCC GCT GGA TCT AAG TGC CTG TTA GC-3'
	wt antisense	5'-ACC GTT CGA AAT CTA GCC CAG T-3'
	mut sense	5'-GAC TCT AGA GGA TCC ACT AGT GTC GA-3'
	mut antisense	5'-TTT TCT CCC TCT TTA AGC AAG GAT CAA GC-3'
GFP-M	sense	5'-GCA CGA CTT CTT CAA GTC CGC CAT GCC-3'
	antisense	5'-GCG GAT CTT GAA GTT CAC CTT GAT GCC-3'

4.2.5 Postsynaptic density preparation

Post-synaptic densities were prepared as described in Cho et al, Neuron, 1992. In brief, forebrains of 6 wt C57/bl-6 adult male mice were homogenized in a dounce glass Teflon homogenizer in 12ml sol A and centrifuged at 3.000rpm for 10min at 4°C. Pellets were re-extracted with 5ml sol A, centrifuged at 1.000rpm for 10min at 4°C, supernatants combined with the ones from the previous centrifugation and centrifuged at 10.000rpm for 10min at 4°C. Pellets were resuspended in 5ml sol B, overlaid on a 1.2M/1.0M/0.85M sucrose gradient and ultracentrifuged at 25.500rpm for 120min at 4°C. A synaptic membrane fraction was extracted at the interface of 1.2M/1.0M sucrose layers and a control non-synaptic fraction was extracted between the top (0.32M) and the 0.85M sucrose layer. The synaptosome fraction was diluted to 9ml in sol B, 9ml of sol C was added followed by a 15min incubation on ice. The solution was divided into 6 samples and pelleted at 22.300rpm for 20min at 4°C. One pellet was resuspended in 100µl sol D (PSD fraction1), the remaining five pellets in 5ml solB. 2ml of this solution were mixed with 2ml sol C, incubated on ice for 15min and centrifuged at 50.100rpm for 60min at 4°C. The resulting pellet was resuspended in 100 µl sol D, 0.3% SDS (PSD fraction 2). The remaining 3ml were mixed with 3ml sol E, incubated on ice for 15min, centrifuged at 50.100rpm for 60min and the pellet resuspended in 100 µl sol D (PSD fraction 3). For a description of solutions used, please refer to the Materials section.

4.2.6 Western blotting

Samples obtained by biochemical procedures described elsewhere in the Methods section of this work as well as total cell lysates were denatured by boiling in SDS sample buffer and resolved by SDS PAGE according to standard procedures. Gels were transferred to nitrocellulose membranes (Protran, Schleicher&Schuell) by semi-dry blotting at 1mA/cm^2 of membrane surface for 45 to 120 min. After completion, protein transfer was validated by PonceauS staining, membranes were blocked either in a 5% BSA solution in PBT or a 7.5% nonfat milk solution in PBT for 1h at RT and incubated o/n at 4°C with primary antibodies diluted in blocking solution. Subsequently, membranes were washed in PBT for 1h at RT with several changes of PBT before incubation with secondary antibodies conjugated to HRP for

30-60min at RT in blocking solution. Finally, membranes were washed for 1h at RT in PBT before incubation with ECL solution (Amersham) for 1min and exposure to X-ray films (Kodak) to visualise signals. Membranes were stripped in 1x PBS, 2% SDS and β–MercaptoEthanol (14µl per 100ml of PBS/SDS) for 30min at 65°C and washed 3x for 10min each in PBT at RT, if subsequent detection of another protein was necessary. After stripping, membranes were again blocked and treated as described above.

4.2.7 Tissue lysis and Immunoprecipitation

Dishes of cultured cells or neurons were placed on ice, washed 2x with PBS and cells were scraped in 0.5ml Cell Lysis Buffer (CLB) per 10cm dish. Lysates were left to rotate at 4°C for 30min and non-soluble debris was pelleted at 13.200rpm for 5min at 4°C. Brain samples were lysed in 3x volume to weight, e.g. 0.5g of tissue were lysed in 1.5ml CLB in a glass Teflon dounce homogenizer and subsequently treated as cell lysates. Lysates were frozen in liquid nitrogen and stored at -80°C or used immediately. Protein concentration was estimated using the DC Protein Assay (Biorad).
A specific antibody directed against the protein of interest was coupled to proteinA- (for rabbit polyclonal antibodies, Amersham) or proteinG-sepharose (for mouse monoclonal or goat polyclonal antibodies, Amersham) by rotating on a wheel at RT for 30min. Unbound antibody was removed from the beads by washing 2x with CLB. Lysates containing equal amounts of total protein were then incubated with the pre-coupled antibody-sepharose for 2h on a rotating wheel at 4°C and washed 3x with CLB to remove traces of unbound proteins. Equal amount of 2x sample buffer was added to the packed beads and samples heated to 95°C for 5min to elute proteins. Samples were further analysed using Western blot analysis.

4.2.8 GST pulldowns

Equal amounts of GST fusion proteins in solution were coupled to Glutathione sepharose for 2 hours at 4°C, washed three times with lysis buffer and incubated with lysate from cultured cells overexpressing potential interactors or total forebrain lysate for 2 hours at 4°C. After

additional washes with lysis buffer, beads were boiled in equal volume of 2x loading buffer for 5min at 95°C and loaded on a SDS gel. Standard western blotting procedures were applied to identify proteins of interest.

4.2.9 Surface biotinylation

Surface biotinylation of cells was carried out similar to the procedure described in (Lin et al., 2000). In brief, stable HeLa-EphA4wt were split at a ratio of 1:10 from a confluent dish, transfected 24h later with either control plasmid (pEGFP-C/N1, Invitrogen) or Rin1FLmycHis, washed with PBS^{CaMg} the following morning and supplied with starving medium (0.5% FBS). On the fourth day, starving medium was aspirated; cells were rinsed once with warm PBS^{CaMg} and incubated with EZlink-NHS-SS-Biotin (Pierce, Rockford, Illinois) 300µg/ml PBS^{CaMg} for 2min at 37 °C/5% CO_2 to label all surface proteins. Subsequently, the biotin solution was aspirated, the cells rinsed once with warm PBS^{CaMg} and incubated with starving medium supplemented with either Fc (control) or ephrinB3-Fc for different time points to trigger EphA4 internalisation. Endocytosis was halted by placing dishes on ice and rinsing them with cold PBS^{CaMg}. Remaining biotin was stripped form the cell surface by incubation with reduced L-Glutathione (2.3g/50ml 150mM NaCl, pH8.75, Sigma) for 30min at 4 °C and glutathione was neutralized by incubation with Iodoacetamide (0.46g/50ml PBS^{CaMg}, Sigma) for 10min at 4 °C. Cells were lysed with CLB and lysates corresponding to equal amounts of total protein were incubated with Neutravidin sepharose (Pierce, Rockford, Illinois) on a rotating wheel at 4°C for 2h. Beads were washed 2x with CLB and boiled in 2x sample buffer before Western blot analysis.

4.2.10 Tissue culture

4.2.10.1 Cell culture

Standard cell lines used in this work are Cos, HeLa, SK-N-BE2, PC12 and NIH-3T3. They were cultured on Falcon dishes according to ATCC's (American Type Culture Collection) recommendations concerning splitting ratios and media requirements.

4.2.10.2 Transfection by $CaPO_4$ method

Cells were split the day before transfection at a ratio dependent on the number of cells required. Transfection reactions for a 10cm dish were setup as follows. Usually, 10-15µg of plasmid-DNA were diluted in H_2O to a total volume of 450µl. 50µl of 2.5M $CaCl_2$ were added, followed by 500 µl 2x BBS (pH 6.96) and gentle vortexing. Reactions were left at RT for 15 minutes before carefully dripping them onto cells. Cells were washed with PBS 4-12 hours after transfection and either supplied with fresh growth medium or starving medium depending on experimental design. Typically, cells were incubated 24-48 hours before analysis by Western blotting or immunofluorescence.

4.2.10.3 Generation of stable cell lines

HeLa cells were split 1:5 from a confluent dish onto 10cm dishes the day before transfection with 15µg pcDNA-EphA4wt or –EphA4KD by $CaPO_4$ method. Cells were split into selection medium (growth medium, 400ng/ml Geneticin [Gibco]) upon reaching confluence on the transfection dish. Selection media was replaced daily to remove dead cells. Clones were picked after 2-3 weeks by removing the cellmass of individual islands mechanically with a sterile pipet tip. Clones were transferred to a 96well plate and eventually expanded to 10cm dishes by splitting when appropriate. One confluent 10cm dish for each clone was frozen in liquid nitrogen, another dish lysed and analysed by

Western Blotting with anti-EphA4 antibody. Positive clones were further analyzed by immunofluorescence.

4.2.10.4 Primary neuron culture

Glass coverslips were treated with 65% nitric acid at RT for 18-36h, washed extensively with H_2O for 6-12h, rinsed several times in 100% Ethanol and dried. Coverslips were usually sterilized by baking at 175°C o/n then coated with poly-lysine o/n at 37°C, 5% CO_2. The following day, coverslips were washed twice with sterile H_2O and dried completely, then coated with laminin o/n at 37°C, 5% CO_2. Finally, they were rinsed twice with PBS and neurobasal/B27 media was added at least 3h prior to plating of neurons.

Hippocampal, cortical or forebrain (hippocampus and cortex) neurons were taken from E18-E19 embryos. Mothers were killed by cervical dislocation and embryos were taken out of the uterus and kept in HBSS on ice. Heads were cut off, the skull opened and brains were placed in dissociation media. Cortices were separated and meninges removed before the cortex and hippocampus were dissected in fresh HBSS from unwanted brain tissue and placed at 37°C in enzyme sol for 10-15min. Samples were washed three times at RT in inhibitor solution and then resuspended in neurobasal medium. Cells were dissociated with a rounded glass Pasteur pipette, counted and plated on coated glass coverslips in neurobasal/B27 medium. Cultures were incubated at 37°C, 5% CO_2 until analysed.

4.2.10.5 Stimulation with ephrin-Fc fusion proteins

As an in vitro system stimulation for Eph-receptors, soluble ephrin-Fc fusion proteins (R&D) were pre-clustered with goat-α-humanFc (R&D). Ephrin-Fc protein was used at a concentration of 1μg/ml of medium and incubated with α-humanFc antibody at a ratio of 10:1 for 1h at RT, diluted in PBS. Pre-clustering of the Fc fusion proteins was applied to mimic the higher-order clusters of Eph-receptor and ephrin ligands believed to occur in vivo.

4.2.11 Immunofluorescence

Cells or neurons grown on 12mm Ø glass coverslips (Marienfeld) were manipulated according to experimental design, placed on ice and rinsed once with cold PBS^{CaMg}. Cells were fixed with 4% PFA/8% sucrose for 20min on ice, rinsed with PBS^{CaMg}, incubated with 50mM Ammoniumchloride for 10min at RT, rinsed again with PBS^{CaMg} and permeabilised with PBS^{CaMg}/0.1% TritonX-100 for 5min on ice. Samples were washed 3x 5min with cold PBS^{CaMg} and blocked at RT for 30min with PBS^{CaMg}/2% BSA/4% serum. Serum was chosen depending on the species where secondary antibodies were raised in, or a combination of different species sera was used if the combination of secondary antibodies demanded it. All the following steps of the protocol were carried out in a dark, humidified chamber to prevent drying of the coverslips. Cells were incubated with the specific primary antibodies diluted in blocking solution for 1h at RT, washed 3x with PBS^{CaMg} and incubated for 30min at RT with secondary antibodies conjugated to fluophores, also diluted in blocking solution. For a list of fluophor-conjugated secondary antibodies, please refer to the Materials section. Coverslips were washed 5min at RT with PBS^{CaMg} and incubated with a 1:3000 dilution of Hoechst in PBS for 5min at RT. After a last washing step with PBS^{CaMg} for 5min at RT, samples were rinsed briefly in ddH_2O, carefully drained of excess liquid and mounted on glass slides with "Antifade Prolong" mounting medium (Molecular Probes). Samples were stored o/n in the dark to allow for complete hardening of mounting medium before analysis with a fluorescence microscope.

4.2.11.1 Pre-/post-permeabilisation staining

To monitor internalisation of surface proteins by immunofluorescence, the aforementioned protocol was altered as follows. After treatment of coverslips with Ammoniumchloride, samples were rinsed with PBS^{CaMg}, blocked for 30min at RT and directly incubated with primary antibodies (pre-permeabilisation staining). Cells were washed and incubated with secondary antibodies as described before, rinsed with PBS^{CaMg} and then permeabilized. Subsequently, samples were subjected to a second round of blocking, primary and secondary antibody incubation, this time the secondary antibody conjugated to a different colour fluophor (post-permeabilisation staining). This staining procedure allows for distinction between internalized receptor molecules and surface receptor molecules.

4.2.11.1.1 Quantification of internalisation

The assay was performed as follows. In brief, HeLa cells stably expressing EphA4-receptor were transiently transfected with eGFP as a control or Rin1-FL and eGFP (ratio 1:5). were stimulated for 30min with pre-clustered ephrinB3Fc, then fixed and stained with a Cy5-conjugated anti-Fc antibody (pre-permeabilisation staining) to reveal all surface clusters of EphA indirectly through detecting all clusters of ephrinB3Fc. Then cells were treated with 0.1% Tx-100 and stained with a TR-conjugated anti-Fc antibody to identify all internal receptor-ligand complexes that had been protected from staining inside the cell in the previous step. Quantification of internalisation was done as follows. Pictures were acquired blind to the nature of the transfected plasmid and with equal exposure times for all pictures acquired in each channel. Ananlysis of pictures was performed with the MetaMorph software (version 6.3r7, Molecular Devices). Outlines of transfected cell shapes were marked in the GFP channel, outlines transferred to the surface staining channel and all surface clusters within the outline identified. A mask of marked surface clusters was then transferred to the total Fc stain channel and additional receptor-ligand clusters counted. Internalisation was expressed as a ratio for each cell analysed of internal divided by total number of clusters counted. The mean of all ratios in one group (either eGFP alone or Rin1 and eGFP) was assessed and standard deviations and statistical revelance was calculated using the excel software (Microsoft® Office Excel 2003).

4.2.12 Histology

4.2.12.1 Cardiac perfusion

Mice were anaesthetised with chloralhydrate (400µl of a 5% solution in H_2O, injected into the abdomen), skin and ribcage were cut open and the diaphragm was removed. A small incision was made into the right auriculum and a syringe connected to an electrical pump was inserted into the left ventricle to replace the animal's blood by cold PBS. Blood removal was monitored by whitening of the liver, normally dark red. This was followed by approximately 25ml of 4% paraformaldehyde (PFA) solution for fixation. The level of fixation was assessed by checking tail stiffness. Brains were dissected out and postfixed overnight at 4°C in 4% PFA.

4.2.12.2 Cryosections

Fixed brains were cryo-protected first by an overnight incubation in 15% sucrose solution in PBS at 4°C, then a 30% step again overnight. Samples were carefully dried, then embedded in OCT on dry ice. Embedded brains were kept at -20°C or the cryostat chamber until sectioning. Usually 50 µm sections were cut for a floating staining protocol.

4.2.12.3 Vibratome sections

Perfused and postfixed brains were embedded in a gelatine-albumin (gel/alb) mixture (0.5g gelatine in 100ml PBS, then dissolved 30g egg albumin in this solution). A layer of 2ml gel/alb was poured into a small plastic mould and polymerisation started by vigorously stirring in 160µl 25% glutaraldehyde solution. The brain was placed on top and another 3ml gel/alb with 240 µl glutaraldehyde poured over it. The mould was left to set for 5minutes at RT before either storage in cold PBS or cutting with a vibratome. Generally, 80 -100 µm coronal sections were cut for the in situ hybridisation protocol.

4.2.12.4 Antibody stainings on tissue sections

Antibody stainings were generally performed on 40µm to 50µm floating cryostat sections. Immunofluorescence stainings were carried out as described for dissociated cells except all incubation times were prolonged to adjust for increased diffusion lengths of all compounds applied. Antibody stainings revealed by a HRP-conjugated secondary antibody were performed according to manufacturer's instructions (vectastain), and pre-treated with a 10% MetOH/3% H_2O_2 solution to quench endogenous peroxidase activity.

4.2.12.5 In situ hybridisation

All solutions used were prepared RNAse free. Sections were subjected to a MetOH dehydration series (25%, 50%, 75%, 2x100% MetOH, all steps 5min incubation at RT) and stored at least o/n at -20°C. Samples were rehydrated in the reverse order and incubated 3x 5min in PBT (PBS, 0.1% Tween20). Sections were digested with with 20µg/ml ProteinaseK in PBT for 13min at RT, rinsed 2x on ice with PBT and fixed for 40min on ice with freshly prepared 4% PFA, 0.2% glutaraldehyde before incubation with (pre-)hybridisation solution (50ml contain 25ml de-ionised formamide, 12.5ml 20x SSC pH 4.5, 100µl Tween20, 5ml 5% Chaps, 1g blocking reagent [Roche], 250 µl 10mg/ml tRNA, 50 µl 50mg/ml heparin and 500 µl 0.5M EDTA pH 8.1) for 1h at 70 °C. Probes were prepared as follows. For antisense probes, plasmids were digested at the 5' end verifying complete digestion on an agarose gel before phenol-chloroform extracting the DNA. The transcription reaction was performed with 2 µl template DNA (100ng/µl), 2 µl 10x transcription buffer, 2 µl 0.1M DTT, 2 µl DIG, 1 µl RNasin and 1 µl of the respective RNA polymerase (T3, T7 or sp6) for 3h at 37°C. 1 µl of the transcription reaction was checked on an agarose gel to verify efficiency. The RNA was precipitated by adding 100 µl TE buffer, 10 µl 4M LiCl and 300 µl EtOH before centrifuging at 13.000rpm for 20min at 4°C. Pellets were washed twice with 70% EtOH and dried briefly before resuspending in 100µl TE buffer. 10-30 µl of probe was used per 1ml of hybridisation buffer. Sections were incubated with this hybridisation solution at 70°C o/n. The following day samples were subjected to the following washing steps. 5min, then 3x 30min in solution I (50%

formamide, 5x SSC pH 4.5, 0.2% Tween20, 0.5% Chaps) at 70°C, 5min, then 3x 30min in solution II (50% formamide, 2x SSC pH 4.5, 0.2% Tween20, 0.1% Chaps) at 66°C, 5min, then 3x 30min in solution III (0.1% Chaps, 2x SSC pH4.5, 0.2% Tween20) at 66-68°C, 2x 5min in MABT (MAB pH 7.5, 0.2% Tween20) at RT and 2x 30min in MABT at 70°C. Subsequently, sections were blocked for 90min at RT in blocking solution (MABT, 2% blocking reagent and 20% sheep serum) before incubation with the anti-DIG antibody (1:2000 in blocking solution) o/n at 4°C. The following day, samples were washed 10x 30min with TBT (TBS, 0.1% Tween20), rinsed in NTMT (for 200ml: 4ml 5M NaCl, 20ml 1M Tris·HCl pH 9.5, 10ml 1M $MgCl_2$, 200µl Tween20) and equilibrated in NTMT for 20min at RT before developing the colour reaction in 1.4 µl NBT, 1.1 µl BCIP/ml NTMT. Development was stopped by rinsing in PBT. Samples were post-fixed in 4% PFA and mounted on glass slides with a 1:1 solution of 4% PFA and glycerol.

4.2.13 Electrophysiology

4.2.13.1 Slice preparation

Adult EphA4$^{-/-}$ and EphA4$^{wt/wt}$ littermate controls were used for the investigation. The brains were removed rapidly and placed in ice-cold artificial cerebro-spinal fluid (ACSF) containing 125mM NaCl, 2.5mM KCl, 25mM $NaHCO_3$, 2mM $CaCl_2$, 1mM $MgCl_2$, 25mM D-Glucose, 1.25mM NaH_2PO_4 (pH 7.4) and bubbled with a 95% O_2/5% CO_2 mixture. Coronal slices of the amygdala (400µm) were prepared using a vibroslicer (FTB). After incubation in a holding chamber with ACSF (22-25°C) for at least 60min, the slices were placed in the recording chamber of the setup and superfused with ACSF at a flow rate of 1.ml/min.

4.2.13.2 Electrophysiological recordings

Stimuli were delivered via bipolar concentric tungsten electrodes insulated to the tip (50μm diameter), and positioned on the border between the lateral amygdala (LA) and the external capsule to evoke field potentials (FPs). All recordings were performed in the LA at room temperature (22-25°C). FPs were recorded using glass microelectrodes (1-2MΩ) filled with ACSF. The stimulus intensities were adjusted in a manner to produce a FP of ~50% of the maximum amplitude. The voltage differences between the sharp negative onset and the negative peak (a), and between the negative peak and succeeding positive peak (b), were measured, and the amplitudes of the FPs were calculated as (a+b)/2.

4.2.14 Microscopy

Pictures of in situs in Figure 26, panels A, B, E and F were acquired with a LeicaMZFLIII stereomicroscope connected to a LeicaDC500 camera and the Leica image manager 1000 software. All other antibody stainings and in situs were analysed with a Zeiss Axioplan 2 imaging microscope. Images were acquired using either a Spot RT slider (colour images) or a Spot RT monochrome (immunofluorescence/ monochrome images) camera (Diagnostic Instruments, Inc.) and the MetaMorph software (version 6.3r7 and earlier versions, Molecular Devices). Confocal images were obtained with the LeicaTCS SP2 microscope and the Leica confocal software (version 2.61, Leica microsystems).

5 Bibliography

Adams, R.H., and R. Klein. 2000. Eph receptors and ephrin ligands. essential mediators of vascular development. Trends Cardiovasc Med. 10:183-8.

Adams, R.H., F. Diella, S. Hennig, F. Helmbacher, U. Deutsch, and R. Klein. 2001. The cytoplasmic domain of the ligand ephrinB2 is required for vascular morphogenesis but not cranial neural crest migration. Cell. 104:57-69.

Afar, D.E., L. Han, J. McLaughlin, S. Wong, A. Dhaka, K. Parmar, N. Rosenberg, O.N. Witte, and J. Colicelli. 1997. Regulation of the oncogenic activity of BCR-ABL by a tightly bound substrate protein RIN1. Immunity. 6:773-82.

Alberts B, et al. Molecular Biology of the Cell, 3rd ed. Garland Publishing, Inc., New York, 1994

Alory, C., and W.E. Balch. 2001. Organization of the Rab-GDI/CHM superfamily: the functional basis for choroideremia disease. Traffic. 2:532-43.

Amorapanth, P., J.E. LeDoux, and K. Nader. 2000. Different lateral amygdala outputs mediate reactions and actions elicited by a fear-arousing stimulus. Nat Neurosci. 3:74-9.

Apodaca, G. 2001. Endocytic traffic in polarized epithelial cells: role of the actin and microtubule cytoskeleton. Traffic. 2:149-59.

Armstrong, J.N., M.J. Saganich, N.J. Xu, M. Henkemeyer, S.F. Heinemann, and A. Contractor. 2006. B-ephrin reverse signaling is required for NMDA-independent long-term potentiation of mossy fibers in the hippocampus. J Neurosci. 26:3474-81.

Arthur, W.T., L.A. Quilliam, and J.A. Cooper. 2004. Rap1 promotes cell spreading by localizing Rac guanine nucleotide exchange factors. J Cell Biol. 167:111-22.

Atkins, C.M., J.C. Selcher, J.J. Petraitis, J.M. Trzaskos, and J.D. Sweatt. 1998. The MAPK cascade is required for mammalian associative learning. Nat Neurosci. 1:602-9.

Baass, P.C., G.M. Di Guglielmo, F. Authier, B.I. Posner, and J.J. Bergeron. 1995. Compartmentalized signal transduction by receptor tyrosine kinases. Trends Cell Biol. 5:465-70.

Bar-Sagi, D., and J.R. Feramisco. 1986. Induction of membrane ruffling and fluid-phase pinocytosis in quiescent fibroblasts by ras proteins. Science. 233:1061-8.

Barbieri, M.A., A.D. Kohn, R.A. Roth, and P.D. Stahl. 1998. Protein kinase B/akt and rab5 mediate Ras activation of endocytosis. J Biol Chem. 273:19367-70.

Barbieri, M.A., R.L. Roberts, A. Gumusboga, H. Highfield, C. Alvarez-Dominguez, A. Wells, and P.D. Stahl. 2000. Epidermal growth factor and membrane trafficking. EGF receptor activation of endocytosis requires Rab5a. J Cell Biol. 151:539-50.

Barbieri, M.A., C. Kong, P.I. Chen, B.F. Horazdovsky, and P.D. Stahl. 2003. The SRC homology 2 domain of Rin1 mediates its binding to the epidermal growth factor receptor and regulates receptor endocytosis. J Biol Chem. 278:32027-36.

Battaglia, A.A., K. Sehayek, J. Grist, S.B. McMahon, and I. Gavazzi. 2003. EphB receptors and ephrin-B ligands regulate spinal sensory connectivity and modulate pain processing. Nat Neurosci. 6:339-40.

Berdnik, D., T. Torok, M. Gonzalez-Gaitan, and J.A. Knoblich. 2002. The endocytic protein alpha-Adaptin is required for numb-mediated asymmetric cell division in Drosophila. Dev Cell. 3:221-31.

Bergemann, A.D., L. Zhang, M.K. Chiang, R. Brambilla, R. Klein, and J.G. Flanagan. 1998. Ephrin-B3, a ligand for the receptor EphB3, expressed at the midline of the developing neural tube. Oncogene. 16:471-80.

Bertet, C., L. Sulak, and T. Lecuit. 2004. Myosin-dependent junction remodelling controls planar cell intercalation and axis elongation. Nature. 429:667-71.

Binns, K.L., P.P. Taylor, F. Sicheri, T. Pawson, and S.J. Holland. 2000. Phosphorylation of tyrosine residues in the kinase domain and juxtamembrane region regulates the biological and catalytic activities of Eph receptors. Mol Cell Biol. 20:4791-805.

Birgbauer, E., C.A. Cowan, D.W. Sretavan, and M. Henkemeyer. 2000. Kinase independent function of EphB receptors in retinal axon pathfinding to the optic disc from dorsal but not ventral retina. Development. 127:1231-41.

Blair, H.T., G.E. Schafe, E.P. Bauer, S.M. Rodrigues, and J.E. LeDoux. 2001. Synaptic plasticity in the lateral amygdala: a cellular hypothesis of fear conditioning. Learn Mem. 8:229-42.

Bliss, T.V., and T. Lomo. 1973. Long-lasting potentiation of synaptic transmission in the dentate area of the anaesthetized rabbit following stimulation of the perforant path. J Physiol. 232:331-56.
Bliss, T.V., and G.L. Collingridge. 1993. A synaptic model of memory: long-term potentiation in the hippocampus. Nature. 361:31-9.

Bonhoeffer, T., and R. Yuste. 2002. Spine motility. Phenomenology, mechanisms, and function. Neuron. 35:1019-27.

Bonifacino, J.S., and J. Lippincott-Schwartz. 2003. Coat proteins: shaping membrane transport. Nat Rev Mol Cell Biol. 4:409-14.

Bossing, T., and A.H. Brand. 2002. Dephrin, a transmembrane ephrin with a unique structure, prevents interneuronal axons from exiting the Drosophila embryonic CNS. Development. 129:4205-18.

Boyle, M., A. Nighorn, and J.B. Thomas. 2006. Drosophila Eph receptor guides specific axon branches of mushroom body neurons. Development. 133:1845-54.

Braisted, J.E., T. McLaughlin, H.U. Wang, G.C. Friedman, D.J. Anderson, and D. O'Leary D. 1997. Graded and lamina-specific distributions of ligands of EphB receptor tyrosine kinases in the developing retinotectal system. Dev Biol. 191:14-28.

Brambilla, R., N. Gnesutta, L. Minichiello, G. White, A.J. Roylance, C.E. Herron, M. Ramsey, D.P. Wolfer, V. Cestari, C. Rossi-Arnaud, S.G. Grant, P.F. Chapman, H.P. Lipp, E. Sturani,

and R. Klein. 1997. A role for the Ras signalling pathway in synaptic transmission and long-term memory. Nature. 390:281-6.

Brown, T.C., I.C. Tran, D.S. Backos, and J.A. Esteban. 2005. NMDA receptor-dependent activation of the small GTPase Rab5 drives the removal of synaptic AMPA receptors during hippocampal LTD. Neuron. 45:81-94.

Bruckner, K., E.B. Pasquale, and R. Klein. 1997. Tyrosine phosphorylation of transmembrane ligands for Eph receptors. Science. 275:1640-3.

Bruckner, K., J. Pablo Labrador, P. Scheiffele, A. Herb, P.H. Seeburg, and R. Klein. 1999. EphrinB ligands recruit GRIP family PDZ adaptor proteins into raft membrane microdomains. Neuron. 22:511-24.

Cagan, R.L., H. Kramer, A.C. Hart, and S.L. Zipursky. 1992. The bride of sevenless and sevenless interaction: internalization of a transmembrane ligand. Cell. 69:393-9.

Cajal R, La fine structure des centres nerveux. Proc R Soc Lond, 55:444-68, 1894

Carvalho, R.F., M. Beutler, K.J. Marler, B. Knoll, E. Becker-Barroso, R. Heintzmann, T. Ng, and U. Drescher. 2006. Silencing of EphA3 through a cis interaction with ephrinA5. Nat Neurosci. 9:322-30.

Cavalli, V., M. Corti, and J. Gruenberg. 2001. Endocytosis and signaling cascades: a close encounter. FEBS Lett. 498:190-6.

Chen, H., and P. De Camilli. 2005. The association of epsin with ubiquitinated cargo along the endocytic pathway is negatively regulated by its interaction with clathrin. Proc Natl Acad Sci U S A. 102:2766-71.

Cheng, H.J., M. Nakamoto, A.D. Bergemann, and J.G. Flanagan. 1995. Complementary gradients in expression and binding of ELF-1 and Mek4 in development of the topographic retinotectal projection map. Cell. 82:371-81.

Chiu, V.K., T. Bivona, A. Hach, J.B. Sajous, J. Silletti, H. Wiener, R.L. Johnson, 2nd, A.D. Cox, and M.R. Philips. 2002. Ras signalling on the endoplasmic reticulum and the Golgi. Nat Cell Biol. 4:343-50.

Cho KO, H.C., Kennedy MB. 1992. The rat brain postsynaptic density fraction contains a homolog of the Drosophila discs-large tumor suppressor protein. Neuron. 9:929-42.

Choi, S.I., R. Vidal, B. Frangione, and E. Levy. 2004. Axonal transport of British and Danish amyloid peptides via secretory vesicles. Faseb J. 18:373-5.

Christoforidis, S., M. Miaczynska, K. Ashman, M. Wilm, L. Zhao, S.C. Yip, M.D. Waterfield, J.M. Backer, and M. Zerial. 1999. Phosphatidylinositol-3-OH kinases are Rab5 effectors. Nat Cell Biol. 1:249-52.

Christoforidis, S., H.M. McBride, R.D. Burgoyne, and M. Zerial. 1999. The Rab5 effector EEA1 is a core component of endosome docking. Nature. 397:621-5.

Clague, M.J., and S. Urbe. 2001. The interface of receptor trafficking and signalling. J Cell Sci. 114:3075-81.

Classen, A.K., K.I. Anderson, E. Marois, and S. Eaton. 2005. Hexagonal packing of Drosophila wing epithelial cells by the planar cell polarity pathway. Dev Cell. 9:805-17.

Cohen, P. 1992. Signal integration at the level of protein kinases, protein phosphatases and their substrates. Trends Biochem Sci. 17:408-13.

Colicelli, J., C. Nicolette, C. Birchmeier, L. Rodgers, M. Riggs, and M. Wigler. 1991. Expression of three mammalian cDNAs that interfere with RAS function in Saccharomyces cerevisiae. Proc Natl Acad Sci U S A. 88:2913-7.

Conner, S.D., and S.L. Schmid. 2003. Regulated portals of entry into the cell. Nature. 422:37-44.
Constantine-Paton, M., and H.T. Cline. 1998. LTP and activity-dependent synaptogenesis: the more alike they are, the more different they become. Curr Opin Neurobiol. 8:139-48.

Contractor, A., C. Rogers, C. Maron, M. Henkemeyer, G.T. Swanson, and S.F. Heinemann. 2002. Trans-synaptic Eph receptor-ephrin signaling in hippocampal mossy fiber LTP. Science. 296:1864-9.

Couso, J.P., M. Bate, and A. Martinez-Arias. 1993. A wingless-dependent polar coordinate system in Drosophila imaginal discs. Science. 259:484-9.

Cowan, C.A., and M. Henkemeyer. 2001. The SH2/SH3 adaptor Grb4 transduces B-ephrin reverse signals. Nature. 413:174-9.

Cowan, C.A., N. Yokoyama, A. Saxena, M.J. Chumley, R.E. Silvany, L.A. Baker, D. Srivastava, and M. Henkemeyer. 2004. Ephrin-B2 reverse signaling is required for axon pathfinding and cardiac valve formation but not early vascular development. Dev Biol. 271:263-71.

Cowan, C.W., Y.R. Shao, M. Sahin, S.M. Shamah, M.Z. Lin, P.L. Greer, S. Gao, E.C. Griffith, J.S. Brugge, and M.E. Greenberg. 2005. Vav family GEFs link activated Ephs to endocytosis and axon guidance. Neuron. 46:205-17.

Cutforth, T., L. Moring, M. Mendelsohn, A. Nemes, N.M. Shah, M.M. Kim, J. Frisen, and R. Axel. 2003. Axonal ephrin-As and odorant receptors: coordinate determination of the olfactory sensory map. Cell. 114:311-22.

da Costa, S.R., C.T. Okamoto, and S.F. Hamm-Alvarez. 2003. Actin microfilaments et al.--the many components, effectors and regulators of epithelial cell endocytosis. Adv Drug Deliv Rev. 55:1359-83.

Davare, M.A., T. Saneyoshi, E.S. Guire, S.C. Nygaard, and T.R. Soderling. 2004. Inhibition of calcium/calmodulin-dependent protein kinase kinase by protein 14-3-3. J Biol Chem. 279:52191-9.

Davis, S., N.W. Gale, T.H. Aldrich, P.C. Maisonpierre, V. Lhotak, T. Pawson, M. Goldfarb, and G.D. Yancopoulos. 1994. Ligands for EPH-related receptor tyrosine kinases that require membrane attachment or clustering for activity. Science. 266:816-9.

Davis, M. The role of the amygdala in conditioned and unconditioned fear and anxiety. In: The amygdala, edited by Aggleton, JP. Oxford, UK: Oxford Univ. Press, 2000

Davy, A., N.W. Gale, E.W. Murray, R.A. Klinghoffer, P. Soriano, C. Feuerstein, and S.M. Robbins. 1999. Compartmentalized signaling by GPI-anchored ephrin-A5 requires the Fyn tyrosine kinase to regulate cellular adhesion. Genes Dev. 13:3125-35.

Davy, A., and S.M. Robbins. 2000. Ephrin-A5 modulates cell adhesion and morphology in an integrin-dependent manner. Embo J. 19:5396-405.

Davy, A., J. Aubin, and P. Soriano. 2004. Ephrin-B1 forward and reverse signaling are required during mouse development. Genes Dev. 18:572-83.

Davy, A., and P. Soriano. 2005. Ephrin signaling in vivo: look both ways. Dev Dyn. 232:1-10.

De Matteis, M.A., and A. Godi. 2004. PI-loting membrane traffic. Nat Cell Biol. 6:487-92.

Delcroix, J.D., J.S. Valletta, C. Wu, S.J. Hunt, A.S. Kowal, and W.C. Mobley. 2003. NGF signaling in sensory neurons: evidence that early endosomes carry NGF retrograde signals. Neuron. 39:69-84.

Dhaka, A., R.M. Costa, H. Hu, D.K. Irvin, A. Patel, H.I. Kornblum, A.J. Silva, T.J. O'Dell, and J. Colicelli. 2003. The RAS effector RIN1 modulates the formation of aversive memories. J Neurosci. 23:748-57.

Di Guglielmo, G.M., P.C. Baass, W.J. Ou, B.I. Posner, and J.J. Bergeron. 1994. Compartmentalization of SHC, GRB2 and mSOS, and hyperphosphorylation of Raf-1 by EGF but not insulin in liver parenchyma. Embo J. 13:4269-77.

Di Guglielmo, G.M., C. Le Roy, A.F. Goodfellow, and J.L. Wrana. 2003. Distinct endocytic pathways regulate TGF-beta receptor signalling and turnover. Nat Cell Biol. 5:410-21.

Dityatev, A.E., and V.Y. Bolshakov. 2005. Amygdala, long-term potentiation, and fear conditioning. Neuroscientist. 11:75-88.

Dravis, C., N. Yokoyama, M.J. Chumley, C.A. Cowan, R.E. Silvany, J. Shay, L.A. Baker, and M. Henkemeyer. 2004. Bidirectional signaling mediated by ephrin-B2 and EphB2 controls urorectal development. Dev Biol. 271:272-90.

Drescher, U., F. Bonhoeffer, and B.K. Muller. 1997. The Eph family in retinal axon guidance. Curr Opin Neurobiol. 7:75-80.

Drescher, U. 2002. Eph family functions from an evolutionary perspective. Curr Opin Genet Dev. 12:397-402.

Dubois, L., M. Lecourtois, C. Alexandre, E. Hirst, and J.P. Vincent. 2001. Regulated endocytic routing modulates wingless signaling in Drosophila embryos. Cell. 105:613-24.

Duchek, P., and P. Rorth. 2001. Guidance of cell migration by EGF receptor signaling during Drosophila oogenesis. Science. 291:131-3.

Duchek, P., K. Somogyi, G. Jekely, S. Beccari, and P. Rorth. 2001. Guidance of cell migration by the Drosophila PDGF/VEGF receptor. Cell. 107:17-26.

Dufour, A., J. Seibt, L. Passante, V. Depaepe, T. Ciossek, J. Frisen, K. Kullander, J.G. Flanagan, F. Polleux, and P. Vanderhaeghen. 2003. Area specificity and topography of thalamocortical projections are controlled by ephrin/Eph genes. Neuron. 39:453-65.

Egea, J., U.V. Nissen, A. Dufour, M. Sahin, P. Greer, K. Kullander, T.D. Mrsic-Flogel, M.E. Greenberg, O. Kiehn, P. Vanderhaeghen, and R. Klein. 2005. Regulation of EphA 4 kinase activity is required for a subset of axon guidance decisions suggesting a key role for receptor clustering in Eph function. Neuron. 47:515-28.

Ellis, C., F. Kasmi, P. Ganju, E. Walls, G. Panayotou, and A.D. Reith. 1996. A juxtamembrane autophosphorylation site in the Eph family receptor tyrosine kinase, Sek, mediates high affinity interaction with p59fyn. Oncogene. 12:1727-36.

Emery, G., A. Hutterer, D. Berdnik, B. Mayer, F. Wirtz-Peitz, M.G. Gaitan, and J.A. Knoblich. 2005. Asymmetric Rab 11 endosomes regulate delta recycling and specify cell fate in the Drosophila nervous system. Cell. 122:763-73.

Emery, G., and J.A. Knoblich. 2006. Endosome dynamics during development. Curr Opin Cell Biol. 18:407-15.

Entchev, E.V., A. Schwabedissen, and M. Gonzalez-Gaitan. 2000. Gradient formation of the TGF-beta homolog Dpp. Cell. 103:981-91.

Ethell, I.M., and Y. Yamaguchi. 1999. Cell surface heparan sulfate proteoglycan syndecan-2 induces the maturation of dendritic spines in rat hippocampal neurons. J Cell Biol. 144:575-86.

Ethell, I.M., F. Irie, M.S. Kalo, J.R. Couchman, E.B. Pasquale, and Y. Yamaguchi. 2001. EphB/syndecan-2 signaling in dendritic spine morphogenesis. Neuron. 31:1001-13.

Fan, G.H., L.A. Lapierre, J.R. Goldenring, J. Sai, and A. Richmond. 2004. Rab11-family interacting protein 2 and myosin Vb are required for CXCR2 recycling and receptor-mediated chemotaxis. Mol Biol Cell. 15:2456-69.

Fanselow, M.S., and J.E. LeDoux. 1999. Why we think plasticity underlying Pavlovian fear conditioning occurs in the basolateral amygdala. Neuron. 23:229-32.

Farb, C.R., and J.E. Ledoux. 1999. Afferents from rat temporal cortex synapse on lateral amygdala neurons that express NMDA and AMPA receptors. Synapse. 33:218-29.

Fiala, J.C., M. Feinberg, V. Popov, and K.M. Harris. 1998. Synaptogenesis via dendritic filopodia in developing hippocampal area CA1. J Neurosci. 18:8900-11.

Fortini, M.E. 2001. Notch and presenilin: a proteolytic mechanism emerges. Curr Opin Cell Biol. 13:627-34.

Fotinopoulou, A., M. Tsachaki, M. Vlavaki, A. Poulopoulos, A. Rostagno, B. Frangione, J. Ghiso, and S. Efthimiopoulos. 2005. BRI2 interacts with amyloid precursor protein (APP) and regulates amyloid beta (Abeta) production. J Biol Chem. 280:30768-72.

Gauthier, L.R., and S.M. Robbins. 2003. Ephrin signaling: One raft to rule them all? One raft to sort them? One raft to spread their call and in signaling bind them? Life Sci. 74:207-16.

Gavin, A.C., M. Bosche, R. Krause, P. Grandi, M. Marzioch, A. Bauer, J. Schultz, J.M. Rick, A.M. Michon, C.M. Cruciat, M. Remor, C. Hofert, M. Schelder, M. Brajenovic, H. Ruffner, A. Merino, K. Klein, M. Hudak, D. Dickson, T. Rudi, V. Gnau, A. Bauch, S. Bastuck, B. Huhse, C. Leutwein, M.A. Heurtier, R.R. Copley, A. Edelmann, E. Querfurth, V. Rybin, G. Drewes, M. Raida, T. Bouwmeester, P. Bork, B. Seraphin, B. Kuster, G. Neubauer, and G. Superti-Furga. 2002. Functional organization of the yeast proteome by systematic analysis of protein complexes. Nature. 415:141-7.

George, S.E., K. Simokat, J. Hardin, and A.D. Chisholm. 1998. The VAB-1 Eph receptor tyrosine kinase functions in neural and epithelial morphogenesis in C. elegans. Cell. 92:633-43.

Gerges, N.Z., D.S. Backos, and J.A. Esteban. 2004. Local control of AMPA receptor trafficking at the postsynaptic terminal by a small GTPase of the Rab family. J Biol Chem. 279:43870-8.

Gonzalez-Billault, C., E.M. Jimenez-Mateos, A. Caceres, J. Diaz-Nido, F. Wandosell, and J. Avila. 2004. Microtubule-associated protein 1B function during normal development, regeneration, and pathological conditions in the nervous system. J Neurobiol. 58:48-59.

Goodwin, J.S., K.R. Drake, C. Rogers, L. Wright, J. Lippincott-Schwartz, M.R. Philips, and A.K. Kenworthy. 2005. Depalmitoylated Ras traffics to and from the Golgi complex via a nonvesicular pathway. J Cell Biol. 170:261-72.

Goosens, K.A., and S. Maren. 2004. NMDA receptors are essential for the acquisition, but not expression, of conditional fear and associative spike firing in the lateral amygdala. Eur J Neurosci. 20:537-48.

Grimes, M.L., J. Zhou, E.C. Beattie, E.C. Yuen, D.E. Hall, J.S. Valletta, K.S. Topp, J.H. LaVail, N.W. Bunnett, and W.C. Mobley. 1996. Endocytosis of activated TrkA: evidence that nerve growth factor induces formation of signaling endosomes. J Neurosci. 16:7950-64.

Gruenberg, J. 2001. The endocytic pathway: a mosaic of domains. Nat Rev Mol Cell Biol. 2:721-30.

Grunwald, I.C., M. Korte, G. Adelmann, A. Plueck, K. Kullander, R.H. Adams, M. Frotscher, T. Bonhoeffer, and R. Klein. 2004. Hippocampal plasticity requires postsynaptic ephrinBs. Nat Neurosci. 7:33-40.

Halford, M.M., M.J. Chumley, and M. Henkemeyer. 2003. Ephective endocytosis. Dev Cell. 5:536-7.

Hammond, D.E., S. Carter, J. McCullough, S. Urbe, G. Vande Woude, and M.J. Clague. 2003. Endosomal dynamics of Met determine signaling output. Mol Biol Cell. 14:1346-54.

Han, L., and J. Colicelli. 1995. A human protein selected for interference with Ras function interacts directly with Ras and competes with Raf1. Mol Cell Biol. 15:1318-23.

Han, L., D. Wong, A. Dhaka, D. Afar, M. White, W. Xie, H. Herschman, O. Witte, and J. Colicelli. 1997. Protein binding and signaling properties of RIN1 suggest a unique effector function. Proc Natl Acad Sci U S A. 94:4954-9.

Han, W., T. Zhang, H. Yu, J.G. Foulke, and C.K. Tang. 2006. Hypophosphorylation of Residue Y1045 Leads to Defective Downregulation of EGFRvIII. Cancer Biol Ther. 5.

Hancock, J.F. 2003. Ras proteins: different signals from different locations. Nat Rev Mol Cell Biol. 4:373-84.

Harris, K.M., and S.B. Kater. 1994. Dendritic spines: cellular specializations imparting both stability and flexibility to synaptic function. Annu Rev Neurosci. 17:341-71.

Harris, K.M. 1999. Structure, development, and plasticity of dendritic spines. Curr Opin Neurobiol. 9:343-8.

Hattori, M., M. Osterfield, and J.G. Flanagan. 2000. Regulated cleavage of a contact-mediated axon repellent. Science. 289:1360-5.

Hayashi, Y., S.H. Shi, J.A. Esteban, A. Piccini, J.C. Poncer, and R. Malinow. 2000. Driving AMPA receptors into synapses by LTP and CaMKII: requirement for GluR1 and PDZ domain interaction. Science. 287:2262-7.

Hebb D, (1949) The organization of Behavior; a Neuropsychological Theory. Wiley-Interscience, New York. Reprinted by Lauwrence Erlbaum Associates, 2002)

Heisenberg, C.P., M. Tada, G.J. Rauch, L. Saude, M.L. Concha, R. Geisler, D.L. Stemple, J.C. Smith, and S.W. Wilson. 2000. Silberblick/Wnt11 mediates convergent extension movements during zebrafish gastrulation. Nature. 405:76-81.

Henderson, J.T., J. Georgiou, Z. Jia, J. Robertson, S. Elowe, J.C. Roder, and T. Pawson. 2001. The receptor tyrosine kinase EphB2 regulates NMDA-dependent synaptic function. Neuron. 32:1041-56.

Hering, H., and M. Sheng. 2001. Dendritic spines: structure, dynamics and regulation. Nat Rev Neurosci. 2:880-8.

Himanen, J.P., and D.B. Nikolov. 2003. Eph signaling: a structural view. Trends Neurosci. 26:46-51.

Himanen, J.P., and D.B. Nikolov. 2003. Eph receptors and ephrins. Int J Biochem Cell Biol. 35:130-4.

Himanen, J.P., M.J. Chumley, M. Lackmann, C. Li, W.A. Barton, P.D. Jeffrey, C. Vearing, D. Geleick, D.A. Feldheim, A.W. Boyd, M. Henkemeyer, and D.B. Nikolov. 2004. Repelling class discrimination: ephrin-A5 binds to and activates EphB2 receptor signaling. Nat Neurosci. 7:501-9.

Hindges, R., T. McLaughlin, N. Genoud, M. Henkemeyer, and D.D. O'Leary. 2002. EphB forward signaling controls directional branch extension and arborization required for dorsal-ventral retinotopic mapping. Neuron. 35:475-87.

Hoeller, D., S. Volarevic, and I. Dikic. 2005. Compartmentalization of growth factor receptor signalling. Curr Opin Cell Biol. 17:107-11.

Hoepfner, S., F. Severin, A. Cabezas, B. Habermann, A. Runge, D. Gillooly, H. Stenmark, and M. Zerial. 2005. Modulation of receptor recycling and degradation by the endosomal kinesin KIF16B. Cell. 121:437-50.

Holahan, M.R., and N.M. White. 2002. Conditioned memory modulation, freezing, and avoidance as measures of amygdala-mediated conditioned fear. Neurobiol Learn Mem. 77:250-75.

Holash, J.A., and E.B. Pasquale. 1995. Polarized expression of the receptor protein tyrosine kinase Cek5 in the developing avian visual system. Dev Biol. 172:683-93.

Holland, S.J., N.W. Gale, G. Mbamalu, G.D. Yancopoulos, M. Henkemeyer, and T. Pawson. 1996. Bidirectional signalling through the EPH-family receptor Nuk and its transmembrane ligands. Nature. 383:722-5.

Holmberg, J., A. Armulik, K.A. Senti, K. Edoff, K. Spalding, S. Momma, R. Cassidy, J.G. Flanagan, and J. Frisen. 2005. Ephrin-A2 reverse signaling negatively regulates neural progenitor proliferation and neurogenesis. Genes Dev. 19:462-71.

Hori, K., M. Fostier, M. Ito, T.J. Fuwa, M.J. Go, H. Okano, M. Baron, and K. Matsuno. 2004. Drosophila deltex mediates suppressor of Hairless-independent and late-endosomal activation of Notch signaling. Development. 131:5527-37.

Horiuchi, H., R. Lippe, H.M. McBride, M. Rubino, P. Woodman, H. Stenmark, V. Rybin, M. Wilm, K. Ashman, M. Mann, and M. Zerial. 1997. A novel Rab5 GDP/GTP exchange factor complexed to Rabaptin-5 links nucleotide exchange to effector recruitment and function. Cell. 90:1149-59.

Hornberger, M.R., D. Dutting, T. Ciossek, T. Yamada, C. Handwerker, S. Lang, F. Weth, J. Huf, R. Wessel, C. Logan, H. Tanaka, and U. Drescher. 1999. Modulation of EphA receptor function by coexpressed ephrinA ligands on retinal ganglion cell axons. Neuron. 22:731-42.

Hu, H., J.M. Bliss, Y. Wang, and J. Colicelli. 2005. RIN1 is an ABL tyrosine kinase activator and a regulator of epithelial-cell adhesion and migration. Curr Biol. 15:815-23.

Huai, J., and U. Drescher. 2001. An ephrin-A-dependent signaling pathway controls integrin function and is linked to the tyrosine phosphorylation of a 120-kDa protein. J Biol Chem. 276:6689-94.

Hunker, C.M., H. Giambini, A. Galvis, J. Hall, I. Kruk, M.L. Veisaga, and M.A. Barbieri. 2006. Rin1 regulates insulin receptor signal transduction pathways. Exp Cell Res. 312:1106-18.

Hunker, C.M., A. Galvis, I. Kruk, H. Giambini, M.L. Veisaga, and M.A. Barbieri. 2006. Rab5-activating protein 6, a novel endosomal protein with a role in endocytosis. Biochem Biophys Res Commun. 340:967-75.

Hutterer, A., and J.A. Knoblich. 2005. Numb and alpha-Adaptin regulate Sanpodo endocytosis to specify cell fate in Drosophila external sensory organs. EMBO Rep. 6:836-42.

Incardona, J.P., J.H. Lee, C.P. Robertson, K. Enga, R.P. Kapur, and H. Roelink. 2000. Receptor-mediated endocytosis of soluble and membrane-tethered Sonic hedgehog by Patched-1. Proc Natl Acad Sci U S A. 97:12044-9.

Irie, F., and Y. Yamaguchi. 2002. EphB receptors regulate dendritic spine development via intersectin, Cdc42 and N-WASP. Nat Neurosci. 5:1117-8.

Irie, F., M. Okuno, E.B. Pasquale, and Y. Yamaguchi. 2005. EphrinB-EphB signalling regulates clathrin-mediated endocytosis through tyrosine phosphorylation of synaptojanin 1. Nat Cell Biol. 7:501-9.

Iwamasa, H., K. Ohta, T. Yamada, K. Ushijima, H. Terasaki, and H. Tanaka. 1999. Expression of Eph receptor tyrosine kinases and their ligands in chick embryonic motor neurons and hindlimb muscles. Dev Growth Differ. 41:685-98.

Jekely, G., H.H. Sung, C.M. Luque, and P. Rorth. 2005. Regulators of endocytosis maintain localized receptor tyrosine kinase signaling in guided migration. Dev Cell. 9:197-207.

Johannes, L., and C. Lamaze. 2002. Clathrin-dependent or not: is it still the question? Traffic. 3:443-51.

Kajiho, H., K. Saito, K. Tsujita, K. Kontani, Y. Araki, H. Kurosu, and T. Katada. 2003. RIN3: a novel Rab5 GEF interacting with amphiphysin II involved in the early endocytic pathway. J Cell Sci. 116:4159-68.

Kaksonen, M., C.P. Toret, and D.G. Drubin. 2006. Harnessing actin dynamics for clathrin-mediated endocytosis. Nat Rev Mol Cell Biol. 7:404-14.

Kamei, T., T. Matozaki, T. Sakisaka, A. Kodama, S. Yokoyama, Y.F. Peng, K. Nakano, K. Takaishi, and Y. Takai. 1999. Coendocytosis of cadherin and c-Met coupled to disruption of cell-cell adhesion in MDCK cells--regulation by Rho, Rac and Rab small G proteins. Oncogene. 18:6776-84.

Katz, L.C., and C.J. Shatz. 1996. Synaptic activity and the construction of cortical circuits. Science. 274:1133-8.

Kawakatsu, T., H. Ogita, T. Fukuhara, T. Fukuyama, Y. Minami, K. Shimizu, and Y. Takai. 2005. Vav2 as a Rac-GDP/GTP exchange factor responsible for the nectin-induced, c-Src- and Cdc42-mediated activation of Rac. J Biol Chem. 280:4940-7.

Kimura, T., T. Sakisaka, T. Baba, T. Yamada, and Y. Takai. 2006. Involvement of the Ras-Ras-activated Rab5 guanine nucleotide exchange factor RIN2-Rab5 pathway in the hepatocyte growth factor-induced endocytosis of E-cadherin. J Biol Chem. 281:10598-609.

Kirchhausen, T. 2000. Clathrin. Annu Rev Biochem. 69:699-727.

Kirkham, M., A. Fujita, R. Chadda, S.J. Nixon, T.V. Kurzchalia, D.K. Sharma, R.E. Pagano, J.F. Hancock, S. Mayor, and R.G. Parton. 2005. Ultrastructural identification of uncoated caveolin-independent early endocytic vehicles. J Cell Biol. 168:465-76.

Klein, R. 2004. Eph/ephrin signaling in morphogenesis, neural development and plasticity. Curr Opin Cell Biol. 16:580-9.

Knoll, B., K. Zarbalis, W. Wurst, and U. Drescher. 2001. A role for the EphA family in the topographic targeting of vomeronasal axons. Development. 128:895-906.

Knoll, B., and U. Drescher. 2002. Ephrin-As as receptors in topographic projections. Trends Neurosci. 25:145-9.

Koch, C.A., D. Anderson, M.F. Moran, C. Ellis, and T. Pawson. 1991. SH2 and SH3 domains: elements that control interactions of cytoplasmic signaling proteins. Science. 252:668-74.

Koo, E.H., and R. Kopan. 2004. Potential role of presenilin-regulated signaling pathways in sporadic neurodegeneration. Nat Med. 10 Suppl:S26-33.

Kullander, K., S.D. Croll, M. Zimmer, L. Pan, J. McClain, V. Hughes, S. Zabski, T.M. DeChiara, R. Klein, G.D. Yancopoulos, and N.W. Gale. 2001. Ephrin-B3 is the midline barrier that prevents corticospinal tract axons from recrossing, allowing for unilateral motor control. Genes Dev. 15:877-88.

Kullander, K., N.K. Mather, F. Diella, M. Dottori, A.W. Boyd, and R. Klein. 2001. Kinase-dependent and kinase-independent functions of EphA4 receptors in major axon tract formation in vivo. Neuron. 29:73-84.

Kullander, K., and R. Klein. 2002. Mechanisms and functions of Eph and ephrin signalling. Nat Rev Mol Cell Biol. 3:475-86.

Labrador, J.P., R. Brambilla, and R. Klein. 1997. The N-terminal globular domain of Eph receptors is sufficient for ligand binding and receptor signaling. Embo J. 16:3889-97.

Lackmann, M., R.J. Mann, L. Kravets, F.M. Smith, T.A. Bucci, K.F. Maxwell, G.J. Howlett, J.E. Olsson, T. Vanden Bos, D.P. Cerretti, and A.W. Boyd. 1997. Ligand for EPH-related kinase (LERK) 7 is the preferred high affinity ligand for the HEK receptor. J Biol Chem. 272:16521-30.

Lackmann, M., A.C. Oates, M. Dottori, F.M. Smith, C. Do, M. Power, L. Kravets, and A.W. Boyd. 1998. Distinct subdomains of the EphA3 receptor mediate ligand binding and receptor dimerization. J Biol Chem. 273:20228-37.

Lai, E.C., F. Roegiers, X. Qin, Y.N. Jan, and G.M. Rubin. 2005. The ubiquitin ligase Drosophila Mind bomb promotes Notch signaling by regulating the localization and activity of Serrate and Delta. Development. 132:2319-32.

Le Borgne, R., S. Remaud, S. Hamel, and F. Schweisguth. 2005. Two distinct E3 ubiquitin ligases have complementary functions in the regulation of delta and serrate signaling in Drosophila. PLoS Biol. 3:e96.

Le Borgne, R. 2006. Regulation of Notch signalling by endocytosis and endosomal sorting. Curr Opin Cell Biol. 18:213-22.

Le Roy, C., and J.L. Wrana. 2005. Clathrin- and non-clathrin-mediated endocytic regulation of cell signalling. Nat Rev Mol Cell Biol. 6:112-26.

Lecuit, T. 2005. Adhesion remodeling underlying tissue morphogenesis. Trends Cell Biol. 15:34-42.

LeDoux, Neurobiology of emotion. In: LeDoux JE, Hirst W, editors. Mind and brain, New York: Cambridge University Press,1986

LeDoux, J.E. 2000. Emotion circuits in the brain. Annu Rev Neurosci. 23:155-84.

Lemke, G., and M. Reber. 2005. Retinotectal mapping: new insights from molecular genetics. Annu Rev Cell Dev Biol. 21:551-80.

Levkowitz, G., H. Waterman, S.A. Ettenberg, M. Katz, A.Y. Tsygankov, I. Alroy, S. Lavi, K. Iwai, Y. Reiss, A. Ciechanover, S. Lipkowitz, and Y. Yarden. 1999. Ubiquitin ligase activity and tyrosine phosphorylation underlie suppression of growth factor signaling by c-Cbl/Sli-1. Mol Cell. 4:1029-40.

Li, X.F., G.E. Stutzmann, and J.E. LeDoux. 1996. Convergent but temporally separated inputs to lateral amygdala neurons from the auditory thalamus and auditory cortex use different postsynaptic receptors: in vivo intracellular and extracellular recordings in fear conditioning pathways. Learn Mem. 3:229-42.

Lin, J.W., W. Ju, K. Foster, S.H. Lee, G. Ahmadian, M. Wyszynski, Y.T. Wang, and M. Sheng. 2000. Distinct molecular mechanisms and divergent endocytotic pathways of AMPA receptor internalization. Nat Neurosci. 3:1282-90.

Lin, C.H., S.H. Yeh, K.T. Lu, T.H. Leu, W.C. Chang, and P.W. Gean. 2001. A role for the PI-3 kinase signaling pathway in fear conditioning and synaptic plasticity in the amygdala. Neuron. 31:841-51.

Lippe, R., M. Miaczynska, V. Rybin, A. Runge, and M. Zerial. 2001. Functional synergy between Rab5 effector Rabaptin-5 and exchange factor Rabex-5 when physically associated in a complex. Mol Biol Cell. 12:2219-28.

Liu, B.P., and K. Burridge. 2000. Vav2 activates Rac1, Cdc42, and RhoA downstream from growth factor receptors but not beta1 integrins. Mol Cell Biol. 20:7160-9.

Lu, Q., E.E. Sun, R.S. Klein, and J.G. Flanagan. 2001. Ephrin-B reverse signaling is mediated by a novel PDZ-RGS protein and selectively inhibits G protein-coupled chemoattraction. Cell. 105:69-79.

Lu, H., and D. Bilder. 2005. Endocytic control of epithelial polarity and proliferation in Drosophila. Nat Cell Biol. 7:1232-9.

Malenka, R.C. 1994. Synaptic plasticity in the hippocampus: LTP and LTD. Cell. 78:535-8.

Malenka, R.C., and M.F. Bear. 2004. LTP and LTD: an embarrassment of riches. Neuron. 44:5-21.

Mann, F., S. Ray, W. Harris, and C. Holt. 2002. Topographic mapping in dorsoventral axis of the Xenopus retinotectal system depends on signaling through ephrin-B ligands. Neuron. 35:461-73.

Marcoux, N., and K. Vuori. 2003. EGF receptor mediates adhesion-dependent activation of the Rac GTPase: a role for phosphatidylinositol 3-kinase and Vav2. Oncogene. 22:6100-6.

Maren, S. 2001. Neurobiology of Pavlovian fear conditioning. Annu Rev Neurosci. 24:897-931.

Maren, S., and G.J. Quirk. 2004. Neuronal signalling of fear memory. Nat Rev Neurosci. 5:844-52.

Maren, S. 2005. Synaptic mechanisms of associative memory in the amygdala. Neuron. 47:783-6.

Marengere, L.E., and T. Pawson. 1992. Identification of residues in GTPase-activating protein Src homology 2 domains that control binding to tyrosine phosphorylated growth factor receptors and p62. J Biol Chem. 267:22779-86.

Marignani, P.A., and C.L. Carpenter. 2001. Vav2 is required for cell spreading. J Cell Biol. 154:177-86.

Marquardt, T., R. Shirasaki, S. Ghosh, S.E. Andrews, N. Carter, T. Hunter, and S.L. Pfaff. 2005. Coexpressed EphA receptors and ephrin-A ligands mediate opposing actions on growth cone navigation from distinct membrane domains. Cell. 121:127-39.

Marston, D.J., S. Dickinson, and C.D. Nobes. 2003. Rac-dependent trans-endocytosis of ephrinBs regulates Eph-ephrin contact repulsion. Nat Cell Biol. 5:879-88.

Martin, S.J., P.D. Grimwood, and R.G. Morris. 2000. Synaptic plasticity and memory: an evaluation of the hypothesis. Annu Rev Neurosci. 23:649-711.

Matoskova, B., W.T. Wong, N. Seki, T. Nagase, N. Nomura, K.C. Robbins, and P.P. Di Fiore. 1996. RN-tre identifies a family of tre-related proteins displaying a novel potential protein binding domain. Oncogene. 12:2563-71.

Matsuda, S., L. Giliberto, Y. Matsuda, P. Davies, E. McGowan, F. Pickford, J. Ghiso, B. Frangione, and L. D'Adamio. 2005. The familial dementia BRI2 gene binds the Alzheimer gene amyloid-beta precursor protein and inhibits amyloid-beta production. J Biol Chem. 280:28912-6.

Matus, A., H. Brinkhaus, and U. Wagner. 2000. Actin dynamics in dendritic spines: a form of regulated plasticity at excitatory synapses. Hippocampus. 10:555-60.

McBride, H.M., V. Rybin, C. Murphy, A. Giner, R. Teasdale, and M. Zerial. 1999. Oligomeric complexes link Rab5 effectors with NSF and drive membrane fusion via interactions between EEA1 and syntaxin 13. Cell. 98:377-86.

McLaughlin, T., R. Hindges, P.A. Yates, and D.D. O'Leary. 2003. Bifunctional action of ephrin-B1 as a repellent and attractant to control bidirectional branch extension in dorsal-ventral retinotopic mapping. Development. 130:2407-18.

Merrifield, C.J. 2004. Seeing is believing: imaging actin dynamics at single sites of endocytosis. Trends Cell Biol. 14:352-8.

Miaczynska, M., and M. Zerial. 2002. Mosaic organization of the endocytic pathway. Exp Cell Res. 272:8-14.

Miaczynska, M., L. Pelkmans, and M. Zerial. 2004. Not just a sink: endosomes in control of signal transduction. Curr Opin Cell Biol. 16:400-6.

Miller, M., and A. Peters. 1981. Maturation of rat visual cortex. II. A combined Golgi-electron microscope study of pyramidal neurons. J Comp Neurol. 203:555-73.

Moberg, K.H., S. Schelble, S.K. Burdick, and I.K. Hariharan. 2005. Mutations in erupted, the Drosophila ortholog of mammalian tumor susceptibility gene 101, elicit non-cell-autonomous overgrowth. Dev Cell. 9:699-710.

Motley, A., N.A. Bright, M.N. Seaman, and M.S. Robinson. 2003. Clathrin-mediated endocytosis in AP-2-depleted cells. J Cell Biol. 162:909-18.

Murai, K.K., and E.B. Pasquale. 2003. 'Eph'ective signaling: forward, reverse and crosstalk. J Cell Sci. 116:2823-32.

Nabi, I.R., and P.U. Le. 2003. Caveolae/raft-dependent endocytosis. J Cell Biol. 161:673-7.

Nader, K., P. Majidishad, P. Amorapanth, and J.E. LeDoux. 2001. Damage to the lateral and central, but not other, amygdaloid nuclei prevents the acquisition of auditory fear conditioning. Learn Mem. 8:156-63.

Nagerl, U.V., N. Eberhorn, S.B. Cambridge, and T. Bonhoeffer. 2004. Bidirectional activity-dependent morphological plasticity in hippocampal neurons. Neuron. 44:759-67.

O'Connor-Giles, K.M., and J.B. Skeath. 2003. Numb inhibits membrane localization of Sanpodo, a four-pass transmembrane protein, to promote asymmetric divisions in Drosophila. Dev Cell. 5:231-43.

Orioli, D., M. Henkemeyer, G. Lemke, R. Klein, and T. Pawson. 1996. Sek4 and Nuk receptors cooperate in guidance of commissural axons and in palate formation. Embo J. 15:6035-49.

Palmer, A., M. Zimmer, K.S. Erdmann, V. Eulenburg, A. Porthin, R. Heumann, U. Deutsch, and R. Klein. 2002. EphrinB phosphorylation and reverse signaling: regulation by Src kinases and PTP-BL phosphatase. Mol Cell. 9:725-37.

Palmer, A., and R. Klein. 2003. Multiple roles of ephrins in morphogenesis, neuronal networking, and brain function. Genes Dev. 17:1429-50.

Pare, D., G.J. Quirk, and J.E. Ledoux. 2004. New vistas on amygdala networks in conditioned fear. J Neurophysiol. 92:1-9.

Parker, M., R. Roberts, M. Enriquez, X. Zhao, T. Takahashi, D. Pat Cerretti, T. Daniel, and J. Chen. 2004. Reverse endocytosis of transmembrane ephrin-B ligands via a clathrin-mediated pathway. Biochem Biophys Res Commun. 323:17-23.

Parks, A.L., K.M. Klueg, J.R. Stout, and M.A. Muskavitch. 2000. Ligand endocytosis drives receptor dissociation and activation in the Notch pathway. Development. 127:1373-85.

Parton, R.G. 2003. Caveolae--from ultrastructure to molecular mechanisms. Nat Rev Mol Cell Biol. 4:162-7.

Pasquale, E.B. 2004. Eph-ephrin promiscuity is now crystal clear. Nat Neurosci. 7:417-8.

Pasquale, E.B. 2005. Eph receptor signalling casts a wide net on cell behaviour. Nat Rev Mol Cell Biol. 6:462-75.

Pawson, T., and J. Schlessinger. 1993. SH2 and SH3 domains. Curr Biol. 3:434-42.

Pelkmans, L., and A. Helenius. 2002. Endocytosis via caveolae. Traffic. 3:311-20.

Penzes, P., A. Beeser, J. Chernoff, M.R. Schiller, B.A. Eipper, R.E. Mains, and R.L. Huganir. 2003. Rapid induction of dendritic spine morphogenesis by trans-synaptic ephrinB-EphB receptor activation of the Rho-GEF kalirin. Neuron. 37:263-74.

Pereira-Leal, J.B., and M.C. Seabra. 2001. Evolution of the Rab family of small GTP-binding proteins. J Mol Biol. 313:889-901.

Perret, E., A. Lakkaraju, S. Deborde, R. Schreiner, and E. Rodriguez-Boulan. 2005. Evolving endosomes: how many varieties and why? Curr Opin Cell Biol. 17:423-34.

Pfeffer, S.R. 2001. Rab GTPases: specifying and deciphering organelle identity and function. Trends Cell Biol. 11:487-91.

Pfeffer, S. 2003. Membrane domains in the secretory and endocytic pathways. Cell. 112:507-17.

Poliakov, A., M. Cotrina, and D.G. Wilkinson. 2004. Diverse roles of eph receptors and ephrins in the regulation of cell migration and tissue assembly. Dev Cell. 7:465-80.

Polo, S., and P.P. Di Fiore. 2006. Endocytosis conducts the cell signaling orchestra. Cell. 124:897-900.

Posada, J., and J.A. Cooper. 1992. Molecular signal integration. Interplay between serine, threonine, and tyrosine phosphorylation. Mol Biol Cell. 3:583-92.

Radhika, V., D. Onesime, J.H. Ha, and N. Dhanasekaran. 2004. Galpha13 stimulates cell migration through cortactin-interacting protein Hax-1. J Biol Chem. 279:49406-13.

Radtke, F., F. Schweisguth, and W. Pear. 2005. The Notch 'gospel'. EMBO Rep. 6:1120-5.

Raiborg, C., K.G. Bache, D.J. Gillooly, I.H. Madshus, E. Stang, and H. Stenmark. 2002. Hrs sorts ubiquitinated proteins into clathrin-coated microdomains of early endosomes. Nat Cell Biol. 4:394-8.

Rappoport, J.Z., S.M. Simon, and A. Benmerah. 2004. Understanding living clathrin-coated pits. Traffic. 5:327-37.

Riccio, A., B.A. Pierchala, C.L. Ciarallo, and D.D. Ginty. 1997. An NGF-TrkA-mediated retrograde signal to transcription factor CREB in sympathetic neurons. Science. 277:1097-100.

Rigaut, G., A. Shevchenko, B. Rutz, M. Wilm, M. Mann, and B. Seraphin. 1999. A generic protein purification method for protein complex characterization and proteome exploration. Nat Biotechnol. 17:1030-2.

Rocks, O., A. Peyker, M. Kahms, P.J. Verveer, C. Koerner, M. Lumbierres, J. Kuhlmann, H. Waldmann, A. Wittinghofer, and P.I. Bastiaens. 2005. An acylation cycle regulates localization and activity of palmitoylated Ras isoforms. Science. 307:1746-52.

Rocks, O., A. Peyker, and P.I. Bastiaens. 2006. Spatio-temporal segregation of Ras signals: one ship, three anchors, many harbors. Curr Opin Cell Biol. 18:351-357.

Rodrigues, S.M., G.E. Schafe, and J.E. LeDoux. 2004. Molecular mechanisms underlying emotional learning and memory in the lateral amygdala. Neuron. 44:75-91.

Rogan, M.T., and J.E. LeDoux. 1996. Emotion: systems, cells, synaptic plasticity. Cell. 85:469-75.

Rubino, M., M. Miaczynska, R. Lippe, and M. Zerial. 2000. Selective membrane recruitment of EEA1 suggests a role in directional transport of clathrin-coated vesicles to early endosomes. J Biol Chem. 275:3745-8.

Rumpel, S., J. LeDoux, A. Zador, and R. Malinow. 2005. Postsynaptic receptor trafficking underlying a form of associative learning. Science. 308:83-8.

Saito, K., J. Murai, H. Kajiho, K. Kontani, H. Kurosu, and T. Katada. 2002. A novel binding protein composed of homophilic tetramer exhibits unique properties for the small GTPase Rab5. J Biol Chem. 277:3412-8.

Sanson, B., C. Alexandre, N. Fascetti, and J.P. Vincent. 1999. Engrailed and hedgehog make the range of Wingless asymmetric in Drosophila embryos. Cell. 98:207-16.

Sass, P., J. Field, J. Nikawa, T. Toda, and M. Wigler. 1986. Cloning and characterization of the high-affinity cAMP phosphodiesterase of Saccharomyces cerevisiae. Proc Natl Acad Sci U S A. 83:9303-7.

Satoh, K., M. Takeuchi, Y. Oda, M. Deguchi-Tawarada, Y. Sakamoto, K. Matsubara, T. Nagasu, and Y. Takai. 2002. Identification of activity-regulated proteins in the postsynaptic density fraction. Genes Cells. 7:187-97.

Schafe, G.E., C.M. Atkins, M.W. Swank, E.P. Bauer, J.D. Sweatt, and J.E. LeDoux. 2000. Activation of ERK/MAP kinase in the amygdala is required for memory consolidation of pavlovian fear conditioning. J Neurosci. 20:8177-87.

Schlessinger, J. 2000. Cell signaling by receptor tyrosine kinases. Cell. 103:211-25.

Schuebel, K.E., N. Movilla, J.L. Rosa, and X.R. Bustelo. 1998. Phosphorylation-dependent and constitutive activation of Rho proteins by wild-type and oncogenic Vav-2. Embo J. 17:6608-21.

Schweisguth, F. 2004. Notch signaling activity. Curr Biol. 14:R129-38.

Scully, A.L., M. McKeown, and J.B. Thomas. 1999. Isolation and characterization of Dek, a Drosophila eph receptor protein tyrosine kinase. Mol Cell Neurosci. 13:337-47.

Segev, N. 2001. Ypt and Rab GTPases: insight into functions through novel interactions. Curr Opin Cell Biol. 13:500-11.

Selkoe, D., and R. Kopan. 2003. Notch and Presenilin: regulated intramembrane proteolysis links development and degeneration. Annu Rev Neurosci. 26:565-97.

Servitja, J.M., M.J. Marinissen, A. Sodhi, X.R. Bustelo, and J.S. Gutkind. 2003. Rac1 function is required for Src-induced transformation. Evidence of a role for Tiam1 and Vav2 in Rac activation by Src. J Biol Chem. 278:34339-46.

Seugnet, L., P. Simpson, and M. Haenlin. 1997. Requirement for dynamin during Notch signaling in Drosophila neurogenesis. Dev Biol. 192:585-98.

Shang, W.H., Y. Adachi, A. Nakamura, T. Copeland, S.R. Kim, and T. Kamata. 2004. Regulation of amphiphysin1 by mitogen-activated protein kinase: its significance in nerve growth factor receptor-mediated endocytosis. J Biol Chem. 279:40890-6.

Sharma, P., S. Sabharanjak, and S. Mayor. 2002. Endocytosis of lipid rafts: an identity crisis. Semin Cell Dev Biol. 13:205-14.

Sharma, D.K., J.C. Brown, A. Choudhury, T.E. Peterson, E. Holicky, D.L. Marks, R. Simari, R.G. Parton, and R.E. Pagano. 2004. Selective stimulation of caveolar endocytosis by glycosphingolipids and cholesterol. Mol Biol Cell. 15:3114-22.

Sherrington CS, The integrative action of the nervous system. 2nd edition, New Haven (CT): Yale University Press, 1906

Shevchenko, A., M. Wilm, O. Vorm, and M. Mann. 1996. Mass spectrometric sequencing of proteins silver-stained polyacrylamide gels. Anal Chem. 68:850-8.

Shintani, T., M. Ihara, H. Sakuta, H. Takahashi, I. Watakabe, and M. Noda. 2006. Eph receptors are negatively controlled by protein tyrosine phosphatase receptor type O. Nat Neurosci. 9:761-9.

Sigismund, S., T. Woelk, C. Puri, E. Maspero, C. Tacchetti, P. Transidico, P.P. Di Fiore, and S. Polo. 2005. Clathrin-independent endocytosis of ubiquitinated cargos. Proc Natl Acad Sci U S A. 102:2760-5.

Silvius, J.R. 2002. Mechanisms of Ras protein targeting in mammalian cells. J Membr Biol. 190:83-92.

Skoulakis, E.M., and R.L. Davis. 1998. 14-3-3 proteins in neuronal development and function. Mol Neurobiol. 16:269-84.

Smith, F.M., C. Vearing, M. Lackmann, H. Treutlein, J. Himanen, K. Chen, A. Saul, D. Nikolov, and A.W. Boyd. 2004. Dissecting the EphA3/Ephrin-A5 interactions using a novel functional mutagenesis screen. J Biol Chem. 279:9522-31.

Somsel Rodman, J., and A. Wandinger-Ness. 2000. Rab GTPases coordinate endocytosis. J Cell Sci. 113 Pt 2:183-92.

Song, J., W. Vranken, P. Xu, R. Gingras, R.S. Noyce, Z. Yu, S.H. Shen, and F. Ni. 2002. Solution structure and backbone dynamics of the functional cytoplasmic subdomain of human ephrin B2, a cell-surface ligand with bidirectional signaling properties. Biochemistry. 41:10942-9.

Song, J. 2003. Tyrosine phosphorylation of the well packed ephrinB cytoplasmic beta-hairpin for reverse signaling. Structural consequences and binding properties. J Biol Chem. 278:24714-20.

Sonnichsen, B., S. De Renzis, E. Nielsen, J. Rietdorf, and M. Zerial. 2000. Distinct membrane domains on endosomes in the recycling pathway visualized by multicolor imaging of Rab4, Rab5, and Rab11. J Cell Biol. 149:901-14.

Sorkin, A., and M. Von Zastrow. 2002. Signal transduction and endocytosis: close encounters of many kinds. Nat Rev Mol Cell Biol. 3:600-14.

Sprenger, R.R., D. Speijer, J.W. Back, C.G. De Koster, H. Pannekoek, and A.J. Horrevoets. 2004. Comparative proteomics of human endothelial cell caveolae and rafts using two-dimensional gel electrophoresis and mass spectrometry. Electrophoresis. 25:156-72.

Stahlhut, M., and B. van Deurs. 2000. Identification of filamin as a novel ligand for caveolin-1: evidence for the organization of caveolin-1-associated membrane domains by the actin cytoskeleton. Mol Biol Cell. 11:325-37.

Suzuki, Y., C. Demoliere, D. Kitamura, H. Takeshita, U. Deuschle, and T. Watanabe. 1997. HAX-1, a novel intracellular protein, localized on mitochondria, directly associates with HS1, a substrate of Src family tyrosine kinases. J Immunol. 158:2736-44.

Szabo, K., G. Jekely, and P. Rorth. 2001. Cloning and expression of sprint, a Drosophila homologue of RIN1. Mech Dev. 101:259-62.

Tall, G.G., M.A. Barbieri, P.D. Stahl, and B.F. Horazdovsky. 2001. Ras-activated endocytosis is mediated by the Rab5 guanine nucleotide exchange activity of RIN1. Dev Cell. 1:73-82.

Tamas, P., Z. Solti, P. Bauer, A. Illes, S. Sipeki, A. Bauer, A. Farago, J. Downward, and L. Buday. 2003. Mechanism of epidermal growth factor regulation of Vav2, a guanine nucleotide exchange factor for Rac. J Biol Chem. 278:5163-71.

Thien, C.B., and W.Y. Langdon. 2001. Cbl: many adaptations to regulate protein tyrosine kinases. Nat Rev Mol Cell Biol. 2:294-307.

Thompson, B.J., J. Mathieu, H.H. Sung, E. Loeser, P. Rorth, and S.M. Cohen. 2005. Tumor suppressor properties of the ESCRT-II complex component Vps25 in Drosophila. Dev Cell. 9:711-20.

Thomsen, P., K. Roepstorff, M. Stahlhut, and B. van Deurs. 2002. Caveolae are highly immobile plasma membrane microdomains, which are not involved in constitutive endocytic trafficking. Mol Biol Cell. 13:238-50.

Toda, T., I. Uno, T. Ishikawa, S. Powers, T. Kataoka, D. Broek, S. Cameron, J. Broach, K. Matsumoto, and M. Wigler. 1985. In yeast, RAS proteins are controlling elements of adenylate cyclase. Cell. 40:27-36.

Topp, J.D., N.W. Gray, R.D. Gerard, and B.F. Horazdovsky. 2004. Alsin is a Rab5 and Rac1 guanine nucleotide exchange factor. J Biol Chem. 279:24612-23.

Ulrich, F., M.L. Concha, P.J. Heid, E. Voss, S. Witzel, H. Roehl, M. Tada, S.W. Wilson, R.J. Adams, D.R. Soll, and C.P. Heisenberg. 2003. Slb/Wnt11 controls hypoblast cell migration and morphogenesis at the onset of zebrafish gastrulation. Development. 130:5375-84.

Ulrich, F., M. Krieg, E.M. Schotz, V. Link, I. Castanon, V. Schnabel, A. Taubenberger, D. Mueller, P.H. Puech, and C.P. Heisenberg. 2005. Wnt11 functions in gastrulation by controlling cell cohesion through Rab5c and E-cadherin. Dev Cell. 9:555-64.

Vaccari, T., and D. Bilder. 2005. The Drosophila tumor suppressor vps25 prevents nonautonomous overproliferation by regulating notch trafficking. Dev Cell. 9:687-98.

Verveer, P.J., F.S. Wouters, A.R. Reynolds, and P.I. Bastiaens. 2000. Quantitative imaging of lateral ErbB1 receptor signal propagation in the plasma membrane. Science. 290:1567-70.

Wang, X., P.J. Roy, S.J. Holland, L.W. Zhang, J.G. Culotti, and T. Pawson. 1999. Multiple ephrins control cell organization in C. elegans using kinase-dependent and -independent functions of the VAB-1 Eph receptor. Mol Cell. 4:903-13.

Wang, Y., R.T. Waldron, A. Dhaka, A. Patel, M.M. Riley, E. Rozengurt, and J. Colicelli. 2002. The RAS effector RIN1 directly competes with RAF and is regulated by 14-3-3 proteins. Mol Cell Biol. 22:916-26.

Wang, W., and G. Struhl. 2004. Drosophila Epsin mediates a select endocytic pathway that DSL ligands must enter to activate Notch. Development. 131:5367-80.

Wang, W., and G. Struhl. 2005. Distinct roles for Mind bomb, Neuralized and Epsin in mediating DSL endocytosis and signaling in Drosophila. Development. 132:2883-94.

Weeber, E.J., and J.D. Sweatt. 2002. Molecular neurobiology of human cognition. Neuron. 33:845-8.

Wilkinson, D.G. 2001. Multiple roles of EPH receptors and ephrins in neural development. Nat Rev Neurosci. 2:155-64.

Wilkinson, D.G. 2003. How attraction turns to repulsion. Nat Cell Biol. 5:851-3.

Wimmer-Kleikamp, S.H., P.W. Janes, A. Squire, P.I. Bastiaens, and M. Lackmann. 2004. Recruitment of Eph receptors into signaling clusters does not require ephrin contact. J Cell Biol. 164:661-6.

Wybenga-Groot, L.E., B. Baskin, S.H. Ong, J. Tong, T. Pawson, and F. Sicheri. 2001. Structural basis for autoinhibition of the Ephb2 receptor tyrosine kinase by the unphosphorylated juxtamembrane region. Cell. 106:745-57.

Yamaguchi, Y., and E.B. Pasquale. 2004. Eph receptors in the adult brain. Curr Opin Neurobiol. 14:288-96.

Ye, H., R. Kuruvilla, L.S. Zweifel, and D.D. Ginty. 2003. Evidence in support of signaling endosome-based retrograde survival of sympathetic neurons. Neuron. 39:57-68.

Yuste, R., and T. Bonhoeffer. 2001. Morphological changes in dendritic spines associated with long-term synaptic plasticity. Annu Rev Neurosci. 24:1071-89.

Zerial, M., and H. McBride. 2001. Rab proteins as membrane organizers. Nat Rev Mol Cell Biol. 2:107-17.

Zhu, J.J., Y. Qin, M. Zhao, L. Van Aelst, and R. Malinow. 2002. Ras and Rap control AMPA receptor trafficking during synaptic plasticity. Cell. 110:443-55.

Zimmer, M., A. Palmer, J. Kohler, and R. Klein. 2003. EphB-ephrinB bi-directional endocytosis terminates adhesion allowing contact mediated repulsion. Nat Cell Biol. 5:869-78.

Zisch, A.H., M.S. Kalo, L.D. Chong, and E.B. Pasquale. 1998. Complex formation between EphB2 and Src requires phosphorylation of tyrosine 611 in the EphB2 juxtamembrane region. Oncogene. 16:2657-70.

Zisch, A.H., C. Pazzagli, A.L. Freeman, M. Schneller, M. Hadman, J.W. Smith, E. Ruoslahti, and E.B. Pasquale. 2000. Replacing two conserved tyrosines of the EphB2 receptor with glutamic acid prevents binding of SH2 domains without abrogating kinase activity and biological responses. Oncogene. 19:177-87.

Ziv, N.E., and S.J. Smith. 1996. Evidence for a role of dendritic filopodia in synaptogenesis and spine formation. Neuron. 17:91-102.

Curriculum vitae

Personal data

Name	Katrin Deininger
Date of Birth	August, 19th, 1975
Place of Birth	Scheßlitz, Germany
Nationality	German

Education

since October 2001	**Doctoral thesis** Laboratory of Prof. Dr. Rüdiger Klein Department of Molecular Neurobiology Max Planck Institute of Neurobiology, Martinsried
Jan 2000 – Jan 2001	**Diploma thesis**, final degree "sehr gut" Laboratory of Francesco Ramirez, PhD Department of Molecular, Cell & Developmental Biology Mount Sinai School of Medicine, New York, NY, USA
Nov 1995 – Jan 2001	**Diploma in Biology**, final degree "sehr gut" Julius-Maximilians-University, Würzburg major: Genetics minors: Cell and Developmental Biology Immunobiology and Virology

Publication

Rentschler S, Linn H, Deininger K, Bedford MT, Espanel X, Sudol M, The WW domain of dystrophin requires EF-hands region to interact with beta-dystroglycan, Biol Chem, 1999